**The Dissertation Committee for Eusebio Mercedes Ingol Blanco Certifies that this is the approved version of the following dissertation:**

**Modeling Climate Change Impacts on Hydrology and Water Resources: Case Study Rio Conchos Basin**

**Committee:**

Daene C. McKinney, Supervisor

David R. Maidment

Randall J. Charbeneau

Ben R. Hodges

David J. Eaton

**Modeling Climate Change Impacts on Hydrology and Water Resources:**

**Case Study Rio Conchos Basin**

**by**

**Eusebio Mercedes Ingol Blanco, B.S.; M.S.**

**Dissertation**

Presented to the Faculty of the Graduate School of

The University of Texas at Austin

in Partial Fulfillment

of the Requirements

for the Degree of

**Doctor of Philosophy**

**The University of Texas at Austin**

**May, 2011**

## Dedication

To memory of my parents for guiding me at the time by the right way.

To my professors from United States, Peru, and Mexico, for their great lessons.

To my wife, Juliana, for her love, patience, and support to achieve this goal.

To my children Nathaly, Gavin, and my little baby, for their love and tenderness.

To my sisters, brother, nephews, nieces, and family, for their affection and support.

# Acknowledgements

I wish express my deep and sincere gratitude to Dr. Daene McKinney, my supervisor, for his excellent support and guidance during the development of this research. Dr. McKinney has been a wonderful mentor for me and thank you for giving the opportunity to work in your projects during my graduate studies. My total thanks to Dr. Randall Charbeneau, Dr. David Maidment, Dr. Ben Hodges, and Dr. David Eaton not only for being members of my committee but also for their excellent teachings and support to achieve my professional and academic goals.

I would like to thank the Ford Foundation International Fellowships Program for providing funding for my English training and for my doctoral program during three years at the University of Texas at Austin. In particular, I would like to thank the Ford IFP's Executive Director, Joan Dassin, for her strong support to students with academic potential in developing countries. In addition, I want to thank to IFP Peru, Cecilia Isrrael, Anita Rojas, and Elsa Elias, and IFP UT Austin, Paloma Diaz and Darcy McGillicuddy, for their support during my staying as fellow. I would like to thank the University of Texas at Austin for its funding support to complete my doctoral studies.

I appreciate the support of members of our research group, especially for Samuel Sandoval for his advising in the water planning model, and for his friendship during the development of this research. Thank you to my EWRI UT friends, for their fantastic

# Modeling Climate Change Impacts on Hydrology and Water Resources: Case Study Rio Conchos Basin

Publication No._____

Eusebio Mercedes Ingol Blanco, Ph.D.

The University of Texas at Austin, 2011

Supervisor: Daene C. McKinney

Water resources availability could be affected by alterations of hydrologic processes as a result of climate change. Global projections of climate change indicate negative impacts on water systems with increasing flooding and drought events. This investigation presents the modeling of climate change effects on the hydrology and water resources availability in the Rio Conchos basin, the main tributary of the lower portion of the bi-national Rio Grande/Bravo basin, and its impact on the water treaty signed between the United States of America and Mexico in 1944. One of the problems most relevant to the study basin is the frequent occurrence of long drought periods. Coupled with increased water demands and low irrigation efficiencies, the competition for water resources is high on both sides of the border. Three main parts are addressed in this research. First, a hydrologic model has been developed using the one-dimensional, 2 layer soil moisture accounting scheme embedded in a water evaluation and planning model. Second, downscaled precipitation and temperature data, from five general circulation models for two emission scenarios,

A1B and A2, were used as inputs to the Rio Conchos hydrologic model to determine the effect on basin hydrology. A multi-model ensemble is developed and several techniques, such as probability density functions, wavelet analysis, and trend analysis, are used to assess the impacts. Third, a water resources planning model for the basin has been developed, which integrates the hydrologic model and water management modeling, to evaluate the impacts on the entire water system and simulate adaptive strategies to mitigate climate change in the study basin. Skill-weighted multi-model ensemble results show that annual average runoff may be reduced by 12% ± 53% and 20% ± 45% in 2080-2099 relative to 1980-1999 for the A1B and A2 scenarios, respectively. Likewise, results show that reliability and resiliency of the water system will tend to decrease; consequently, the vulnerability of the system increases over time. Proposed adaptation measures could make the system more reliable and less vulnerable in meeting water demands for irrigation and municipal uses.

# Table of Contents

# List of Tables

# List of Figures

xxiii

# Chapter 1: Introduction

In many river basins in the world, water availability is vulnerable to the potential effects of climate change. Furthermore, the irregular distribution of precipitation in space and time plays an important role in defining the hydrologic features of a basin, being even more complicated if alterations in the hydrologic cycle occur as a consequence of climatic variability. Changes in temperature and precipitation patterns, due to the increase in concentrations of greenhouse gases affect the hydrologic processes; consequently, negative impacts are expected on water resources for agriculture, urban uses, mining and industry, aquatic life in rivers and lakes, and hydropower production. Likewise, spatial changes in intensity and frequency of precipitation may affect the magnitude and frequency of streamflows, increasing the intensity of floods and droughts, with substantial impacts on economic activities at local and regional levels.

In this direction, at global scale, studies indicate that temperature will increase more than 3.0 $^{o}$C (under the A2 emission scenario) by the end of the 21$^{st}$ century and precipitation will decrease in lower and mid-latitudes by 5-25%, and increase in high latitudes (IPCC, 2008). Regionally, precipitation will decrease in part of North America (south of the United States and Mexico), Central America and South America, Caribbean regions, sub tropical western coasts, and over the Mediterranean. Likewise, evaporation, soil moisture content, and groundwater recharge will also be affected; consequently, drought conditions and increased evapotranspiration rates are projected in summer for sub-tropical regions, low- and mid-latitudes.

Several studies have evaluated the impacts of climate change on hydrology and water resources at regional and local scales (Hamlet and Lettenmaier 2000, Christensen and Wood et el. 2004, Zhu et el. 2005, and Joyce et el. 2006). Most of these investigations predict a seasonal reduction of flows due to an increase in temperature and decrease of precipitation. On the other hand, few studies have been developed to evaluate the impacts of climate change in transboundary river basins. Some of these include Draper and Kundell (2007) and Beyene et el. (2008). Since existing transboundary treaties were signed by countries and states under historical climatic conditions, transboundary water planning may be unreliable under future, changed climate conditions (Draper and Kundell 2008). Therefore, treaties need to consider future changes in water availability as a consequence of climate change events, such as, longer drought periods and increased flooding, adopting water management and design strategies to face and mitigate the negative effects of climatic variability.

This investigation evaluates the effects of climate change on hydrology and water resources in the Rio Conchos basin, with a special emphasis on the water treaty signed between the US and Mexico in 1944. Streamflow inputs for the basin's main reservoirs are evaluated and their effect on agricultural and municipal uses in the study area. The Rio Conchos basin is located in the Mexican state of Chihuahua, with a drainage area around 67,800 km$^2$; it is the most important Mexican tributary of the binational Rio Grande/Bravo basin. The Rio Conchos contributes about 55% to the 1944 water treaty deliveries to the United States, which represents a higher value than the other Mexican

2

rivers considered in the treaty. During drought periods, there are serious conflicts and competition for the water resources on both sides of the border, and, as a consequence, Mexico can accumulate important deficits of water delivery to the US. Additionally, the hydrologic behavior of the basin produces recurrent periods of water stress, long drought periods, and water pollution.

## 1.1 THE PROBLEM

Water allocation in the Rio Conchos basin is governed by Mexican rules based on rights and demands of each water user taking account of the water availability in the main reservoirs and control stations along the basin. The main water demands are for agricultural and municipal use, with 91% and 7% (CONAGUA 2004 and 2009), respectively. The agricultural sector has more than 100,000 hectares (CONAGUA 2004) located in different irrigation districts. One of the most important problems for this sector is the low water efficiency which averages between 30% and 40% (Collado 2002 and CONAGUA 2003).

On the other hand, the Rio Conchos basin is the main tributary of the bi-national Rio Grande/Bravo basin delivering specified minimum amounts of water from Mexico to the United States as established in the 1944 water treaty. This agreement has been affected in the last decades due to frequent drought periods and increased water demands. As mentioned above, one problem in the basin is the recurrent and long drought periods. Natural variability, climate change, human activities such as deforestation in the upper basin, could be influencing the current hydrologic pattern. In the last 70 years, extreme

droughts have occurred from 1940 to 1965 and 1992 to 2002. This hydrologic behavior of the basin has contributed to Mexican difficulties in treaty compliance several times, causing serious conflicts for the water resources in both countries. In the coming decades, this problem may be more acute if we consider the potential effects of climate change.

The research developed here aims to answer the following questions:

1. *What will the hydrologic response of the Rio Conchos basin be under the potential effects of climate change?*

2. *What will happen to water availability in the basin over the coming decades taking into account the climate change impacts in the basin?*

3. *What will happen to the water treaty between Mexico and the US under the potential effects of climate change?*

4. *How can the water infrastructure, such as dams and channels for irrigation districts, be operated to reliably adapt to climate change in the basin?*

5. *What kind of management strategies could be implemented in order to face future drought periods?*

To answer these questions, the development and use of hydrologic and planning models is necessary. In this research, the Water Evaluation and Planning (WEAP) software is used (SEI, 2007) to model and assess the hydrologic behavior of the Rio Conchos basin under potential climate change. The model is spatially continuous with areas configured as a set of sub-catchments that cover the entire river basin under study, considering them to be a complete network of rivers, reservoirs, channels, aquifers,

demand points, etc. Likewise, this model includes methods to simulate catchment processes, such as evapotranspiration, runoff and infiltration, as a dynamic integrated rainfall-runoff model including various components of the hydrologic cycle (Yates et al. 2006). The model was calibrated and validated comparing the simulated flows with historical naturalized flows in the Rio Conchos basin; moreover, climate change scenarios from 5 GCMs are used to assess impacts of climate change on the water resources in the Rio Conchos basin.

## 1.2 OBJECTIVES

To answer the questions formulated above, this research has the following main objectives:

1. Model the hydrological behavior of the Rio Conchos basin (rainfall – runoff) using the soil moisture method;

2. Process and analyze statistically downscaled climate outputs from 5 General Circulation Models (GCMs) for emission scenarios A2 (high emission path) and A1B (middle emission path);

3. Simulate and assess the result of climate change on the hydrologic system of the Rio Conchos;

4. Assess climate change impacts on water resources management in basin and their effect on the 1944 Treaty between the US and Mexico; and

5. Simulate and evaluate water management scenarios to adapt to the climate change effects in the next decades.

## 1.3 STUDY AREA DESCRIPTION

### 1.3.1 Location

The Rio Conchos basin, main Mexican tributary of the Binational Rio Grande/Bravo basin, is located in the Mexican State of Chihuahua (Figure 1-1), with a drainage area of 67,808 km$^2$ and a length of the main river of 720 km. It provides about 55% of the water deliveries to the US under the water sharing treaty signed between Mexico and the US in 1944, representing the highest amount of all the Mexican tributaries considered on this treaty.
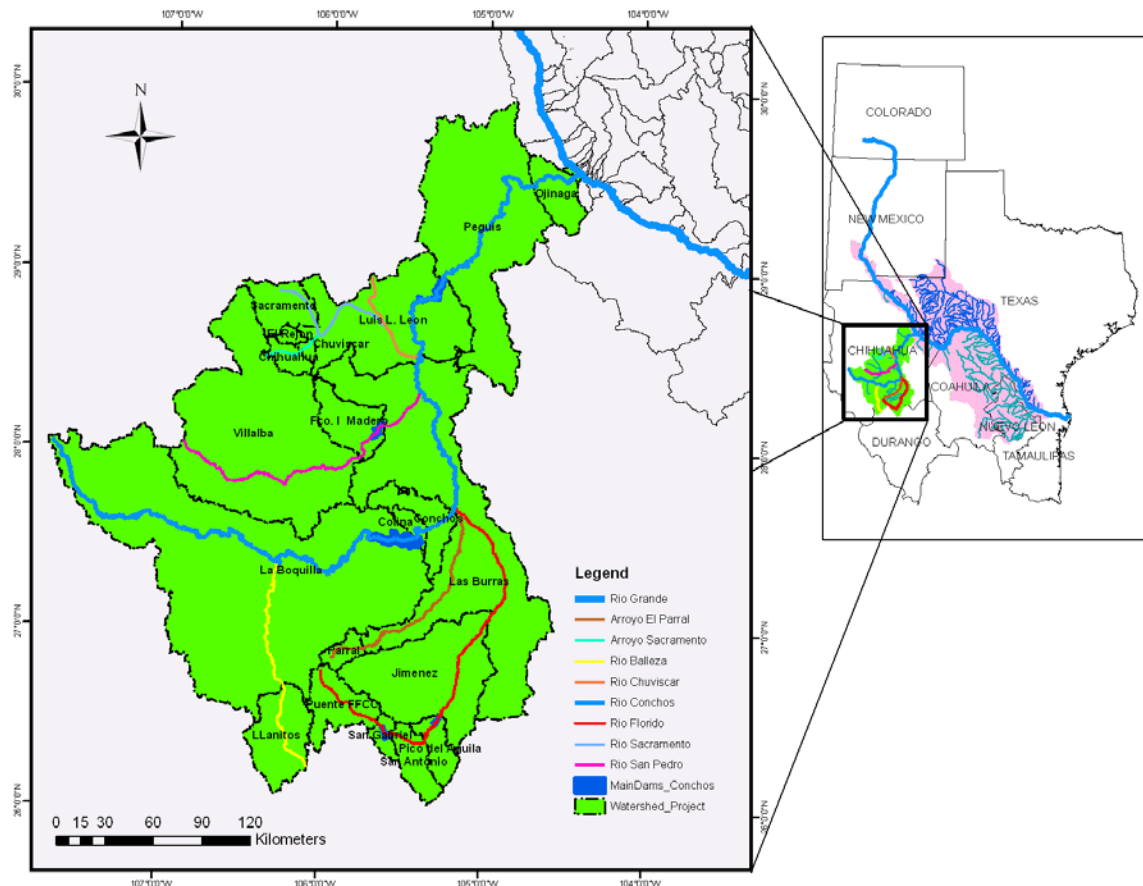


Figure 1-1: Location of the Rio Conchos basin

**1.3.2 Climate**

The study area is characterized by a dry climate and desert, especially in the middle and lower basin. In the upper basin, the prevailing climate is warm and semi – humid with rainfall occurring mostly in the summer. Maximum temperatures occur from June to August (summer period) and minimum from November to February (winter period). Moreover, the annual average temperature is around 19 $^{o}$C, with maximum that occurs from June to August (summer period) and minimum from November to February (winter period). The spatial variation indicates an annual maximum of 32 $^{o}$C for the lower basin and 27 $^{o}$C for the upper basin, with average minimum that ranges from 12 to 9 $^{o}$C (Ingol and McKinney, 2008), respectively. To characterize the precipitation in the study area, three main areas can be identified: (1) A small region located above about 2500 m above sea level comprised of mountains with massive plateaus (Chihuahua Mountains) in which the precipitation is around 1,000 mm per year on average; (2) A transition region, with an annual precipitation of about 450 mm per year, formed by valleys surrounded by mountainous areas; and (3) A desert zone at an altitude of about 1200 m with an annual precipitation of around 300 mm per year (Kim and Valdes, 2002).

**1.3.3 Soils**

In the upper basin, Podzoles soils are found whose geological composition corresponds to the volcanic half Cenozoic period, with vegetation of coniferous forest and pastizal amacollado arborescent types. In addition, in areas close to the la Boquilla reservoir, the main soils are of alluvial origin, with a grassland vegetation medium of

arbosufrutescente type. Mostly, the middle basin is characterized by soils of alluvial origin with vegetation of medium shrubland sibinerme kind and grassland whose geological formation belongs to the upper Cenozoic classic period. In the lower basin, the soils are alluvial belonging to the upper Cenozoic classic period and lower and upper cretaceous, with high shrub as vegetation (Pro-Fauna, 2003). In the upper basin, the terrain topography is very irregular, with steep and hillsides.

**1.3.4 Hydrology and Water Resources**

*1.3.4.1 General Description of the River*

The Rio Conchos originates in the high mountains in the southwest of Chihuahua State, specifically in the Sierra Madre Occidental near Bocoyna in Chihuahua, where it flows toward the east adding several tributaries along its journey. In the river reach at Zaragoza valley, La Boquilla reservoir is located, which is the largest reservoir forming Toronto Lake. After that, the Rio Conchos continues eastward forming the Colina Lake and passes through Camargo, Chihuahua, the main agricultural sector in this region where it joins the Rio Florido. From there, it continues northward and close to the Delicias, it receives flow from the San Pedro River which has another important reservoir, F. I. Madero. From there, the Rio Conchos enters the Chihuahua Desert and turns to the northeast where it is impounded by the Luis L. Leon dam, and finally the river cuts across the Peguis Canyon near Ojinaga. At Ojinaga, the river joins the Rio Bravo/Grande at river km 750.

### 1.3.4.2  Hydrologic Regimens

The hydrology of the Rio Conchos is characterized by two different regimens. The first one is a rainy period starts in late summer or early fall in the Sierra Madre Occidental (upper basin), with annual maximum streamflows reached in September. A long dry period occurs from November to June in which the base flow component is predominant for the river. Both hydrologic regimes have seasonal variations that are quite high. The main flows are produced in the upper basin. The hydrological behavior of the basin indicates recurrent periods of water stress, with long drought periods, allocation and release, and water pollution.

### 1.3.4.3  Water Sources and Availability

Total water availability in the basin is around 4,077 million $m^3$ ($Mm^3$) of which 67% is surface water and 33% is groundwater. Of the total water, 3,165.8 $Mm^3$ (77.6%) is allocated in the basin: 52.8% is from surface water, 41.3% is from aquifers, and 5.9% is from agricultural return flows (Jimenez 2002). In addition, it is estimated that in normal conditions around 800 $Mm^3$ per year flow to the confluence with the Rio Bravo.

### 1.3.4.4  Water Uses

The main water uses in the study area are for agricultural and municipal users, with 91% and 7%, respectively (Jimenez 2002). The difference (2%) corresponds to other uses in the following order of importance: livestock, mining, industry, and power production. The Rio Conchos basin has several reservoirs that store and regulate water

supply for agriculture; such as, La Boquilla, F.I. Madero, San Gabriel, Pico Aguila, and Luis L. Leon, although the last one generally is used for flood control. Low water efficiencies exist in the agriculture sector, ranging from 30% to 40% on average.

### *1.3.4.5 Drought Conditions*

One of the most important aspects of the basin is the competition for water resources whose distribution is complicated because of recurrent drought periods, causing conflicts among user organizations in the middle and lower basin. In the state of Chihuahua, where the study area is located, over a 50 year period normal precipitation occurred in only 8 years. Droughts have been identified when rainfall in the basin is less than 80% of the annual mean, and extreme events are on the order of 50% (CNA 1997, reported by Jimenez 2002). For instance, the basin was under extreme drought conditions from 1940 to early 1960 (more pronounced in 1951, 1953, and 1956) and wetter conditions in the late 1970s and at the beginning of the 1990s (Kim et el. 2002). The last drought period occurred from 1992 to 2002 and it was most severe in 1994.

Because of the desert conditions of most area of the watershed, the lack of rain causes negative impacts on all economic activities and ecosystems for both sides of the boundary since the Rio Conchos is the most important tributary of the Rio Grande/Bravo. Dry soil and high surface temperatures increase the evapotranspiration affecting the water use by stakeholders (Kim et el. 2002). Drought periods in the Rio Conchos basin have caused strong conflicts in water allocation, such as that stipulated in the 1944 US –

Mexico water treaty; consequently, Mexico experienced a deficit in water treaty deliveries in the last drought.

**1.3.5 Water Treaty**

The international water treaty signed between United States of America and Mexico in 1944 establishes the use of the waters of the Colorado and Tijuana rivers, and the Rio Grande/Basin. Specifically, in its article 4, incise c; it establishes the water allocation from The Rio Bravo for both countries (from Fort Quitman, Texas to Gulf Mexico). Essentially for the main Mexican tributaries, the water is allocated in the following way: two-thirds of the flow reaching the Rio Grande/Bravo from the Conchos, San Diego, San Rodrigo, Escondido, and Salado rivers, and Arroyo Las Vacas belongs to Mexico, and one–third of the flow reaching the main river from the tributaries mentioned above belongs to the United States, and that this one-third part shall not be less, as an average amount in cycles of five years, than 431,721,000 cubic meters annually (Water Treaty of the Colorado and Tijuana Rivers and of the Rio Grande, 1944). Likewise, the agreement specifies that in the event of extraordinary drought making it difficult of Mexico to allocate the minimum amount of water pointed above, the five-year cycle deficit shall be made up in the following five-year cycle with water from the same tributaries.

**1.4 DISSERTATION ORGANIZATION**

This dissertation describes the impacts of climate change on hydrology and water availability in the Rio Conchos basin. It is divided into eight chapters. Chapter two provides an extensive literature review of previous studies about the development and use of hydrological models to assess climate change, Global Climate Models, and downscaling methods. Chapter three describes the methodology to model the hydrologic dynamic of the Rio Conchos basin, the water system, and methods to evaluate the climate impacts. The methodology includes (1) the development of a hydrologic model; (2) analyzing multiple, downscaled General Circulation Model (GCM) outputs under two emission scenarios, A2 and A1B; (3) simulating the response of the basin hydrologic system to the resulting climate change; (4) deriving skill-weighted multi-model ensemble outputs describing the basin response to climate change; (5) assessing climate change impacts on hydrology in the basin; and (6) assessing climate impacts on water availability and the simulation of adaptive strategies. Chapter four presents the results of hydrological modeling which includes the calibration and validation model. Chapter five evaluates the impacts of climate change on the streamflow in the Rio Conchos, including a short and long term analysis. Chapter six presents the results of climate change impacts on reliability, resiliency, and vulnerability of the entire water system. Chapter seven describes adaptive water managements to mitigate climate change. Finally, conclusions and recommendations are addressed in chapter eight.

# Chapter 2: Literature Review

This section describes a review of major studies related to the development and application of models to evaluate potential climate change impacts on water resources in many basins in the world. Impacts at the global, regional, and local scales, as well as a description of downscaling techniques, the main advantages and disadvantages, and uncertainty of climate change estimates are discussed.

## 2.1 DEVELOPMENT AND USE OF HYDROLOGIC AND WATER PLANNING MODELS FOR CLIMATE CHANGE STUDIES

Several hydrological models have been applied to evaluate climate impacts on the hydrology and water resources at the basin scale. However, few of them evaluate widely the impacts on availability of water and possible management strategies to face increasing scarcity due to climate change. In addition, there are few hydrological studies that evaluate the effects of climate change in trans-boundary basins. Most studies have used separate hydrological and water resources models and integrated models have been neglected. Loukas and Quick (1996) used the University British Columbia (UBC) watershed model to simulate the hydrological response of two British Columbia basins under the potential effects of climate change. Basically, this model computes the total contribution of both rainfall runoff and snowmelt to basin water resources. The results indicated good model performed well in reproducing streamflows under historical conditions and for simulating climate change scenarios, for which annual runoff will increase due to the increment of precipitation and snowmelt. Yates and Strzepek (1998)

developed a lumped hydrological model based on a monthly water balance method for the Nile river basin to assess changes in runoff due to climate change. The hydrologic model showed a strong response to climate variability of the Nile River.

Hamlet and Lettenmaier (1999) assessed the impact of climate change on the water resources in the Columbia River basin. They used two models: (1) the Variable Infiltration Capacity (VIC) hydrological model developed by the University of Washington and Princeton University to simulate the hydrologic processes in the basin; and (2) the ColSim reservoir model to simulate and represent the current water system and operating policies. VIC is a semi-distributed grid-based hydrologic model, which parameterizes the hydro-meteorological processes in the interaction between the land surface and the atmosphere (Wood et el., 2004). This study showed that the macro-scale hydrologic model reproduced well the historical pattern and the effects of temperature and precipitation changes on streamflow. On the other hand, the ColSim model was less accurate than VIC; although, it was able to simulate, at a macro-scale level, the response of the water system.

Similarly, Wood et al. (2002), Wood et al. (2004), Payne et al. (2004), and Christensen et al. (2004), used VIC model to evaluate the hydrologic response in the Ohio, Columbia, and Colorado River basins under climate change conditions. In terms of water resources impacts, the Colorado River basin is one the most interesting. In addition to the VIC model, the Colorado River Reservoir model (CRRM) was used to evaluate the performance of the Colorado water system under potential effects of climatic variability.

Changes in streamflows, reservoir storage, water distribution for irrigation districts, hydropower production, and some water policies were evaluated, with a slight probabilistic analysis whose results showed that climate change will lead to a possible degradation of the water system performance in the next decades since total demand will likely exceed annual reservoir inflows.

More recent studies include Joyce et al. (2006), Kang and Ramirez (2007), Vicuna et al. (2007), Wiley and Palmer (2008), Li et al. (2008), Xie et al. (2008), and Sulis et al. (2009). Joyce et al.(2006) used WEAP (SEI, 2007) to assess the impact of future climate scenarios on agricultural water in the Sacrament basin. This study simulated the hydrologic processes and water resources changes in the same model, evaluating some water policies to mitigate the impact of climatic variability.

On the other hand, impact studies on hydrology also include the development and application of several models. For instance, the HEC-HMS distributed hydrological model has been used for the analysis of the response of streamflows under climate change in the Colorado Rockies (Kang and Ramirez 2007).   In this study, despite the fact that they only considered precipitation changes and neglected the temperature increase, the model reproduced acceptably the trends of flow changes due to the climate scenario considered for this end. Li et al. (2008) developed a simple hydrologic model to assess the impacts of precipitation and temperature changes from different GCMs on the runoff in the upper basin of the Yellow river in China. Snow and frozen soils were also included in the model that showed good performance in reproducing seasonal and annual climatic

15

variability. The Soil and Water Assessment Tool (SWAT) is another model used for climate change impact analysis. Applications with this model include Xie et al. (2008) and Sulis et al. (2008) who used SWAT to simulate hydrologic processes under potential effects of climate change in Mackinaw and upper Sangamon River basins in US, and the Caia River basin in Portugal.

## 2.2 GLOBAL CLIMATE MODELS

Global Climate Models (GCMs) are computational models that solve several mathematical equations governing atmospheric processes and project climate changes under different greenhouse gas emission scenarios. Since 1960, several global atmospheric models have been created, whose components were developed separately and later coupled into compressive climate models (IPCC, 2001). Initially, the models did not consider land and ocean interaction (e.g., Phillips 1956, Smagorinsky 1963, and Smagorinsky et al., 1965); however, these were capable of reproducing the general circulation of the atmosphere.

Later, in 1990 with the advance of computer skills, most atmospheric models included the major components of the climate system such as the atmosphere, land surface, ocean, cryosphere and biosphere, which are represented as sub-models (IPCC, 2001). Global Circulation Models (GCMs) that include the coupled interaction between the atmosphere and ocean components are called Atmosphere-Ocean General Circulation Models (AOGCMs). These models solve the fundamental conservation laws of

16

momentum, mass, and energy, which are discretized by finite difference, finite element, or spectral methods.

Climate models require an equation of state and a moisture equation for the atmosphere and ocean. The state equation for the atmosphere relates pressure, density, and temperature, and for the oceans, it relates pressure, temperature, density, and salinity (Warren, 2005). At the present time, climate models have reproduced adequately the observed features of recent climate and past climate changes. In that sense, AOGCMs present an important tool to estimate future climate change at continental and larger scales, with more confidence in temperature than precipitation (IPCC, 2007). The models are based on physical laws capable of simulating features of the current and past climate. Despite growing confidence in the GCMs ability to represent the physical phenomena of the climatic system, there remain important uncertainties in the simulated outputs. Currently, scale resolution (vertical and horizontal), aerosols, and cloud feedback are the main sources of uncertainties; the last one (clouds) is the most important due to the difficulty in representing them in GCMs.

GCMs provide weather data at global scale (e.g. grid resolution of 200x200 km) whose use in local applications is restricted due to their coarse spatial resolution. In that sense, for assessing climate change impacts at the basin scale, the GCM outputs, such as temperature and precipitation, need be downscaled to increases their resolution.

Moreover, models outputs for past and future climate differ among GCMs for the same region or basin due to the differences in mathematical algorithms, space-time

17

resolution, atmospheric physics representation, etc., used in each global model. In 2007, the results of 23 coupled AOGCMs with multiples realizations forced by various 21$^{st}$ century emission scenarios were reported by the Intergovernmental Panel on Climate Change (IPCC) in their fourth assessment report (AR4, 2007) indicating the advances and improvements in the modeling and their performance to reproduce the features of the global climate system. Since then, vertical and horizontal resolution has been improved in many models and more climate processes, such as aerosols, sea ice, and land surface, have been incorporated (Taylor et el. 2009).

## 2.3 EVALUATION OF CLIMATE MODELS

For researchers, it is not an easy task to assess the ability of GCMs in predicting past and future climate since each model uses a different spatial resolution, numerical technique, atmospheric physics representation, parameterization of local climate processes, etc. Probably, these are the main reasons why GCMs predict different results for the same region. Some studies have been carried out to evaluate the performance of GCMs at global and regional scales to reproduce temperature and precipitation. For instance, Karl (2002) reported an evaluation of temperature and precipitation from 17 GCMs across North America carried out by the IPCC and the Lawrence Livermore National Laboratory in 2001, with more emphasis placed on the Canadian climate model (CCC) and the Hadley Center Model (HadCM). Results showed that there is agreement with the observed long-term temperature over the 20$^{th}$ century. However, the CCC model is more

18

sensitive to greenhouse gases than other models. Likewise, HadCM model simulations represented precipitation better than the CCC model.

Likewise, Ruiz-Barradas et al. (2006), in a study of North American climate variability, evaluated four U.S models, CCSM3 and PCM from the National Center for Atmospheric Research (NCAR), GFDL-CM2.1 from the Geophysical Fluid Dynamic Laboratory, and GISS-EH from the NASA Goddard Institute for Space Studies, a British model from the Hadley Centre Coupled Ocean-Atmospheric (UKMO-HadCM3), and a Japanese model from the Center for Climate System Research at University of Tokyo (MIROC3.2). Comparisons were made with the NCEP's North American Regional Reanalysis, and the U.S and Mexico precipitation datasets. In general, they concluded that UKMO-HadCM3 model is closest to the observations than the other models, but it was not over all of the southeastern United States.

## 2.4 DOWNSCALING CLIMATE DATA FROM GCMs

Global Circulation Models (GCMs) provide weather data at global scale and low resolution (currently about 200 km x 200 km) which are unable to resolve subgrids at higher resolution, say 12 km x 12 km (Fowler et al., 2007). Climatic variables used directly from GCMs are restricted due to their coarse spatial and temporal resolution. To assess the impact of climatologic variables such as temperature and precipitation on water resources at the basin scale, GCM outputs need to be resolved (downscaled) to the higher resolution for use in hydrologic models.

Downscaling can be defined as a technique that increases the resolution of GCMs to obtain local-scale weather. There are two fundamental methods to downscale large-scale data from GCM outputs: Statistical and dynamic downscaling, whose concepts have been discussed in several papers (e.g., Wilby and Wigley, 1997; Chong-Yu, 1999; Wilby et al., 2004; and Fowler et al., 2007). This section presents a basic description of these techniques used to downscale climate data from GCMs; as well as advantages and disadvantages in their application, and some studies are discussed.

## 2.4.1 Statistical Downscaling

Statistical downscaling (SDS) is based on statistical relationships between the large-scale climate variables generated by GCMs, such as temperature and precipitation, and local-scale meteorological variables. Statistical methodologies have the advantage of using less computational resources and generating a large number of realizations for climate change studies; however, physical phenomena of the climate system are not represented in the process. Statistical downscaling can be classified into three main groups (Wilby and Wigley 1997):  (1) regression models; (2) a weather pattern based approach; and (3) stochastic weather generators. Multiple linear regression or nonlinear, artificial neural network relationships between local-scale parameters and low-resolution predictor variables (GCM data) are frequently used in the *regression methods*. On Downscaling based on the *weather pattern* approach uses the probability distribution of weather patterns and involves statistically relating meteorological data (observed station) to a determined weather classification scheme (Wilby and Wigley, 1997). S*tochastic*

*weather generators* produce large synthetic time series of weather data (for instance Markov models of precipitation) for a location based on the statistics of historical variables.

For water resources impacts, many statistical techniques have been developed and applied to translate large-scale GCM outputs to higher resolution. This proposal does not review all the papers on this issue; however, some of the more important recent ones are discussed, taking into account technical developments and performance. The *delta change* or *perturbation factors method* is a common technique widely used to downscale CGM outputs (e.g. Hay et al., 2000; Diaz-Nieto and Wilby, 2005; Minville et al., 2008). This approach consists of finding the differences between GCMs simulations of future and recent (past century) climate and then, adding these changes to the historical (observed) climate time series. This method assumes that GCMs are more reliable in simulating relative changes than absolute values, adopting a constant bias through time (Fowler et al., 2007; Xu et al., 2005). Additionally, the method ignores changes in the range and variability of variable; assuming the spatial pattern of the current climate does not change in the future (Diaz-Nieto and Wilby, 2005).

More sophisticated statistical downscaling techniques have been developed and applied, including linear and nonlinear regression methods. For example, Wilby et al. (2000) used linear least-squares regression to estimate the parameters (three predictor variables were used, mean sea level pressure, surface specific humidity, and 500 hPa geopotential) to downscale daily precipitation and temperature in the Animas River basin,

Colorado. The approach allows carrying out any number of simulations and the performance of the method was better in spring and autumn but worse during winter and summer.

More recent studies have applied multiple regression models (Hertig and Jacobeit, 2007; Chu et al., 2009) and conical correlation analysis (Hertig and Jacobeit, 2007) for downscaling precipitation and temperature, respectively. Both methods were used to determine predictor-predictand relationships for different periods of calibration, indicating the importance of selecting the best predictor combination to get good performance of statistical downscaling models. Local weather and spatial terrain conditions can limit the performance of these models, despite the fact that they can simulate trends of changes and mean values (Chu et al., 2009).

Weather typing is another technique that has been applied to downscale data from GCMs (Conway and Jones 1998; Brinkmann 2000). Weather generator (WG) techniques have been applied to generate precipitation, temperature, and other variables for climate change studies. The WG method, used by many researchers, was developed by Richardson (1981). It is a stochastic technique to generate daily precipitation, temperature, and solar radiation. For instance, the more recent studies of Elshamy et al. (2006) and Kim et al. (2006) used a first-order Markov chain model to predict precipitation from which other weather variables are generated. Likewise, Minville et al. (2008) used a third-order Markov chain (Richardson type weather generator) to produce time series of daily precipitation. The advantage of this method lies in fact that it can

generate any number of time series with the same statistical properties as the historical series (Minville et al., 2008). However, the most important drawback to WGs is that cannot be applied immediately in other climates due to the fact that they are conditioned on local climate relationships (Fowler et el., 2007).

As noted above, there are several statistical downscaling techniques that could be applied to the case study (Rio Conchos basin); however the use of more complicated methods may underestimate the trend of changes in climate variables causing more uncertainty in the streamflows predictions. Despite this, it is of urgent necessity to downscale climate data since GCM outputs are for climate change applications at global, not regional, scale.

Hence, in order to reproduce more realistic simulations for assessing hydrology impacts, the basic requirement of any downscaling method is that historic trends of climate must be reproducible (Good et al., 2004). Additionally, it is important to note that hydrological models do not show good performance when climate data is used directly from GCMs (Fowler et al., 2007). Wood et al. (2004) used three simple statistical methods to downscale outputs of climate simulations from the NCAR-DOE Parallel Climate Model (PCM) and Regional Model (RCM) for hydrological simulations: (1) linear interpolation; (2) spatial disaggregation without bias correction; and (3) bias correction followed by spatial disaggregation. The most interesting thing in this study was that bias correction with spatial disaggregation reproduced well the main features of observed data for both kinds of climate models. Linear interpolation and spatial

23

disaggregation produced similar and better results for RCM than PCM. However with both methods, significant biased hydrologic simulations are noted, indicating that for both climate model outputs the downscaling results did not show any improvement without a bias correction step.

The Lawrence Livermore National Laboratory, US Bureau of Reclamation, and Santa Clara University used a similar approach to that described by Wood et al. (2002), Wood et al. (2004), and Maurer (2007) to downscale climate projections from the World Climate Research Programme's (WCRP's) Coupled Model Intercomparison Project (CMIP3) multimodel dataset for the US and northern Mexico, which are stored and served at the LLNL Green Data Oasis (http://gdo-dcp.ucllnl.org/downscaled_cmip3_projections/). In essence, the methodology has two important steps: bias-correction and spatial downscaling. The first step consists of detecting if the GCM past climate simulations relative to historic observations tend to be too cool, wet, or dry. After that, quantile mapping techniques are used to remove those identified trends from future GCM projections. The second one translates the adjusted GCM output (as a bias correction on a $2^o$ spatial grid) to a basin-scale high resolution ($1/8°$ grid, i.e., approximately 12km square). The procedure consists in finding factor values at each $2°$ grid point in the domain (relation: Adjusted GCM / observational data); and after that applies an inverse-distance-squared interpolation from $2°$ factor values to $1/8°$ resolution.

**2.4.2 Dynamical Downscaling**

This technique refers to fine spatial-scale atmospheric models which use complex algorithms to describe atmospheric process embed within GCM outputs. The goal of this procedure is to extract local–scale weather data from large-scale GCM data developing and using Limited Area Models (LAMs) or Regional Climate Models (RCMs) in which coarse GCM data are used as boundary conditions (Wilby and Wigley, 1997; Xu, 1999). Applications of this technique include the increase of spatial and temporal resolution as well as parameterizations of some physical climate processes. Regional climate characteristics, such as extreme events, orographic precipitation, anomalies, and non-linear effects, can be truly simulated by this method (Fowler et al., 2007). On the other hand, many assessments have shown the skill of RCMs to downscale and simulate regional scale climate variables, and important differences have been found with GCM projections (influence of orographic conditions, land coverage, etc).

For hydrological impacts at regional scale, many studies have illustrated the application and performance of this technique (e.g., Wood et al. 2004; Fowler and Kilsby 2007; Akhtar et al. 2008). Fowler and Kilsby (2007), in a study carried out to assess climate change impacts of future river flows in northwest England, concluded that an RCM may be used directly as input for hydrological models; however, it is necessary to apply a bias-correction procedure on a monthly basis before using the RCMs outputs. A similar conclusion was reached by Wood et al., (2004) using a quantile-mapping, bias-correction scheme to correct RCMs outputs. In contrast, Akhtar et al., (2008) using

PRECIS RCM 9 (developed by the Hadley Centre) at a spatial resolution of 25 x 25 km$^2$, to simulate present (1961-1990) and future (2071-2100) climate scenarios and evaluate impacts of climate change in the Karakorum–Himalaya river basins, found the direct use of RCM climate data in the hydrologic model performed well, with monthly and annual streamflow trends acceptable for the end of the 20$^{th}$ century.

As pointed out before, this technique allows improvement of the course resolution GCM outputs for their later use in assessing water resources impacts. One of the main advantages of this is the RCM's ability to respond consistently to external forces since climate process at regional and local scale can be physically represented. Moreover, with RCMs it is possible to represent most vertical levels of the atmosphere to assess local climate change impacts (Fowler and Kilsby, 2007). However, uncertainty associated with parameterization of local and regional climate processes, model initialization, and boundary conditions can affect performance. Additionally, it is possible to say that dynamic downscaling followed by bias-correction is necessary to improve the performance of hydrological models.

### 2.4.3 Comparisons between Both Techniques

Few studies have addressed the assessment and comparison of the abilities of statistical and dynamical downscaling for hydrologic and water resources impacts. Wilby et al. (2000) assessed the performance of both techniques on the hydrologic response of the Animas River basin in southwest Colorado. Multiple regression methods were used to downscale precipitation and temperature. In general, SDS provided better results than the

Regional Climate Model (RCM) method for predicting daily streamflows. But both techniques showed better performance than the course resolution data, indicating that an elevation bias correction improved the raw RCM results.

Similarly, Hay and Clark (2003) used statistically and dynamically downscaled GCM model output to evaluate the performance of a hydrologic model in three snowmelt basins in the western United States (Animas river in Colorado, East Carson river in Nevada, and Cle Elum river in Washington). Their main conclusions indicated that the estimation of daily streamflows improved notably after the application of a bias correction to RCM method outputs. In that sense, dynamically downscaling RCM outputs can be useful for hydrological modeling (at the basin scale) after bias correction is carried out. In addition, this study indicates that SDS simulations were better than those obtained by the RCM method.

Other studies include Wood et al. (2004), Christensen et al.(2004), and Payne et al. (2004) who evaluated the climate change impacts on water resources in the western United States. The most interesting finding, also reported by Fowler (2007), is from Wood et al. (2004) who assessed the performance of statistical and dynamic downscaling techniques on the hydrology in the Columbia River basin which was discussed in previous sections. They concluded that dynamic downscaling does not lead to large improvements in hydrologic simulations relative to the direct use of GCM outputs. Most SDS methods assume that atmospheric processes are linear in contrast with the real, nonlinear climate system. Moreover, "the statistical relationships developed for the

27

present day climate also hold under the different forcing conditions of possible future climates" (Wilby et al., 2004). Nonetheless, most studies showed that SDS is a viable technique able to reproduce historical climate conditions for use in hydrology impact assessments. The advantages and weaknesses of RCMs are discussed in the next section.

**2.4.4 Advantages and Disadvantages**

Both statistical and dynamic downscaling are able to translate the course resolution of CGMs to a fine spatial resolution. Some advantages and disadvantages in the application of both techniques are discussed which were adapted from Wilby and Wigley (1997), and Fowler et al. (2007).

- Statistical downscaling (SDS) needs few computational resources; therefore it is less costly. In addition to this, SDS can generate a large number of statistically similar realizations, which are useful in assessing uncertainties; which allows selecting properly a climate dataset for water resources studies at the basin scale. In contrast, dynamic downscaling (DDS) provides a limited number of realizations, and it is a complex method that requires intensive computational resources.

- DDS produces scenarios based on physical processes of the climate system. In contrast, most SDS methods assume that the local climate variables are a simple function of atmospheric circulation. However, in DDS, all vertical levels of the atmosphere are considered to impact the local climate (Fowler, 2007).

- SDS can compute climatic variables at point-scale from CGM outputs. In the same way, DDS produces finer resolution data from GCM outputs and is capable of resolving small-scale atmospheric processes. However, both techniques require a large amount of historical data for calibration.

- Other advantages of SDS are related to the ability to incorporate observation into the downscaling based on historical patterns and accepted statistical techniques.

- DDS is strongly dependent on GCM boundary forcing such as lateral and bottom boundary conditions, and initial conditions. SDS is also dependent on GCM boundary forcing affected by biases in the underlying GCM.

- Other disadvantages of SDS have to do with the choice of predictors and non-stationarities in the predictor-predictand relationship. In addition, feedbacks in the climate system cannot be included in SDS.

- Most studies have shown that after the application of DDS, a statistical bias correction is need for assessing hydrological and water resources impacts. In addition, DDS is infeasible for application to long time periods.

## 2.5 UNCERTAINTY OF CLIMATE CHANGE AT THE BASIN LEVEL

In assessing climate change impacts on water resources, uncertainties are propagated through a modeling chain, since this process requires the development and application of climate, hydrology, and water resources models in order to evaluate impacts at the local (basin) scale. In addition to this, GCMs provide climate data at low resolution; therefore, it needs be downscaled, introducing another source of uncertainty.

Basically, uncertainty in climate modeling includes spatial and temporal resolution, predictions of anthropogenic climate change, parameterizations of some climate processes, and initial and boundary conditions of the models. On the other hand, hydrologic modeling is usually used for applications of flood forecasting and water management under climate change conditions. The typical approach used for this is the split sampling strategy (Wood et al. 2004), with a set of observations used for calibration, and another set for validation. Here, the problem lies in the assumption that the parameters estimated with historical data are invariant when simulating climate change scenarios. However, errors in computations as a result of this are expected be less than those resulting from the GCMs and downscaling procedure (Wood et al. 2004).

In water resources models, uncertainty is often related to system operation, which is based on historical inflows and demands to get an optimal system performance. Likewise, the projected future trends in demands for the water system are another source of uncertainty.

Few studies have addressed the uncertainties of climate change effects on water resources. For instance, recent papers include to Maurer and Duffy (2005), Maurer (2007), and Minville et al. (2007) who used probability distribution functions (PDFs) of climate change variables to assess uncertainties on hydrology in basins in the Sierra Nevada, US and Quebec, Canada, respectively.

**2.6 SUMMARY**

One of the more relevant problems in our study basin is frequent and extensive drought periods. Natural conditions and variability, climate change, human activities (deforestation in the upper basin) and other factors influence the current hydrologic pattern in the basin. In the last 70 years, extreme droughts have occurred, e.g., 1940 to 1965 and 1992 to 2002. Since the Rio Conchos is the main tributary of the bi-national Rio Grande/Bravo, this hydrologic behavior of the basin has contributed to difficulties in implementing the 1944 water treaty; causing serious conflicts for the water resources among both countries. This situation requires studying potential effects of climate change on the basin in the coming decades and how it could increase even more the competition for water resources.

On the other hand, many studies have been performed to assess climate change impacts on hydrology and water resources, but few of them have evaluated the impacts on water availability and possible management strategies to face this important problem. Few studies have addressed the analysis of climatic variability impacts on transboundary river basins, especially using integrated water resources models that include hydrology and water planning together. This research integrates a hydrological model into a water management model to simulate some adaptive strategies under a changing climate.

In the complex process of assessing climate change impacts on water resources, several models need be developed and applied. This is a modeling chain that includes general circulation models (GCMs), hydrologic models, and water planning models.

31

Statistical and dynamical downscaling was discussed. The literature review indicates that both techniques can translate the coarse resolution of GCM outputs. SDS requires low computational resources, generates multiple realizations, and is less expensive. In contrast, DDS (with Regional Climate Models) provides a limited number of realizations, and is a complex method that requires intensive computational tasks. One of advantages of DDS is that it can simulate the physical processes of the local climate system; however, "a bias-correction is necessary to correct both the absolute magnitude of precipitation amount and the seasonality to observations, and therefore produce realistic runoff series when input to a hydrologic model" (Hay et al. 2002; Wood et al. 2004; Fowler and Kilsby 2007).

Uncertainty in the climate models, the downscaling procedure, hydrologic models, and water planning models need to be taken into account to assess climate change effects on water availability. Under the optical that is a very complex process, a combination of quantitative and probabilistic analysis is necessary to evaluate such impacts. This investigation considers this kind of analysis to assess potential climate in the Rio Conchos Basin. Given the importance of the Rio Conchos Basin as a major tributary of the Rio Grande and one containing one of Mexico's largest irrigation areas, hydrologic modeling of the Rio Conchos basin needs further studies in order to develop tools that allow water planners to make decisions in the context of water management and climate change.

## 2.7 CONTRIBUTIONS OF THE RESEARCH

As with other studies, this investigation will help to develop the current state of the art of a complex process, evaluating climate change impacts on hydrology and water availability. Given the importance of the Rio Conchos Basin as a major tributary of the Rio Grande and one containing one of Mexico's largest irrigation areas, as well as the frequency of long drought periods, future climate change needs to be studied. This study is the first investigation integrating hydrologic and water management modeling to evaluate climate change in the Rio Conchos basin. Empirical equations were used to calibrate the hydrologic model, which could be very useful to build hydrologic models for water management studies. A multi-model ensemble from five general circulation models was developed using the root mean square error weighting approach. Moreover, several techniques were used to assess impacts, such as cumulative distribution functions, trend analysis, and wavelet. Wavelet analysis was used to examine the connections with long and short-term climate patterns. Another research contribution is the development and evaluation of some adaptive water management alternatives to mitigate potential climate change.

# Chapter 3: Methodology

In this section, methods and procedures are described to achieve the objectives proposed in this investigation. The methodology includes (1) the development of a hydrologic model, which addresses the model calibration and validation; (2) analyzing multiple, downscaled General Circulation Model (GCM) outputs under two emission scenarios, A2 and A1B; (3) simulating the response of the basin hydrologic system to the resulting climate change; (4) deriving skill-weighted multi-model ensemble outputs describing the basin response to climate change; (5) assessing climate change impacts on hydrology in the basin; and (6) assessing climate impacts on water availability and the simulation of adaptive strategies. Results are evaluated in two parts: first, impact on the hydrology using several techniques, and second, impact on water availability and its effect on the water uses and the 1944 water treaty in terms of reliability, resiliency, and vulnerability of the system to future climate change. Finally, adaptive measures are simulated in order to propose some alternatives to mitigate the climate change impacts on the water system. Figure 3-1 shows the general methodology used to achieve the proposed objectives.
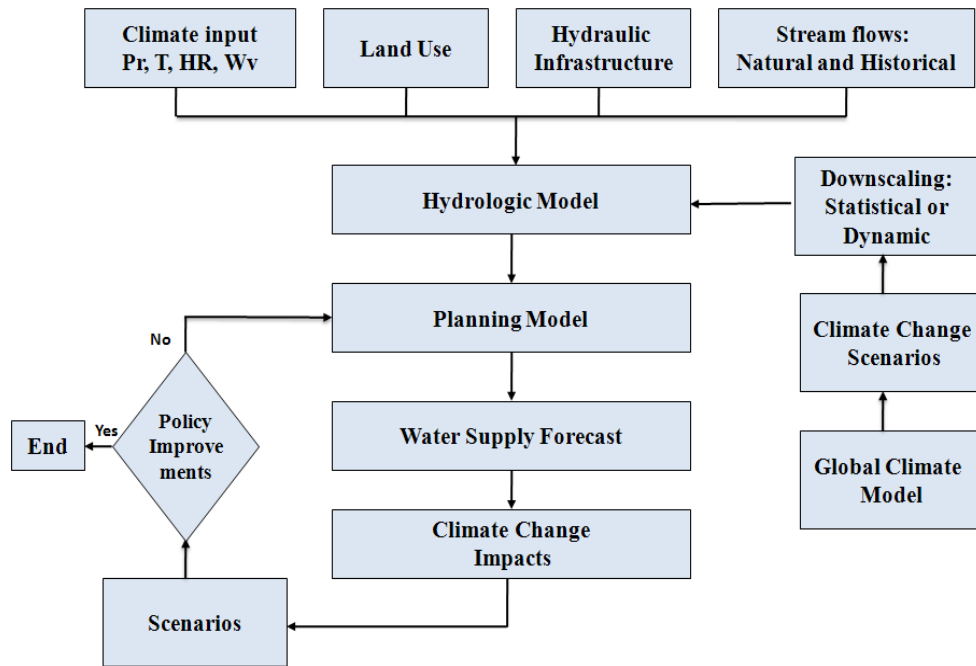
Figure 3-1: Methodological flow chart to assess climate change impacts on water resources

## 3.1 CLIMATE DATA

### 3.1.1 Precipitation

Twenty years (1980-1999) daily time series of precipitation from the Mexican Institute of Water Technology (Gomez-Martinez et al. 2005) were used from climate stations in each sub catchment. To feed the hydrologic model, cumulative monthly was computed. Monthly maximum values ranges from 80 mm to 190 mm and the minimum values from 1.3 mm to 11 mm on average. The seasonal variation indicates a wet period located from June to September and a marked dry period from October to May (Figure 3.2). An annual average around 445 mm/year was computed for the basin during this time period. Precipitation variation is depicted by the altitude, with higher values for Llanitos

sub catchment, 740 mm/year on average, located in the upper basin. The lowest values were recorded in the Luis Leon and Peguis sub catchments, lower basin, with annual averages of about 325 mm. In the middle basin, annual precipitation varies from 350 to 400 mm. Figure 3.2 shows the monthly average precipitation for each catchment in the Rio Conchos basin.
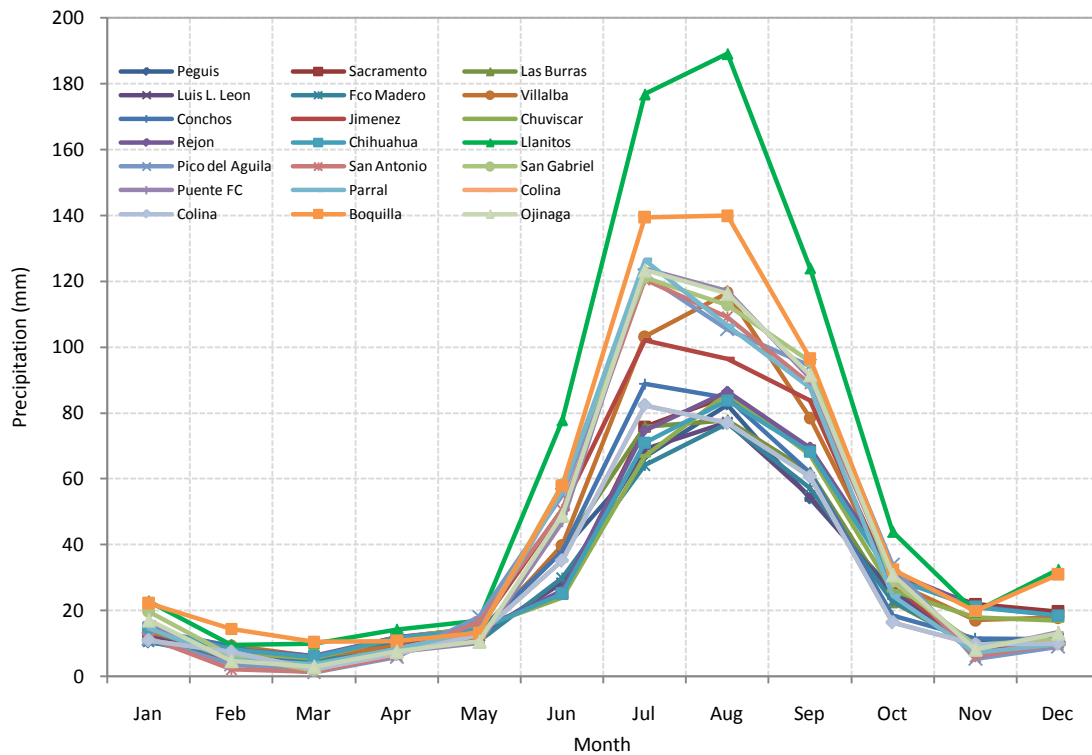


Figure 3-2: Monthly average precipitation in the Rio Conchos basin, 1999-2000

### 3.1.2 Temperature

There is not enough data on air surface temperature for the study area. Monthly surface temperature in degree Celsius from the North American Regional Reanalysis

36

(NARR, http://nomads.ncdc.noaa.gov/thredds/catalog/narr/) for the period 1980 – 1999 was used. Data are downloaded in NetCDF format and processed using GIS tools. Maximum temperatures occur from June to August and minimum from November to February (Figure 3-3, monthly average of 20 years). For the first period (June-August), the spatial variation indicates that high values occur in the lower basin (desert region), with values around 32 $^{o}$C for the Ojinaga and Peguis sub basins, and 21 $^{o}$C for the Llanitos and Puente FFCC sub basins.  For the second period (November to February), the temperature varies from 7 – 11 $^{o}$C and 12 - 16 $^{o}$C for the lower and upper basin, respectively.

Under historical conditions, temperature and precipitation showed a negative correlation during the period of analysis. This means that when temperature tends to rise, rainfall tends to decrease. It shows interesting evidence about climate change impacts on the basin during the last 20 years (Figure 3-4); whose annual analysis indicates that the temperature is increased by one degree Celsius and the precipitation was reduced by 5% in average.
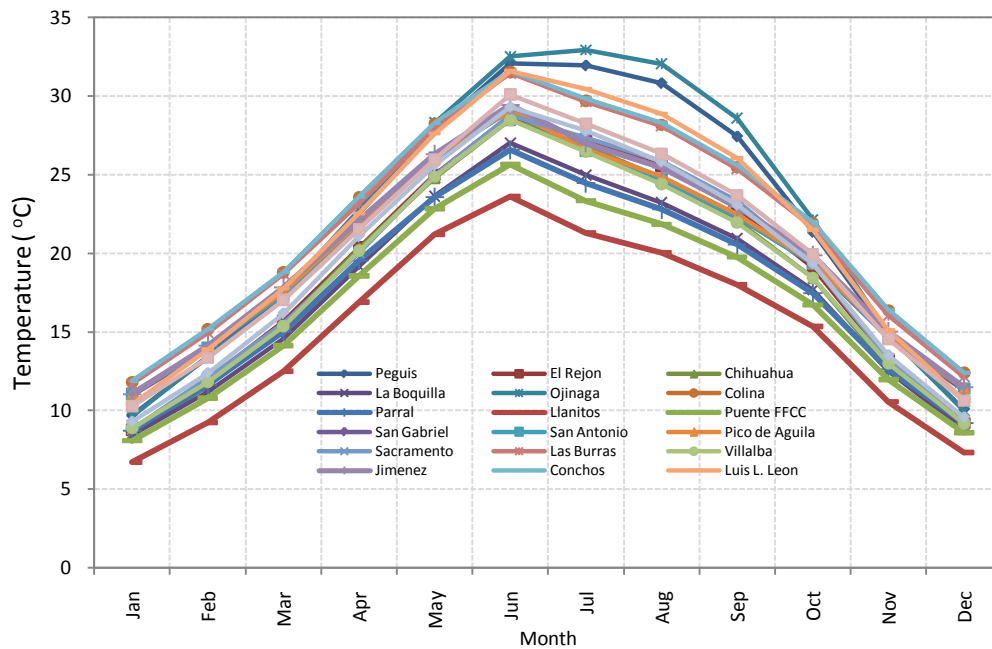
Figure 3-3:  Monthly average temperature in the Rio Conchos basin, 1999-2000
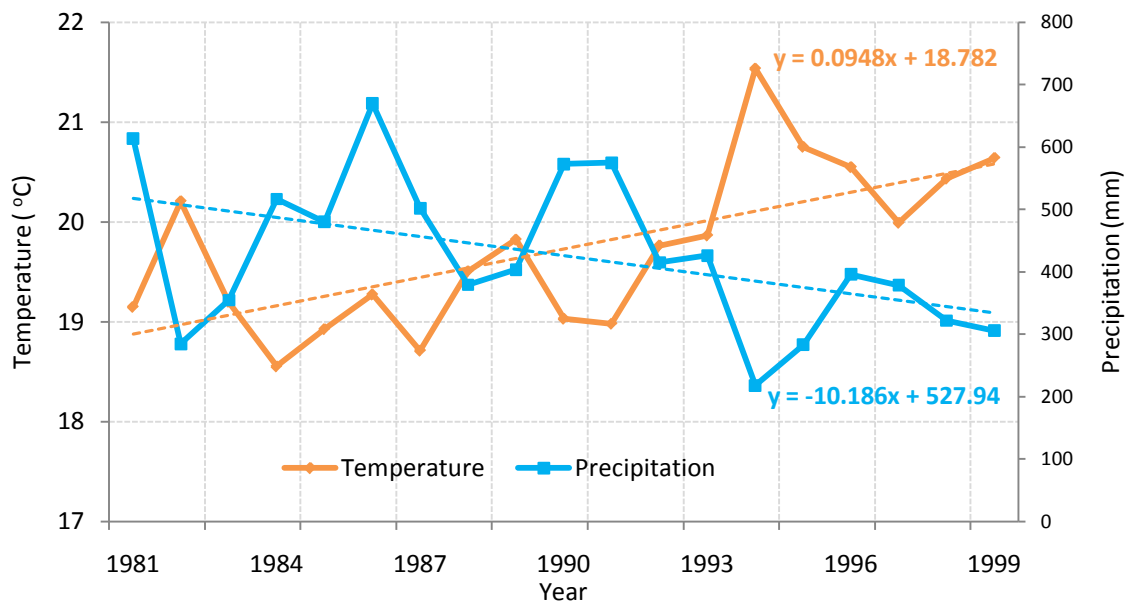


Figure 3-4:  Annual variations of temperature and precipitation

### 3.1.3 Relative Humidity

This parameter is also obtained from the NARR. A Spatial Analyst tool in GIS is used to compute the average monthly relative humidity for each sub catchment. Spatial variation indicates that lowest values of relative humidity occur in Fco Leon, Pegui, and Ojinaga catchments located in the lower basin, and the highest values occur in the upper basin. The average for the whole basin is around 42% and the temporal variation indicates that maximum values occur from July to September. On the other hand, the minimum values of relative humidity are observed from March to June.

### 3.1.4 Wind Velocity

Wind velocity is downloaded from the NARR. Velocity vectors for East-West (U) and North-South (V) are processed to get the wind velocity magnitude. In the Rio Conchos basin, the dominant winds come from Southwest to Northeast. Two components of velocity were obtained from the NARR for different sub catchments of the basin. Velocity vectors for East-West (U) and North-South (V) were processed in to get the wind velocity. The wind speed during the year indicates a seasonal variation with high values from November to April, with an average of 12 km/h for the whole basin. In general, in the upper basin (La Boquilla, Llanitos, Parral sub basins) the wind speed is greater than in the lower basin (Luis Leon, Peguis, Ojinaga sub basins), with 18 km/h and 6 km/h, respectively. On the other hand, the minimum wind speed is observed from May to October (6.1 km/h average), period in which the maximum temperature occurs.

### 3.1.5 Latitude

The latitude in degrees is entered for the centroid of each sub-catchment in order to estimate solar radiation and computing the Penman-Monteith reference crop potential evapotranspiration (PET).

### 3.1.6 Melting Point, Freezing Point, and Initial Snow

At the study area, snow is not important; therefore, these parameters are not modeled. However, it should be noted that the Melting Point is the threshold for snow melt and the freezing point is the threshold for snow accumulation in degrees Celsius. For the Rio Conchos basin, the threshold for snow melt was set as +5 degrees Celsius and the threshold for snow accumulation as -5 degrees Celsius. The Initial Snow is the snow accumulation at the beginning of the simulation and it was set in to an initial value of zero for all catchments.

### 3.2 LAND USE

The twenty sub-basins (see Figure 3-5) were sub-divided again by soil groups and land use categories (Amato *et al.*, 2006). The land use and soil coverage data from IMTA (Gomez-Martinez et al. 2005) are applied for the Soil Moisture Method in the WEAP model. LAI values estimated by Scurlock et al., 2001 are shown in Table 3-1. Table 3-1a shows a summary about the land use area for each category (Amato *et al.*, 2006) as well the crop coefficient and Leaf Area Index (LAI). Soils characteristics for this method are described in later sections.

40

Table 3-1: LAI Values Scurlock et al., 2001 (cited by Amato et al., 2006).

| Biome | Original Data | | | Data after IQR analysis | | |
|---|---|---|---|---|---|---|
| | Number of observations | Mean | Standard Deviation | Number of outliers removed | Mean | Standard deviation |
| All | 931 | 5.23 | 4.08 | 53 | 4.51 | 2.52 |
| Forest/BoDBL | 58 | 2.64 | 1.03 | 5 | 2.58 | 0.73 |
| Forest/BoENL | 94 | 3.50 | 3.34 | 8 | 2.65 | 1.31 |
| Crops | 88 | 4.22 | 3.29 | 5 | 3.62 | 2.06 |
| Desert | 6 | 1.31 | 0.85 | 0 | 1.31 | 0.85 |
| Grassland | 28 | 2.50 | 2.98 | 3 | 1.71 | 1.19 |
| Plantation | 77 | 8.72 | 4.32 | 0 | 8.72 | 4.32 |
| Shrub | 5 | 2.08 | 1.58 | 0 | 2.08 | 1.58 |
| Forest/BoTeDNL | 17 | 3.63 | 2.37 | 0 | 4.63 | 2.37 |
| Forest/TeDBL | 187 | 5.12 | 1.84 | 3 | 5.06 | 1.6 |
| Forest/TeEBL | 58 | 5.82 | 2.57 | 1 | 5.7 | 2.43 |
| Forest/TeENL | 215 | 6.70 | 5.95 | 16 | 5.47 | 3.37 |
| Forest/TrDBL | 18 | 3.92 | 2.53 | 0 | 3.92 | 2.53 |
| Forest/TrEBL | 61 | 4.90 | 1.95 | 1 | 4.78 | 1.7 |
| Tundra | 13 | 2.69 | 2.39 | 2 | 1.88 | 1.47 |
| Wetlands | 6 | 6.34 | 2.29 | 0 | 6.34 | 2.29 |

IQR = Inter-Quartile Range

Table 3-1a: Land use category used in the hydrologic model

| Land use code | Land use category | Area $(km^2)$ | % total area | Crop Coefficient Kc | Leaf Area Index LAI |
|---|---|---|---|---|---|
| 10 | Forest | 7268.78 | 10.72 | 0.35 | 5.18 |
| 20 | Forrest Grasses | 6455.13 | 9.52 | 0.38 | 3.07 |
| 30 | Water Bodies | 121.44 | 0.18 | 1.00 | 0.10 |
| 40 | Irrigated Areas | 1218.99 | 1.80 | 0.88 | 4.22 |
| 50 | Naturally Irrigated Areas | 5900.10 | 8.70 | 0.96 | 4.22 |
| 60 | Small Pasture Grasses | 10654.90 | 15.71 | 0.53 | 2.50 |
| 70 | High Grasses and Small | 12266.76 | 18.09 | 0.34 | 2.08 |
| 75 | Other Vegetation | 1295.87 | 1.91 | 0.45 | 2.08 |
| 80 | Grazing Pastures | 22023.66 | 32.48 | 0.46 | 5.00 |
| 85 | Urban Areas | 283.83 | 0.42 | 0.77 | 8.00 |
| 90 | Wetland Vegetation | 206.91 | 0.31 | 0.90 | 6.34 |
| 95 | Without Apparent Vegetation | 111.81 | 0.16 | 0.30 | 1.31 |

## 3.3 STREAMFLOWS

Naturalized streamflow data from six stations located along to the basin (Table 3) is used to calibrate and validate the model performance. Naturalized flows were taken from the Texas Commission on Environmental Quality (Brandes, 2003). In addition, historic flows from (Gomez-Martinez *et al*. 2005) IMTA and the International Boundary Water Commission (IBWC, 2008) are used for the historical calibration in the water planning model. The geographic coordinates of the six stations are shown in Table 3-2, and Figure 3-5 shows the spatial location.

Table 3-2: Latitude and Longitude of hydrometric stations. Rio Conchos basin

| NAME | CRWR_ID | Longitude | Latitude |
|---|---|---|---|
| Rio San Pedro at Villalba | FM4000PCP400 | -105 46' 35.9" | 27 59' 4.45" |
| Rio Florido at Cd. Jimenez | FM5000PCP410 | -104 55' 4.4" | 27 8' 30.88" |
| Rio Conchos at Las Burras | FM3000PCP390 | -105 25' 15.9" | 28 32' 19.68" |
| Rio Conchos at El Granero | FM2000PCP380 | -105 16' 15.2" | 29 1' 2.69" |
| Rio Conchos at Presa La Boquilla | FM6000PCP420 | -105 24' 45.4" | 27 32' 44.23" |
| Rio Conchos at Ojinaga | FM1000PCP370 | -104 26' 25.8" | 29 34' 42.74" |
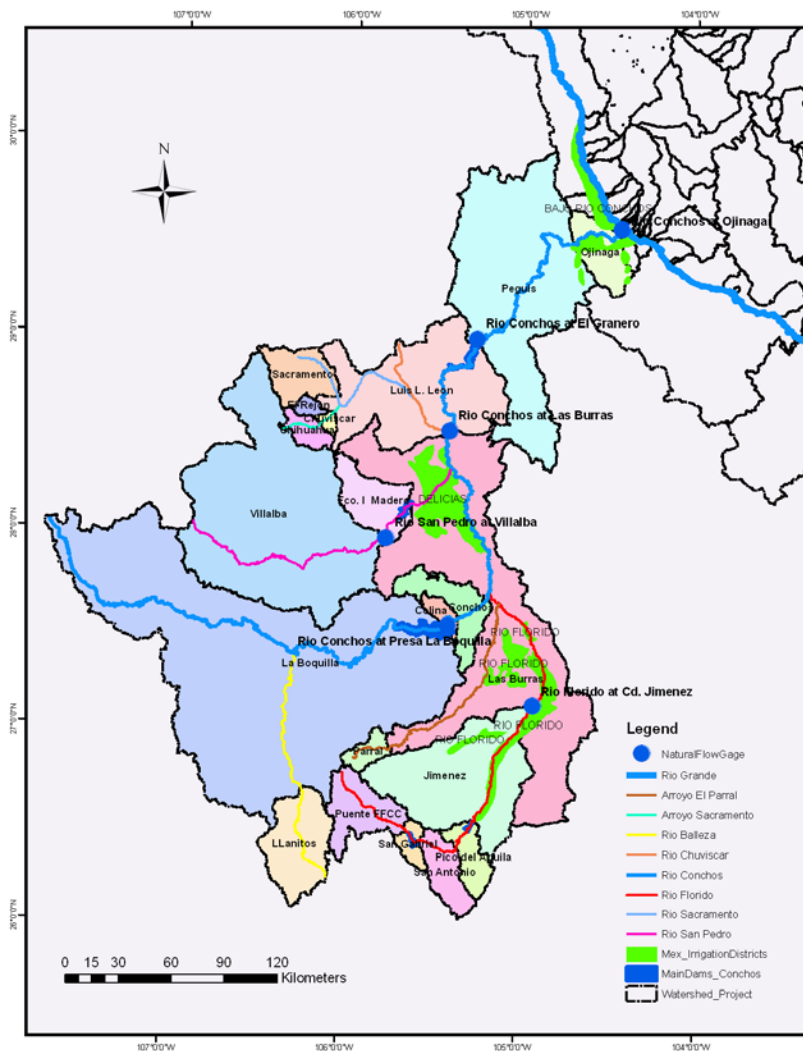


Figure 3-5:  Main Rivers, dams, control stations, catchments, and irrigation districts

**3.4 HYDRAULIC INFRASTRUCTURE**

For this study, basic hydraulic infrastructure in the basin includes the main rivers, tributaries, and reservoirs (Figure 3-5). Five main reservoirs are considered in the model to assess the impact of climate change on water resources in the basin. The main characteristics of the reservoirs are shown in Table 3-3.

Table 3-3: Main characteristics of reservoirs for the modeling (Danner, 2006)

| Feature | | La Boquilla | F. Madero | San Gabriel | Pico de Aguila | Luis L. Leon |
|---|---|---|---|---|---|---|
| Physical | Storage Capacity ($Mm^3$) | 3336 | 565 | 389.6 | 86.8 | 877 |
| | Initial Storage($Mm^3$)[*] | 2334 | 348.9 | 146.9 | 22.8 | 352.5 |
| | Elevation Max. (m) | 1325 | 1245 | 1785 | 1625 | 1050 |
| Operation | Top Conservation ($Mm^3$) | 2903.3 | 348 | 255.43 | 50 | 650 |
| | Top of Buffer ($Mm^3$) | 129.7 | 5.3 | 250 | 4.41 | 450 |
| | Top of Inactive ($Mm^3$) | 129.7 | 5.3 | 7.5 | 4.41 | 42.5 |

* Initial Storage values for 1980

**3.5 WATER SUPPLY AND DEMANDS**

Water supply and demands for agricultural, municipal, and other uses will be used in the model. Demands for the irrigations districts 103 Rio Florido, 005 Las Delicias, 090 Bajo Rio Conchos are considered in the model. Annual water demands as well as the historical monthly variation of demand for 20 years (1980-1999) are considered for historical simulation. Table 3-4 shows the annual demands used in the Rio Conchos water system (CONAGUA 2004).

Table 3-4: Annual water demand at system level and main irrigation district

| Water System | | Main Irrigation Districts | |
|---|---|---|---|
| User | Demand (million m3) | User | Demand (million m3) |
| Groundwater | 1076.15 | ID_005 Delicias | 941.60 |
| Irrigation | 1532.20 | ID_090 Bajo Rio Conchos | 84.99 |
| Municipal | 41.97 | ID_103 Rio Florido | 105.09 |
| Water Treaty | 711.00 | IRR_Labores Viejas | 114.46 |
| Total | 3361.32 | Total | 1246.14 |

## 3.6 HYDROLOGICAL MODELING

A proper representation of the hydrological processes is fundamental to predict changes in the dynamic response of a hydrologic system. This system is composed by a set of interrelated components that includes mainly the precipitation, evapotranspiration, infiltration, base flow, groundwater, and runoff processes. Since the most simples until the most complex models can be used to represent the physical behavior of a hydrological system; however, those that uses mathematical equations are more reliably. Within the classification of deterministic models, distributed where the hydrological processes are evaluated at deferent points in a dimensional space and lumped models whose hydrologic system is spatially averaged with no dimensions (Chow et el. 1987) are essentially developed and applied in hydrology to predict runoff and other hydrologic processes. Furthermore, estimate change in runoff in space and time is the main concern for hydrologists and water resources planners. At basin level, many hydrologic models have been developed for runoff predictions and climate change impacts (e.g. Fleming and

Neary, 2004; Benaman et el. 2005; Barbaro and Zarriello, 2006; Chu and Steinman, 2009, Meselhe et el. 2009; Luizzo et el. 2010). However, few studies evaluate widely the impacts on water availability and possible management strategies to face increasing scarcity due to climate change. Additionally, most of them have used separate hydrological and water resources models; and integrated models have been neglected.

This section describes the methodology to represent the study basin using a physically-based model embedded in an integrated water resources planning model. The main objective in this part is to model and simulate the hydrologic behavior of the Rio Conchos basin (rainfall – runoff), a main Mexican tributary of the Binational Rio Grande/Bravo basin; for which, the soil moisture method of the Water Evaluation and Planning Model (WEAP) is used (Ingol and McKinney 2010). The model is spatially continuous with areas configured as a set of sub-catchments that cover an entire river basin under study, considering them to be a complete network of rivers, reservoirs, channels, aquifers, demand points, etc (Yates et el. 2009).

First, the model is calibrated for 10 years (1980-1989) of streamflow data at six control stations located along of the Rio Conchos basin, normal hydrologic conditions were presented in this time period and a monthly step was used in the simulation. A trail-error method is used to calibrate the model and some empirical equations were used to estimate the hydraulic conductivity. Soil parameters were adjusted for each sub catchment to reproduce the naturalized monthly and annual streamflows. Second, in order to assess the model using data different from the training set used in the calibration, a 10

years independent dataset was used to validate the model (1990-1999). The validation evaluates the ability of the model to predict streamflows in periods and areas outside the data used in the calibration (Benaman et el. 2005). Drought conditions have been found in the Conchos River during the validation. Moreover, a statistic analysis that includes mainly the Nash coefficient and index agreement is carried out to assess the model performance. Additionally, since that the model is used for climate change impacts, it is tasted for the long period 1980-1999 using probability distribution function and confidence levels for annual flows.

### 3.6.1 Model Description

The hydrologic model for the study basin was built using the Water Evaluation and Planning (WEAP) software, developed by the Stockholm Environment Institute (SEI). The model is spatially continuous (lumped model) represented by a set of catchments that covers the entire the river basin under study, considering them to be a complete network of rivers, reservoirs, channels, ground-surface water interaction, and demand points (Ingol and McKinney 2010). Furthermore, the model includes three methods to simulate the catchment processes (evapotranspiration, runoff, infiltration, and irrigation demands).  (1) the Rainfall Runoff; (2) Irrigation Demands only version of the FAO Crop Requirements Approach; and (3) the Soil Moisture Method (SEI, 2007).  The Soil Moisture method is used to model the hydrologic response of the study basin as a dynamic and integrated rainfall-runoff model that includes the main components of the hydrologic processes.

47

### 3.6.2 The Soil Moisture Method

The WEAP Soil Moisture Method is based on empirical functions that describe the behavior of evapotranspiration, surface runoff, interflow, baseflow, and deep percolation for a watershed (SEI 2007). The model considers the movement of water through two vertical soil layers. The first layer represents water retained near the surface, which is available to plant roots; the second layer is deeper and water from this layer can be transmitted as baseflow or groundwater recharge. The main parameters of this model include the water holding capacity for both layers as well as the water movement between them (SEI 2007). For each sub catchment, the model computes the water balance due to inflows, outflows, and storage change in each layer. Figure 3-6 shows the general scheme of main components of the soil moisture model:
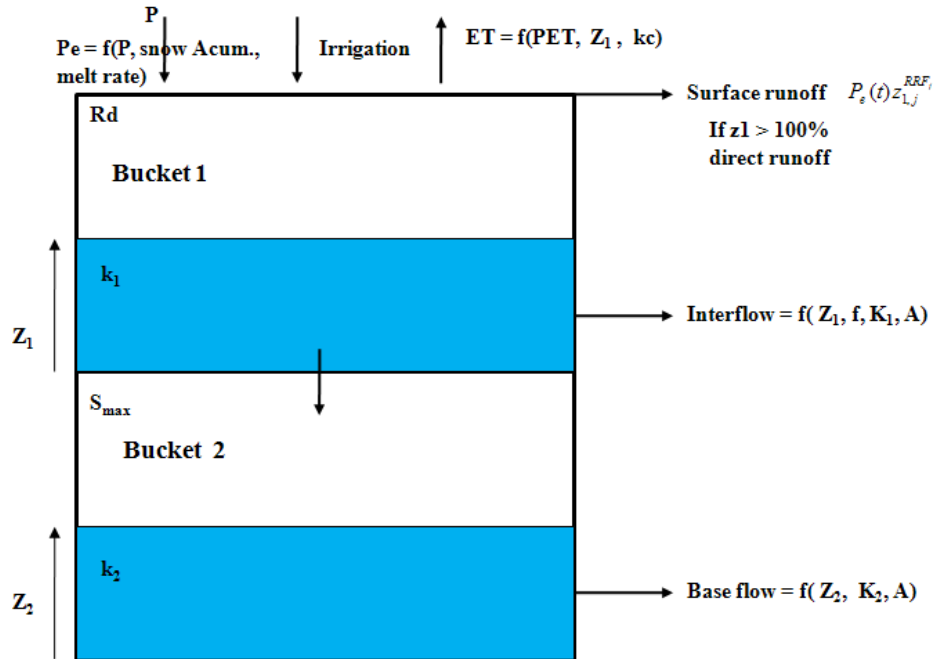


Figure 3-6: Two layers in the Soil Moisture Model in WEAP (SEI, 2007)

For a basin subdivided into a number of sub-basins with different fractional land use or soil type areas, the mathematical formulation to compute the storage change in the first layers is expressed in terms of a water balance as follow (SEI, 2007):

$$Rd_j \frac{dz_{1,j}}{dt} = P_e(t) - PET(t)k_{c,j}(t)(\frac{5z_{1,j} - 2z_{1,j}^2}{3}) - P_e(t)z_{1,j}^{LAI_j} - f_j k_{s,j} z_{1,j}^2 - (1 - f_j)k_{s,j} z_{1,j}^2 \quad \text{Equation 3-1}$$

Where $z_{1,j} \in [0,1]$ is the relative soil water storage, a fraction of the total effective water storage in the root zone layer in area $j$ [dimensionless]; $Rd_j$ is the soil water holding capacity of the area j (mm); $P_e$ is the effective precipitation (mm); PET(t) is the reference potential evapotranspiration (mm/day); $k_{c,j}$ is the crop coefficient for area $j$; LAI$_j$ the leaf and stem area index for area j which depend on the land cover; $P_e(t)z_{1,j}^{LAI_j}$ is the surface runoff; $f_j k_{s,j} z_{1,j}^2$ is the interflow from the first soil layer for area j; $f_j$ is the partition coefficient related to the land cover type, soil, and topography for area $j$, that divides flow into horizontal $f_j$ and vertical $(1 - f_j)$ flows, and $k_{s,j}$ is the saturated hydraulic conductivity of the root zone layer for area j [mm/time].

The change of storage in the second layer ($dz_2/dt$) is computed by:

$$S_{max} \frac{dz_2}{dt} = \left[ \sum_{j=1}^{N} (1 - f)k_{s,j} z_{1,j}^2 \right] - K_{s,2} z_2^2 \qquad \text{Equation 3-2}$$

Where $S_{max}$ is the deep percolation from the upper layer storage and $K_{s2}$ is the saturated hydraulic conductivity of the lower storage [mm/time].

### 3.6.3 Model Calibration

Calibrating the model involved both quantitative and qualitative evaluation of the hydrologic response of each sub-catchment. This was carried out using historical observed data, such as, precipitation, temperature, relative humidity, wind velocity, and soil parameters to produce streamflow output from each sub-catchment. A trial-and-error method and some empirical equations (Ingol and McKinney 2010) were used to calibrate the model to match, as closely as possible, the monthly and annual historical flows in the decade 1980-1989, a wet period in the basin was considered. The calibration parameters considered in each sub-catchment were the water storage capacity, hydraulic conductivity, initial storage and flow direction for each of the two model layers. The resulting values of the parameters are reported in the result section. A validation data set (1990-1999), a drought period in the basin, was used to assess the adequacy of the model. The main parameters of the soil method are described below.

### 3.6.3.1 Root Zone Water Capacity, rzwc

At the beginning of the simulation, the upper zone water cavity was estimated using values of 800-1000 mm for irrigated areas, small pastures grasses, and cultivated grassland, and 2000-2500 mm for forest areas (Canadell et al., 1996). Because of poor model performance with these values, adjustments were made taking into account the soil

50

depth which ranges from 200 mm to 500 mm for the study area (Pro Fauna, 2003). For the upper basin, the values ranged from 250 mm to 350 mm; and for the lower basin, from 400 mm to 600 mm. For instance, in the La Boquilla sub-catchment (upper and middle basin), colluvium Podzols soil is predominant, except in the Zaragosa valley where the soils are of alluvial origin and deeper. On the other hand, in Luis Leon, Peguis, and Ojinaga sub-catchments (lower basin), the soils are of alluvial origin and deeper, more than 50 cm on average. The final values of upper layer water capacity vary from 250-600 mm, with high values for catchments located in the lower basin (e.g. Ojinaga and Peguis) where the soils are deeper.

### 3.6.3.2 Initial Storage for the First Layer, $z_1$

$Z_1$ is the relative soil water storage given as a percentage of the total effective storage which is an approximation of the depth of the root zone (Yates et el, 2006). For each sub catchment, initial water storage value, $z_1$, at the beginning of the simulation was estimated taking account the land use coverage and soil type. Values ranged from 5 to 30% in some sub basins. Because of the desert condition in the lower basin, smaller values were used for catchments such as Luis L. Leon, Peguis, and Ojinaga in which no much water exists in the top layer.

### 3.6.3.3 Root Zone Hydraulic Conductivity, $k_1$

The water flow from the upper layer to the lower layer, as well as the interflow, is regulated by the upper zone hydraulic conductivity. The average interflow (*I*)

51

contribution was estimated from the difference between the 30% and 90% observed

exceedance flows for each station, allowing the estimation of the upper zone conductivity

using the following empirical equation (Ingol and McKinney 2010):

$$k_1 = \frac{I_t / A_i}{z_1^2 f_i}$$
Equation 3-3

where $A_i$ is the area of sub-catchment $i$, $z_1$ is the initial water capacity, and $f_i$ is the flow

direction coefficient that partitions flow into vertical and horizontal components (vertical

$= 0 \leq f \leq 1 =$ horizontal). Flow direction values from 0.05 to 0.20 were used for the upper

and middle sub-catchment as La Boquilla, Villaba, and Las Burras. The flow direction

was taken to be zero for the lower basin indicating vertical flow in those areas and the

upper zone conductivity was estimated as follow (Ingol and McKinney 2010):

$$K_{1,i} = \frac{V_i / A_i}{Z_1^2} * (1 - C_{r,i})$$
Equation 3-4

where $V_i$ is the average precipitation on sub-catchment $i$ over the period and $C_{r,i}$ is the

runoff coefficient which varies from 0.05 to 0.15 in the Rio Conchos Basin. Equations (3-

3) and (3-4) allow an estimation of an initial value of the upper zone conductivity given

an initial storage in the layer. These values were then adjusted in the calibration process.

### 3.6.3.4 Lower Zone Water Capacity, lzwc

Initial values for the lower water capacity ranged from 2000 mm to 3000 mm. These values resulted in high accumulated base flow in the calibration period; consequently, the hydrologic response of the basin was not represented accurately. This behavior was noted after the second year of simulation, with extraordinarily large base flow at the end of calibration period. Therefore, values higher than 12,000 mm were evaluated. High values of lower zone water capacity were estimated, indicating the existence of deep aquifers such those located in the middle and lower basin.

### 3.6.3.5 Initial Storage for the Second Layer, $z_2$

At the beginning of the simulation, lower zone initial storage values from 40% to 50% were used. However, this range resulted in high baseflow values in the river, with more than 50% on the average. Final calibrated values ranged from 5 to 20%, with lower values in the lower basin (Ingol-Blanco and McKinney, 2010).

### 3.6.3.6 Lower Zone Deep Conductivity, $k_2$

Deep hydraulic conductivity controls the transmission of base flow to the river from each sub catchment. Increased base flow in the river indicates high values of $k_2$, together with the existence of deep aquifers. The conductivity is estimated as

$$k_2 = \frac{(B_f / A_i)}{z_2^2} \quad for\ 0 < z \leq 1 \qquad \text{Equation 3-5}$$

where $A_i$ is the area of the land use cover fraction for sub-catchment $i$, $k_2$ is the lower layer hydraulic conductivity in mm/month, $z_2$ is the relative storage given as a percentage of the effective storage of the lower layer, and $B_f$ is the baseflow in the river. Many investigators have developed and applied several techniques to evaluate the contribution of the groundwater to the streamflow in the river. In this research, considering the limited available data in the basin, the straight-line method of baseflow separation (Chow et al. 1988) and the no exceedance probability were used to estimate the initial value of baseflow. The no-exceedance technique assumes that most baseflow is located within the range of 90-95% of no-exceedance probability. With the estimation of the baseflow, values obtained with equation (3-5) were adjusted to match better the calibrated and observed streamflows.

### 3.6.4 Statistical Analysis of Model Performance

The model performance is assessed using several statistics from naturalized and simulated flows, including Mean Absolute Error (MAE), Root Mean Square Error (RMSE), Volume Error (VE), Coefficient of Determination and Correlation. Basically, the MAE and RMSE are used to measure the deviation between the observed and simulated streamflows values. On the other hand, the VE is defined as the ratio of the volume error to the observed streamflow volume expressed as percentage. In addition, this analysis also considers the Nash-Sutcliffe Coefficient(R) and Index of Agreement

(IA), to evaluate the goodness-of-fit of the model performance (Legates and McCabe, 1999; Fleming and Neary, 2004; and Barbaro and Zerriello, 2006).  The parameters are stated as follow:

1. *Mean Absolute Error (MAE)*

$$MAE = \frac{1}{N} \sum_{i=1}^{N} \left| Q_i^o - Q_i^s \right|$$

Equation 3-6

2. *Root Mean Square Error (RMSE)*

$$RMSE = \sqrt{\frac{\sum_{i=1}^{N} (Qo_i - Qs_i)^2}{N}}$$

Equation 3-7

3. *Error in Volume (VE in%)*

$$VE = \frac{(V_o - V_s)}{V_o} x100$$

Equation 3-8

4. *Nash-Sutcliffe Coefficient(R)*

$$R = 1.0 - \frac{\sum_{i=1}^{N} (Qo_i - Qs_i)^2}{\sum_{i=1}^{N} (Qo_i - \bar{Q})^2}$$

Equation 3-9

5. *Index of Agreement (IA)*

Equation 3-10

$$IA = 1.0 - \frac{\sum_{i=1}^{N} (Qo_i - Qs_i)^2}{\sum_{i=1}^{N} \left( \left| Qs_i - \bar{Q} \right| - \left| Qo_i - \bar{Q} \right| \right)^2}$$

where $Q^o{}_i$ is the observed streamflow, $Q^s{}_i$ is the simulated streamflow, $\overline{Q}$ is the average streamflow; *Vo* is the observed streamflow volume; *Vo* is the simulated streamflow

volume; $\bar{Q}$ is the average streamflow ($m^3$/s ). Nash-Sutcliffe Coefficient ranges from minus infinity to 1.0, with high values indicating better agreement. Physically, this parameter expresses the ratio of the mean square error to the variance in the observed values, differenced from unity. If R is equal to zero, the observed mean is as good predictor as the model, and if the R <0 (negative values), the observed mean is a better predictor than the model (Legates and McCabe, 1999). Furthermore, the index of agreement relates the square error to the absolute value of the square differences between simulated and the observed values, with their average of the corresponding time series, reduced by the maximum agreement. Values ranges from 0 to 1, high values indicates a better agreement between modeled and observed streamflows.

Moriasi et al. (2007) conducted an extensive review of published literature related to calibration, validation, and application of watershed models to determine published ranges of values and performance ratings for recommended model evaluation statistics. Table 3-4a lists the recommended performance ratings for monthly time step watershed models.

Table 3-4a: General performance ratings for Nash-Sutcliffe Efficiency Statistic for Monthly Time Step Models (Moriasi et al. (2007).

| Performance Rating | Range |
|---|---|
| Very good | 0.75 – 1.0 |
| Good | 0.65 – 0.75 |
| Satisfactory | 0.50 – 0.65 |
| Unsatisfactory | $-\infty$ – 0.50 |

**3.6.5 Model Validation**

A ten-year hydrologic period (1990-1999) was considered to validate the goodness of the model. Drought conditions were found in the Rio Conchos (1992-1999) in this time period, which flows under the average. Since the model was calibrated for normal conditions, the assessment under hydrological drought is strongly important. Statistical analysis, as calibration process, was used to assess the model performance in each control station. Exceedance probabilities for historical and simulated flow were evaluated to establish ranges of the model prediction under a certainty level.

**3.6.6 Probability and Reliability Analysis**

Differences between simulated and observed values are expected since the physical representation of the basin in the hydrologic model includes assumptions that lead to a significant uncertainty level in flow prediction. Probabilistic analysis can help to establish ranges in the model prediction. On the other hand, as the model is used to assess the effects of climate change on water availability relative to the historical baseline 1980-99, probabilities and confidence limits for annual flow are computed for a twenty-year running model (1980-99).

**3.7 SELECTION OF THE GLOBAL CLIMATE MODELS**

When considering climate change, one of the challenges that water resources managers often face is deciding what general circulation models (GCMs) should be used for evaluating climate change impacts on water supply. This is a perplexing question,

since GCMs all demonstrate uncertainty in predicting historical climate variables (Warren and Parkinson 2005; IPCC 2008). However, some criteria, e.g., spatial resolution, degree of atmospheric-ocean coupling, and availability of multiple realizations, may be taken into account to select a suite of GCMs to reduce uncertainties in water supply forecasts based on any individual GCM. The GCMs chosen for this study were: CGCM31-T47 (Flato and Boer 2001), CCSM3 (Collins et al. 2006), ECHAM5 (Jungclaus et al. 2006), MIROC3.2-Medres (K-1 Model Developers 2004), and UKMO-HadCM3 (Gordon et al. 2000). Table 3-5 shows the main features of the GCMs what were used in this research.

Table 3-5: GCMs selected to assess climate change impacts on water Resources in the Rio Conchos Basin

| Model | Modeling Group, Country | Resolution | | Runs | Land (soils, plant, routing) |
| | | Atmospheric (degrees) | Ocean (degrees) | | |
| --- | --- | --- | --- | --- | --- |
| CGCM3.1 (T47) | Canadian Centre for Climate Modeling and Analysis, Canada | 2.8 x 2.8 | 1.9 X 1.9 | 1,2,3,4, 5 | Layers, canopy, routing |
| CCSM3 | National Center for Atmospheric Research, US | 1.4 x 1.4 | 0.3-1 x 1 | 1,2,3,4, | Layers, canopy, routing |
| ECHAM5/ MPI-OM | Max Planck Institute for Meteorology, Germany | 1.9 x 1.9 | 1. 5 X1.5 | 1,2,3 | Bucket, canopy, routing |
| MIROC3.2 (medres) | Center for Climate System Research (The University of Tokyo), National Institute for Environmental Studies, and Frontier Research Center for Global Change Japan | 2.8 x 2.8 | 0.5-1.4 x1.4 | 1,2,3 | Layers, canopy, routing |
| UKMO-HadCM3 | Hadley Centre for Climate Prediction and Research / Met Office, UK | 2.5 x 3.75 | 1.25 x 1.25 | 1 | Layers, canopy, routing |

**3.8 DOWNSCALED WCRP CMIP3 CLIMATE DATA**

General Climate Model (GCM) simulations are performed at coarse resolution (approximately $2^0$ x $2^0$). For water resources applications at local scale (basin), global climate data need to be downscaled. Statistical and dynamic methods are discussed in previous section indicating their advantages and disadvantages to downscaling climate models outputs. Statistically downscaled climate projections developed by the University of Santa Clara and the Bureau of Reclamation (Maurer et al. 2007) are used in this research. This dataset includes 112 downscaled projections for 16 GCMs and 3 future greenhouse gas emissions scenarios (A1B and A2) for precipitation and temperature variables. The downscaled data are available at the finer spatial resolution of $1/8^o$ latitude-longitude (~12km x 12 km) whose domain covers from 25.125° to 52.875° latitude North and from - 124.625° to -67.000° longitude East (US and contiguous, portion of southern Canada and northern Mexico).

The methodology includes two major steps: A Bias correction, which allows recognizing how a General Circulation Model tends to be too cool/warm/wet/dry in simulating the past climate conditions related to the historical values, and a spatial downscaling that translate spatially adjusted GCM climate data from coarse spatial resolution to a basin resolution for hydrology and other water resources applications. (Wood et al. 2002, Wood et al. 2004, and Maurer 2007). Using the quantile mapping technique, bias correction removes trends from projected climate data.

59

**3.9 SIMULATION OF CLIMATE CHANGE SCENARIOS**

In 2000, the Intergovernmental Panel on Climate Change (IPCC) in its Special Report on Emission Scenarios (SCENARIO) published a new set of emission scenarios to be used in climate change studies. This new group of scenarios was developed to incorporate a wide range of driving forces and emissions. Driving forces such demographic development, technology change, and socio-economic development were considered to estimate the future greenhouse gas emission. This investigation uses downscaled climate data for emission scenarios A2 and A1B. These scenarios have been selected on the base of their emission paths; high and middle respectively, as well the fact that they applied and discussed in several places in the world.

**3.9.1 Emission Scenario A1B**

In general, the A1B scenario is a middle emission path, which considers that technological change in the energy system is balanced across all fossil and non-fossil energy sources. The main key assumptions considered in this scenario are: low population, future world with rapid economic growth, and introduction of new technology. Likewise, economic and cultural convergence, capacity building and significant reduction in differences in per capita income are considered as main themes (IPCC, 2000).

**3.9.2 Emission Scenario A2**

Scenario A2 is a higher emissions path that includes high population growth, and technological change and economic growth are more fragmented. "*The underlying theme is that of strengthening regional cultural identities, with an emphasis on family values and local traditions, high population growth, and less concern for rapid economic development*" (IPPC, 2000). The future time period to be used is from 2040 – 2099, which will be evaluated each 20 years (2040 - 2059, 2060 - 2079, and 2080 - 2099) relative to the period 1980 – 1999.

**3.10 ENSEMBLE OF GCMs OUTPUTS**

Streamflows produced by using the downscaled data from the five GCMs in a hydrologic model form an ensemble response of the basin.  The expected response of the basin can be obtained by, at least, two methods: simple averaging and weighted averaging. The weighting method gives preference to the GCMs that present less error with respect to reproducing historical runoff values.  In this study, weights are assigned according to the performance of each GCM (Ingol and McKinney 2011) to generate the monthly flow from the reference period (1980-1999), providing greater confidence in the model that records less error as indicated by the Root Mean Squared Error (RMSE).  The RMSE in the streamflow for month $j$ and GCM $k$ can be defined as

$$RMSE_{jk} = \sqrt{\frac{\sum\limits_{i=1}^{N}\left(Q_{ij}^{o} - Q_{ij}^{k}\right)^2}{N}}$$

Equation 3-11

where $Q_{ij}^{o}$ is the monthly naturalized flow for month $j$ in year $i$ ($i = 1,2,\ldots,N$), and $Q_{ij}^{k}$ is the simulated streamflow in month $j$ using GCM $k$ downscaled temperature and precipitation as input to the hydrologic model. The total RMSE for month $j$ from all of the GCMs can be defined by

$$TRMSE_{j} = \sum_{k=1}^{5} RMSE_{jk}$$

Equation 3-12

The weight for GCM k in month j is given by

$$\psi_{jk} = \frac{RMSE_{jk}}{TRMSE_{j}}; \qquad 0 < \psi_{jk} < 1; \quad k = 1,\ldots,5$$

Equation 3-13

where larger weights indicate less accuracy in computing the historical streamflow. The streamflow ensemble for month $j$ is

$$Q_{j}^{e} = \frac{1}{\phi_{j}}\sum_{k=1}^{5}\left(\frac{Q_{jk}}{\psi_{jk}}\right)$$

Equation 3-14

where $\phi_{j} = \sum_{k=1}^{5}\left(\frac{1}{\psi_{jk}}\right)$,

Equation 3-15

with $Q_{jk}$ is the streamflow value from using GCM $k$. Finally, expression (7) could be expressed as follow:

$$Q_{j}^{e} = \sum_{k=1}^{5} w_{jk} Q_{jk}$$

Equation 3-16

where $w_{jk} = 1/\phi_j \psi_{jk}$

Table 3-6 shows the weights for each GCM in the Rio Conchos at Ojinaga. Weights were computed using the root mean square error approach described above. For this end, historical period 1980-1999 was used.

Table 3-6: Weights Computed for Flow at Ojinaga

| Month | General Circulation Model | | | | |
|-------|-------|--------|--------|--------|---------|
|       | CCSM3 | CGCM31 | ECHAM5 | HADLEY | MIROC32 |
| Jan   | 0.18  | 0.21   | 0.21   | 0.20   | 0.20    |
| Feb   | 0.19  | 0.20   | 0.22   | 0.19   | 0.19    |
| Mar   | 0.20  | 0.19   | 0.21   | 0.20   | 0.20    |
| Apr   | 0.20  | 0.23   | 0.18   | 0.19   | 0.20    |
| May   | 0.21  | 0.21   | 0.20   | 0.19   | 0.20    |
| Jun   | 0.19  | 0.23   | 0.18   | 0.23   | 0.16    |
| Jul   | 0.20  | 0.25   | 0.22   | 0.21   | 0.13    |
| Aug   | 0.22  | 0.23   | 0.20   | 0.18   | 0.17    |
| Sep   | 0.22  | 0.18   | 0.17   | 0.23   | 0.19    |
| Oct   | 0.21  | 0.18   | 0.21   | 0.21   | 0.19    |
| Nov   | 0.22  | 0.15   | 0.21   | 0.20   | 0.21    |
| Dec   | 0.22  | 0.17   | 0.22   | 0.20   | 0.19    |

## 3.11 IMPACTS ON HYDROLOGY OF THE BASIN

This section describes some tools used to evaluate potential climate change impacts on the hydrology of the Rio Conchos basin. Additionally to the quantitative assessment, a probabilistic analysis is considered. Probability density functions (PDFs) and Cumulative Distribution functions (CDFs) were computed to quantify the monthly and annual flows resulting from the simulated climate scenarios. Wavelet analysis is carried out to detect climate pattern connections. Moreover, changes in annual runoff distribution are evaluated through the Coefficient of Variation (CV), and the streamflow

concentration degree. In addition, the non-parametric Mann-Kendall method is used to detect linear trends in annual streamflows (Kahya and Kalayc, 2004).

### 3.11.1 Mann-Kendall Analysis

The non-parametric method by Mann-Kendall is used to detect the linear trend of annual streamflows. This test assumes for the null hypothesis $H_o$ that time series data are a sample of n independent and distributed random variables, with no trend. The alternative hypothesis $H_1$ states that the distribution of $x_i$ and $x$ are different for all i,j < n (Helsel and Hirsch 2002, and Kahya and Kalayc, 2004). The Mann-Kendall statistic S is as follows:

$$S = \sum_{i=1}^{n-1} \sum_{j=i+1}^{n} sign(x_i - x_j)$$

Equation 3-17

With:

$$sign(x_i - x_j) = \begin{cases} +1 & if\ (x_i - x_j) > 0 \\ 0 & if\ (x_i - x_j) = 0 \\ -1 & if\ (x_i - x_j) < 0 \end{cases}$$

Equation 3-18

The idea with this test is that each data value is compared with the subsequent value. If the subsequent value is higher than the previous value, S is assumed to be +1. On the other hand, if the later value of a time period is lower than the previous value, S is assumed to be -1. The Initial value of the Mann- Kendall statistic, S, is assume to be 0. For this statistic test, the variance of S can be computed by the following expression:

$$\sigma_s = \sqrt{\frac{n(n-1)(2n+5)}{18}}$$

Equation 3-19

Where n is the number of time series data. Then the normalized test statistics of Z is computed as follow:

$$Z = \begin{cases} \dfrac{S-1}{\sigma_s} & if \ S > 0 \\ 0 & if \ S = 0 \\ \dfrac{S+1}{\sigma_s} & if \ S < 0 \end{cases}$$

Equation 3-20

A positive Z indicates a positive trend and a negative Z denotes a negative trend of annual streamflows. Likewise, the null hypothesis is rejected at significance level α if |Zs| > Zcritical, where Zcritical = $Z_{1-\alpha/2}$ and it is the value of the standard normal distribution with an exceeding probability of α / 2. For this research a significance level α of 5% is used.

**3.11.2 Probabilistic Analysis**

*3.11.2.1 Annual Runoff*

Probability density functions (PDFs) and Cumulative Distribution functions (CDF) were computed and evaluated to quantify the annual flows resulting from climate projections in the Rio Conchos. Streamflow was evaluated each 20 years to break the non

stationary conditions due to climate change. Log normal distribution with a sample moments was selected to fit the annual streamflow.

### 3.11.2.2 Maximum and Minimum Flows

Analysis of extreme flows is crucial in water resources management and planning to flood control, drought prediction, and environmental ecosystems. Log Pearson type 3 (LP3) distributions and a General Extreme Value (GEV) were used to model and evaluate the annual maximum and minimum streamflow respectively. Similarly, the assessment was carried out for 20-year segments. LP3 distribution has been used extensively in hydrology (Griffis and Stedinger, 2007) and it is recommended by U.S federal agencies for flood frequency analysis. The procedure for flood analysis is described by the Bulletin 17B of U.S. Geological Survey (1982) based on the analysis of Pearson III distribution with log transformation of the data to define the annual flood series. On the other hand, The GEV distribution with maximum likelihood parameters (Jenkinson 1955; Chow *et al*. 1988; and El-Adlouni *et al*. 2007) was used for annual minimum flows in the Rio Conchos. The GEV distribution has been used to consider climate change impacts on water quality (Towler *et al.* 2010). All computations were carried out in Matlab software. Cumulative distribution function is given as (Jenkinson, 1955)

$$F(x_i) = \exp\left[-\left(1 - \frac{k(x_i - \mu)}{\alpha}\right)^{1/k}\right] \qquad \text{for k} \neq 0 \qquad \text{Equation 3-21}$$

$$F(x_i) = \exp\left[-\exp\left(-\frac{x_i - \mu}{\alpha}\right)\right] \qquad \text{for } k = 0 \qquad \qquad \text{Equation 3-22}$$

Where $x_i$ is the exceedance value, $\mu$ is the location parameter, $\alpha$ is the scale parameter, and $k$ is the shape parameter. This function has three limiting cases (Jenkinson, 1955; Chow, et. el, 1988; and El-Adlouni et. el, 2007): when k = 0, GEV is reduced to the Extreme Value Type I such those expressed in 3-22 (Gumbel distribution); for k < 0, it equals to the Extreme Value Type II (Frechet distribution), for μ+α/k≤ x≤ ∞; and for k > 0, it is an Extreme Value Type III (Weibull distribution), for -∞ ≤ x≤ μ+α/k. μ, α, and k ∈ R. The same analysis was performed for historical conditions period 1980-1999 in order to assess how historical extremes are related to the future extremes under climate change.

### 3.11.3 Evaluating Long Term Natural Variability.

Since significant drought periods are indentified in the study basin, the assessment of long term variability of the streamflow is fundamental for water resources management. An analysis of flow at Ojinaga (the confluence of the Rio Conchos with the Rio Grande) was performed to show how these are linked to naturally varying climatic patterns, such as El Niño-Southern Oscillation (ENSO) and the Pacific Decadal Oscillation (PDO). Then changes in flows under climate change and their connections to climate events are discussed.

### 3.11.3.1 General Description of Selected Climate Indices

The ENSO phenomenon is characterized by a strong sea surface temperature between warm water in the western equatorial Pacific and relatively cool water in the eastern equatorial Pacific (Warren and Parkinson 2005). Warm water is produced by upwelling along the west coast of South America, and it is linked with several climate anomalies in the world. The ENSO index used in this study is the monthly bivariate ENSO Time Series (BEST) index (NOAA 2010), which is based on combining an atmospheric component of the ENSO phenomenon (the Southern Oscillation Index based on the observed sea level pressure differences between Tahiti and Darwin, Australia) and an ocean component Nino 3.4 defined as the surface sea temperature averaged over the region 5N-5S and 170W -120W.

PDO event is defined as a long pattern of Pacific climate variability that shifts inter-decadal time scale, usually 20-30 years. PDO index is computed by spatially averaging the monthly sea surface temperature of the Pacific Ocean north of 20 $^{o}$N. The global average anomaly is subtracted to account for global warming (JISAO, 2010). Index is positive, sea water in the north central Pacific Ocean tend to be cool, and water along the west coast of North America tend to be warm. By contrast happens when the index is negative.

### 3.11.3.2 Wavelet Analysis

Wavelet analysis is used to assess periodic events in non-stationary time series. The decomposition of a signal into different frequencies allows the evaluation of

68

dominant periods and how their distribution changes over time. It can be made by either Fourier or wavelet transforms. Wavelet analysis is preferred for non-stationary signals (Coulibaly and Burn, 2004), and they perform better on signals with high peaks such as the streamflow time series (Bayazit, et al. 2001). Wavelet analysis was applied here to the historical monthly flows to examine the connections with long- and short-term climatologic pattern variability, such as the Pacific Decadal Oscillation (PDO) and El Niño/Southern Oscillation (ENSO) and their influence on the hydrology of the Rio Conchos are investigated.

The Monthly Bivariate ENSO Time Series (BEST) Index (NOAA, 2010) and the PDO index (JISAO, 2010) are used in this research. Likewise, the Morlet wavelet was used, which consists of a plane wave modulated by a Gaussian window (Torrence and Compo, 1998, and Coulibaly and Burn, 2004):

$$\psi_o(\eta) = \pi^{-0.25} e^{i\omega_o \eta} e^{-0.5\eta^2} \qquad \text{Equation 3-23}$$

Where $\omega_o$ is the non-dimensional frequency with $\omega_o=6$ to satisfy the admissibility condition (Torrence and Compo, 1998), and $\psi_o$ is the wavelet function that depend on the non dimensional time parameter $\eta$.

The continue wavelet transform of a discrete sequence time series $x_n$ is defined as the convolution of $x_n$ with a scaled and translated $\psi_o(\eta)$.

$$W_n(s) = \sum_{n'=0}^{N-1} x_{n'} \psi * \left[ \frac{(n'-n)\delta t}{s} \right]$$

Equation 3-24

where, N is the number of point of time series $x_n$, n is the localized time index, s is the wavelet scale, and $\delta t$ is the time space (sampling period). The asterisk symbol indicates the complex conjugate. The scale-averaged wavelet power is defined as the weighted sum of the wavelet power spectrum over the scales $s_1$ and $s_2$ (Coulibaly and Burn, 2004):

$$\overline{W_n}^2 = \frac{\delta_j \delta t}{C_\delta} \sum_{j=j_1}^{j_2} \frac{\left| W_n(s_j) \right|^2}{s_j}$$

Equation 3-25

Where, $\delta_j$ is a factor of scale resolution and $C_\delta$ is the reconstruction factor equal to 0.776 for the Morlet wavelet ($\omega_o=6$). The monthly time series (e.g., flow, ENSO or PDO) was normalized for the wavelet analysis by subtracting the monthly average and dividing by the standard deviation for the period 1940-99.

### 3.12 INTEGRATED WATER RESOURCES MODELING

### 3.12.1 Model Description

In this research, an integrated water resources model is developed using the Water Evaluation and Planning (WEAP) software to perform the hydrologic and water allocation analysis and thereafter, to evaluate climate change impacts on water availability on the entire water system. The model integrates two parts: hydrologic

modeling described in previous sections and water management modeling. Five main reservoirs, operation rules, municipal and irrigation water demand, aquifers, water distribution policies, return flows, stream gages, groundwater aquifers, and transmission links are represented in the water planning model.

A yearly demand with monthly variation is used to represent water demands; priorities and consumptive use are set in the model. Constraints are defined for maximum flow in transmission links for demand points that use water from reservoirs, which are linked to special operation rules. System losses and losses to the Meoqui aquifer were established in the return flows from Irrigation District 005 Delicias. The model is calibrated using historical streamflow, storage reservoir volumes, irrigation and municipal water deliveries, water distribution rules, and priorities. Mostly, reservoirs are for multipurpose, irrigation, energy, and municipal uses. Figure 3.7 below shows the main components of the Rio Conchos water system. Water release from La Boquilla reservoir is used for the ID-005 Delicias irrigation district, Labores Viejas irrigation, Camargo, and for hydropower generation. F. Madero reservoir is used to irrigate part of the ID-005 Delicias. San Gabriel and Pico del Aguila reservoirs are used mainly for irrigation of ID-103 Rio Florido. Luis L. Leon reservoir is used for control flooding and for irrigation of ID-090 Bajo Rio Conchos.
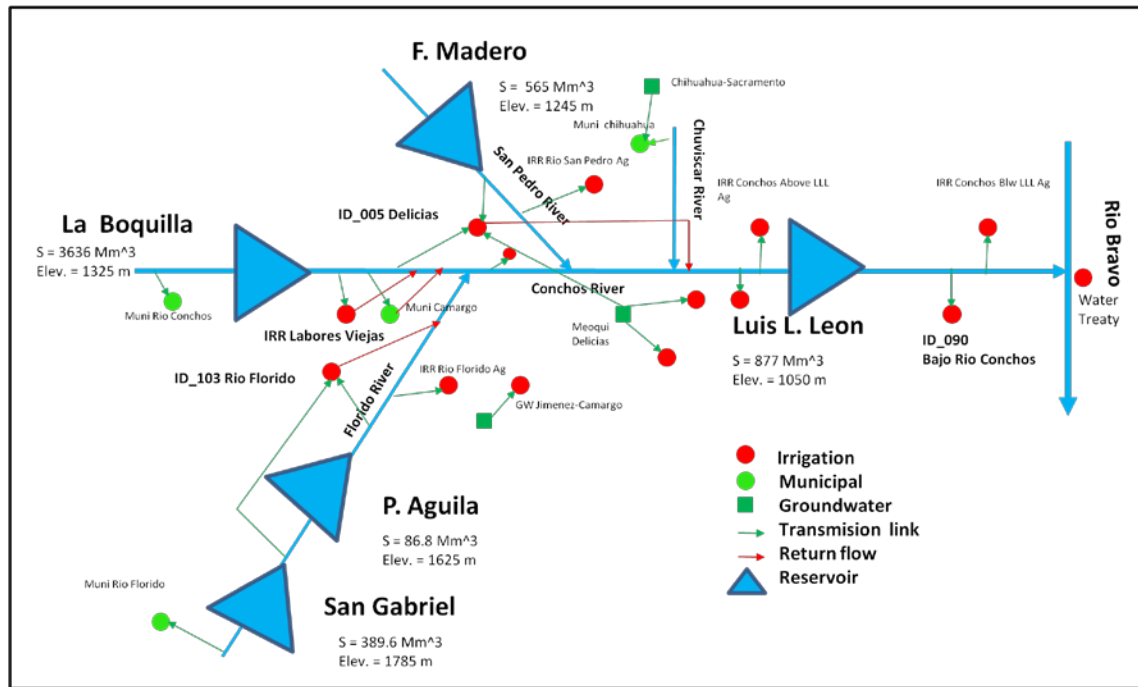
Figure 3-7: Hydraulic scheme of the Rio Conchos basin

### 3.12.2 Groundwater Modeling

Groundwater is used as supplemental irrigation water in dry periods to meet crop and municipal demands in the Rio Conchos system. Despite its relevance, however, there is little information about the groundwater amount supplied for each irrigation district and the hydraulic characteristics of aquifers. Under this constraint, this research intends to show a broad effect of climate change on the main aquifers located along the study area. Table 3-7 shows the main aquifers modeled in WEAP and whose data was extracted from CRWR dataset (Patino and Mckinney 2005). The Meoqui-Delicias and the Jimenez-Camargo aquifers are relevant for irrigation and the Chihuahua-Sacrament aquifer for municipal purposes.

72

Table 3-7: Groundwater aquifers set in the water planning model of the Rio Conchos

| Object ID | Name | Status | Annual Extraction (Million m3) | Annual Recharge (Million m3) | Area (Km2) |
|---|---|---|---|---|---|
| 27 | Laguna de Mexicanos | N.D | N.D | N.D | 961.920 |
| 46 | Chihuahua-Sacramento | overexploitation | 124.800 | 55.000 | 1850.062 |
| 47 | Meoqui-Delicias | Equilibrium | 417.000 | 418.000 | 4927.823 |
| 48 | Jimenez-Camargo | overexploitation | 580.650 | 440.000 | 10019.886 |
| 51 | Tabalaopa-Aldama | N.D | N.D | N.D | 728.473 |
| 52 | Aldama-San Diego | overexploitation | 42.733 | 35.200 | 1603.254 |
| 53 | Bajo Rio Conchos | No exploitation | 18.420 | 90.000 | 8838.877 |
| 54 | Alto Rio San Pedro | No exploitation | 39.040 | 56.300 | 11057.623 |
| 56 | Villalba | No exploitation | 0.000 | 8.000 | 785.238 |
| 57 | Potrero Del Llano | No exploitation | 0.000 | 50.000 | 2493.657 |
| 59 | Bocoyna | No exploitation | 0.150 | 17.000 | 7393.695 |
| 60 | Valle De Zaragoza | No exploitation | 0.470 | 13.000 | 4062.382 |
| 61 | San Felipe De Jesus | No exploitation | 0.000 | 8.000 | 2759.041 |
| 62 | Carichi-Nonoava | No exploitation | 0.820 | 8.000 | 7035.411 |
| 50 | Parral-Valle Del Verano | No exploitation | 22.933 | 26.700 | 1466.159 |

N.D: No Data

WEAP has four options to simulate the interaction between groundwater and surface water (SEI 2007). In this research, we use a combination of the deep soil layer of the Soil Moisture method and the specific Groundwater (GW)-Surface water (SW) flow method. The soil moisture method computes the main hydrologic components for each catchment: precipitation, runoff, evapotranspiration, base flow, and interflow. Then, a water balance in WEAP was developed to estimate the storage change for the second layer that was linked to the groundwater aquifers using the GW-SW method. The aquifer area was related to its respective total area of catchment to compute the fraction of the

recharge contribution in each aquifer. The equation to estimate the monthly recharge is as follow:

$$\frac{ds}{dt} = \Pr ecipiation - Runoff - ET - Baseflow - Interflow$$
Equation 3-26

Fourteen aquifers were included in the WEAP model. Only data on the concessions for the Meoqui Aquifer for irrigation was available with a total of 189 Mm$^3$ for the Irrigation District 005 Las Delicias, and a maximum withdrawal of around 410 Mm$^3$ per year. Further information about the soil moisture method applied to the Rio Conchos, the reader is referred to Ingol-Blanco and McKinney (2010).

**3.12.3 Baseline Scenario Definition**

A time period of twenty years was selected as a baseline for scenario analysis to compare the performance and future water availability under climate change in the Rio Conchos basin. This period assumes that the water demands, water system conditions, historical climate input, and land use do not change over time. Furthermore, a water demand at the river outlet to satisfy the requirements of the 1944 water treaty was set up in the water planning model. This condition assumes a water delivery of about 711 Millions m$^3$ per year on average as is stipulated in the water treaty signed between US and Mexico in 1944. Water demands for agriculture and municipal uses were obtained from the Water Management Scenarios for the Rio Bravo Basin (Sandoval and McKinney 2010). Likewise, future water demand for irrigation was assumed to be

74

constant under the emission scenarios A2 and A1B. Unfortunately, there is not available precipitation data to simulate a long historical period; however, the period chosen covers the normal and drought conditions which are very relevant to assessing the performance of the system under climate change conditions. Changes are assessed relative to the baseline period (1980-1999).

### 3.12.4 Priority

The water use priority was considered taking into account the water distribution policy in the study basin. In WEAP, the priority number varies from 1 to 99; the lowest value means a high priority, and highest, a low priority for allocation water. Three groups of priorities of water distribution were set in the model: 1 for municipal, 2 for irrigation from reservoirs, and 3 for irrigation uses allocated directly from the rivers. A low priority has been considered (97) for the water treaty, which means that the WEAP-Conchos model meets first the target demand for the water users located in the Rio Conchos; and subsequently the treaty. This is in general agreement with Mexican water policy

### 3.13 IMPACTS ON WATER AVAILABILITY

Climate change impacts on water resources are evaluated on supplies to meet the user demands in the Rio Conchos basin and the treaty. The analysis focuses on the performance of the water system as a percentage of change from the baseline scenario. The main users (agricultural, groundwater, and domestic/municipal uses) are evaluated.

### 3.13.1 Performance of the Water System under Climate Change

Indices of reliability, resiliency, and vulnerability are used to assess the performance of the Rio Conchos water system to meeting demand (Hashimoto et al. 1982; Fowler et al. 2003; Ajami et al. 2008) for the baseline, climate change, and mitigation scenarios. First a criterion, C, is established for each water supply source where an unsatisfactory condition occurs when a specified demand is not met (Ajami et al. 2008). In this study, the annual time series of coverage demand, $X_t$ is assessed in meeting the criterion $C_t$ which is defined as the total annual demand that needs to be supplied in each time step. Water supply from four main reservoirs, rivers, and groundwater are considered to satisfy the water demands for municipal and irrigation users under climate change effects. Furthermore, an index $Z_t$ is defined to quantify a satisfactory (S) or unsatisfactory (U) state of the water system on the base of the criterion, $C_t$ (Hashimoto et al. 1982):

$$Z_t = \begin{cases} 1, & if \quad X_t \in S \\ 0, & if \quad X_t \in U \end{cases} \qquad \text{Equation 3-27}$$

The transition between satisfactory and unsatisfactory states is represented through the index $W_t$ as follow:

$$W_t = \begin{cases} 1, & if \quad X_t \in U \ and \quad X_{t+1} \in S \\ 0, & otherwise \end{cases} \qquad \text{Equation 3-28}$$

If the periods of unsatisfactory states of $X_t$ are $K_1,\ldots,K_N$ then the reliability, resilience, and vulnerability indices are computed as follow (Hashimoto et al. 1982; Fowler et al. 2003):

Reliability $\quad C_R = \dfrac{\sum\limits_{t=1}^{T} Z_t}{T}$ $\qquad\qquad\qquad\qquad\qquad$ Equation 3-29

Resilience $\quad C_{RS} = \dfrac{\sum\limits_{t=1}^{T} W_t}{T - \sum\limits_{t=1}^{T} Z_t}$ $\qquad\qquad\qquad\qquad$ Equation 3-30

Vulnerability $\quad C_V = \max\left\{ \sum\limits_{t \in K_i} C - X_t, \quad i = 1,\ldots,N \right\}$ $\qquad$ Equation 3-31

where, T is the total length of the time series considered in the analysis. The reliability is a measure that indicates the frequency with which the water demands are achieved taking into account a specified criterion. On the other hand, the resiliency measures the ability of the Rio Conchos system to recover from an unsatisfactory condition. If the reliability of the system is achieved in the whole time period, the index $Z_t$ will be equal to the total length, *T*; in this case, the resilience computed by equation 3-30 is 100%. The Vulnerability index shows the inability of the system to meet the threshold demand and it is computed on the base of an extended failure period in which the maximum deficit among all unsatisfactory periods is chosen. In this research, we use the relative vulnerability for the average deficit which is expressed as follow:

77

$$C_r = \frac{\sum\limits_{t \in j_i} (D_t - X_t)}{\sum\limits_{t \in j_i} D_t} \quad , \text{ for all } D_t > X_t \qquad \qquad \text{Equation 3-32}$$

Here, $D_t$ represents the criterion demand in time step t and $j_i$ refers to the unsatisfactory period where the user water demands cannot be achieved. In addition, a relative maximum deficit is defined by comparing the volumetric maximum deficit for the period i with its respective target demand:

$$Max\,deficit = \frac{Maxdefict_t^i}{D_t^i} \qquad \qquad \text{Equation 3-33}$$

### 13.13.2 Sustainability Indicator

The sustainability index can be defined as a measure that allows evaluation of the overall performance of the water system under certain conditions and management policies. In this research, we estimate a sustainability measure (Loucks, 1997 and Sandoval et al. 2010) by combining the reliability, resilience, and relative vulnerability as follow:

$$SI = (\text{Re}\,liability * \text{Re}\,silience * (1 - C_r))^{1/3} \qquad \qquad \text{Equation 3-34}$$

Essentially, equation 3-34 expresses the geometric mean of the main indicators (Sandoval et al. 2010) used to assess the global performance of the system.

**3.14 SIMULATION OF WATER MANAGEMENT SCENARIOS**

Water management measures designed to help adapt to or mitigate the effects of climate change are simulated and tested. This will provide water users an understanding of some possible water management alternatives to be implemented in the future. This includes an evaluation of how the water system responds to these new policy changes and how the 1944 treaty might be managed under the effects of climate change. Each alternative is described below.

**3.14.1 Alternative I (SI)**

Maintain current irrigation water demand under an increasing municipal demand for the period 2040-99. This scenario considers no improvement in the current water system and no change in the crop demands, but a significant increase in municipal demand. Future population in the Rio Conchos Basin was projected using an arithmetic method, extrapolated to estimate the future municipal demands.

*Projection of the Municipal Demands*

Water resources for municipal purposes are also expected to be affected by future climate change. This is based on a notable growth of the world population which means major increases in water consumption in the next decades. Mexican population has shown significant increases in the last decades. Furthermore, several methods can be used to estimate the future population such as arithmetic, geometric, exponential, logarithmic methods. However, there is not a specific method that will allow us to project the population for long time periods. Instead, projections for long time periods are based on

the possible scenarios that could occur as those estimated by the United Nations (United

Nations 2008).  In this research, the arithmetic method was used to estimate the future

Mexican population. It assumes a constant growing rate which is stated as follows:

$$\frac{dP}{dT} = Cr$$

Equation 3-35

Where P is the population, T is the time, and $C_r$ is the constant rate. Integrating this

equation for population intervals from $P_2$ and $P_1$, and $T_2$ and $T_1$, respectively, we have:

$$Cr = \frac{P_2 - P_1}{T_2 - T_1}$$

Equation 3-36

Then, the projected population will be:

$$P_j = P_2 + Cr * (T_j - T_2)$$

Equation 3-37

Where, the $P_j$ is the projected population for the time $T_j$.

Finally, changes computed with equation (3-37) are used to project the annual municipal

water demands (period 2040-2099), $D_j$, as follow:

$$D_{j+1} = D_j + \left( \frac{P_{j+1}^{t_{j+1}} - P_j^{t_j}}{P_j^{t_j}} \right) * D_j$$

Equation 3-38

### 3.14.2 Alternative II (SII)

This alternative considers increased water use efficiencies in all irrigation districts in two parts: (1) increased conveyance efficiency in the Rio Conchos Basin from 61% to 76.5% through improvements in the current system such as control structures (gates, dams, and distribution system), lining of main canals with reinforced concrete, improvement of irrigation infrastructure land, training and technical support for farmers and decision makers; and (2) increased average water application efficiency from 54% to 80% using pressurized irrigation systems. It implies a total change of the current irrigation method in the basin through a combination of drip and sprinklers irrigation systems. Groundwater use is also considered to satisfy the water demands in the Rio Conchos basin. In addition, this scenario also considers the same increase in municipal demand as Scenario I.

### 3.14.3 Alternative III (SIII)

This alternative envisions a reduction of the irrigation demands in the Rio Conchos basin by 25%, with increased water application efficiency through a change in crops to those with less water consumption. The municipal water demands remain constant during the time period (2040-2099).

### 3.14.4 Alternative IV (SIV)

The water demand for irrigation is projected to be reduced by 32% through increased water efficiency in the conveyance and application systems. As in Alternative

III, it is assumed that municipal demands do not vary during the analysis period. Likewise, increase of groundwater use as an alternative to meet the irrigation demands in drought periods is considered. Table 3-8 shows a summary of the efficiency of water use for the scenario simulation in the irrigation district 005 Las Delicias.

Table 3-8: Water use efficiency for scenarios simulation under adaptive strategies

| Alternative | Conveyance channel network | | Application | Global |
|---|---|---|---|---|
| | Main | Secondary | | |
| I | 80% | 76% | 54% | 33% |
| II | 85% | 90% | 80% | 61% |
| III | 80% | 76% | 72% | 44% |
| IV | 80% | 80% | 80% | 51% |

Essentially, these alternatives assume that increased water use efficiency will allow saving more water in the reservoirs, which will help to mitigate the impacts of climate change in the study area; reducing the vulnerability of the water system and increasing the reliability of water delivery to municipal and agricultural users. For each alternative, special operation rules were programmed in the Rio Conchos WEAP model to release water from reservoirs according to the efficiencies described in Table 3-8. Coupled with intensive groundwater use, these scenario analyses give information about the behavior of the system and the performance of various adaptive measures to deal with climate change conditions, constituting an important tool for water resources planners in decision making. Table 3-9 presents the surface water distribution to meet the proposed efficiency for the main irrigation district 005 Las Delicias.

Table 3-9: Surface water distribution for the ID-005 Delicias under adaptive strategies

| Alternative | Reservoir Release (million m$^3$ per year) | | Water Distribution (million m$^3$ per year) | | |
|:---:|:---:|:---:|:---:|:---:|:---:|
| | La Boquilla | F. Madero | Total release | Control point | Application |
| I | 927.04 | 246.43 | 1173.46 | 941.59 | 717.12 |
| II | 499.87 | 132.88 | 632.75 | 537.84 | 484.05 |
| III | 695.28 | 184.82 | 880.10 | 706.19 | 537.84 |
| IV | 597.50 | 158.83 | 756.33 | 605.07 | 484.05 |

# Chapter 4: Hydrological Modeling Results

This section presents results of the hydrologic modeling of the Rio Conchos basin. Calibrated soil parameters, flows for calibration and validation periods, statistical performance of the model, and an annual long-term analysis are addressed. Results show, in general, good model performance in representing the hydrologic dynamic of the study basin.

## 4.1 CALIBRATION PARAMETERS

Several simulations were carried out in order to estimate the best parameters of the model. Because of high accumulated base flow at the beginning of the simulations, one of the most difficult tasks was to estimate the hydraulic conductivity for the second model layer to reproduce a satisfactory base flow, especially when the model was run for long periods. The main calibrated parameters for the soil moisture method are shown in Table 4-1 for each catchment located in the study area. Hydraulic conductivity ranges from 45 to 180 mm/month for the first layer, with an initial storage from 5- 30%. Because of the desert zone in the lower basin, the lowest values are estimated for the catchments Ojinaga, Peguis, and Luis L. Leon; in contrast, high values are computed for catchments located in the upper basin such as Llanitos and Pico de Aguila with more than 20%.

For the second layer, hydraulic conductivity ranges from 3-45 mm/month and the initial storage from 5-20%. In addition, the root water capacity varies from 250 mm to 600 mm, with high values for catchments located in the lower basin (e.g., Ojinaga and

Peguis) where the soils are deeper. High values of deep layer water capacity were estimated, which could indicate the existence of deep aquifers such those located in the middle and lower basin.

Table 4-1: Calibrated upper and lower soil parameters for the Rio Conchos Basin

| Catchment | Drainage area (km$^2$) | Upper Zone | | | | Lower Zone | | |
|---|---|---|---|---|---|---|---|---|
| | | Water Capacity (mm) | Conductivity (mm/month) | Water Storage (%) | Flow Direction | Water Capacity (mm) | Conductivity (mm/month) | Water Storage (%) |
| Peguis | 7999.30 | 400 | 120 | 5 | 0.00 | 1500 | 25 | 5 |
| Sacramento | 1042.61 | 280 | 60 | 10 | 0.00 | 6400 | 6 | 20 |
| Las Burras | 11309.47 | 350 | 180 | 20 | 0.05 | 1850 | 45 | 20 |
| Luis L. | 5085.51 | 400 | 60 | 5 | 0.00 | 1200 | 6 | 20 |
| FCO. I | 1211.35 | 280 | 60 | 20 | 0.05 | 2000 | 45 | 20 |
| Villalba | 9556.86 | 250 | 100 | 30 | 0.06 | 2000 | 5 | 20 |
| Conchos | 1114.39 | 250 | 45 | 25 | 0.05 | 1800 | 45 | 20 |
| Jimenez | 4422.96 | 350 | 60 | 20 | 0.05 | 1500 | 5 | 10 |
| Chuviscar | 106.09 | 280 | 70 | 10 | 0.00 | 3600 | 10 | 20 |
| El Rejon | 146.85 | 280 | 70 | 10 | 0.00 | 3600 | 10 | 20 |
| Chihuahua | 399.99 | 280 | 70 | 10 | 0.00 | 6000 | 12 | 15 |
| Llanitos | 1829.93 | 400 | 100 | 30 | 0.05 | 2500 | 7 | 20 |
| Pico de | 647.61 | 350 | 60 | 20 | 0.05 | 1350 | 3 | 10 |
| San | 821.16 | 350 | 60 | 20 | 0.05 | 1200 | 3 | 10 |
| San Gabriel | 305.85 | 350 | 60 | 20 | 0.05 | 1200 | 3 | 10 |
| Puente | 1270.66 | 250 | 60 | 20 | 0.05 | 1500 | 3 | 10 |
| Parral | 363.79 | 275 | 60 | 20 | 0.05 | 4000 | 45 | 20 |
| Colina | 259.06 | 280 | 60 | 25 | 0.05 | 2400 | 45 | 20 |
| La Boquilla | 18931.98 | 300 | 120 | 30 | 0.15 | 3000 | 10 | 15 |
| Ojinaga | 983.47 | 600 | 80 | 5 | 0.00 | 1500 | 25 | 5 |

## 4.2 MODEL PERFORMANCE

### 4.2.1 Calibration Period

Monthly simulated and naturalized streamflows for the calibration period (1980 - 1989) are shown in Figure 4-1 for two stations: La Boquilla and Ojinaga. La Boquilla is an upstream station at the outlet of the largest sub-catchment in the basin and Ojinaga is at the downstream outlet of the basin at the confluence with the Rio Grande. The model reproduces the high flows more accurately than the low flows. Figure 4-2 shows the average monthly flows for the calibration period at the two stations. Simulated flow represents between 85% and 95% of the naturalized flow; the model tends to reproduce well the hydrological response of the basin. Mostly, the differences between naturalized and simulated flows are small.

Figure 4-3 shows the simulated and naturalized annual streamflow where simulated flow for the La Boquilla station is less than naturalized, and the average error for Ojinaga station is about 2%. Relationships between monthly simulated and naturalized flows show a strong correlation (see Figure 4-4), indicating good model performance (correlation of 0.95 for Ojinaga station). The goodness-of-fit of the model is also supported by the Nash index which is described with further detail in the statistical analysis section below.
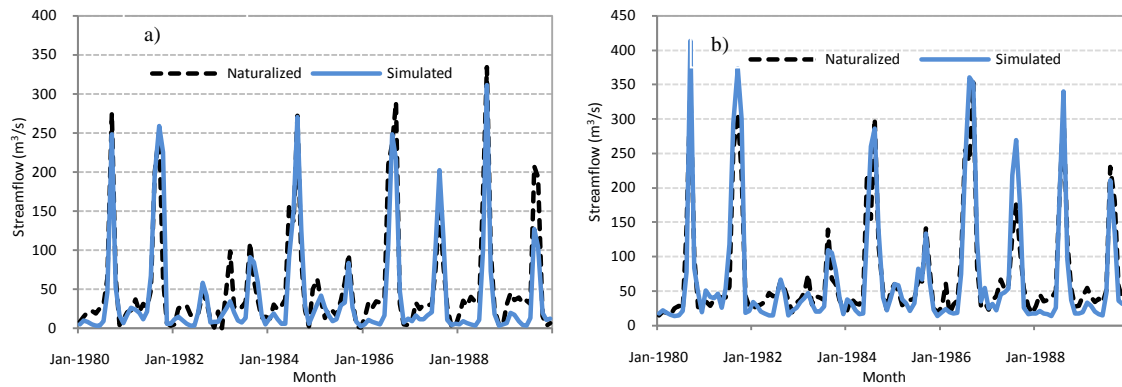
Figure 4-1: Natural and simulated monthly flow for the calibration period. a) La Boquilla and b) Ojinaga.
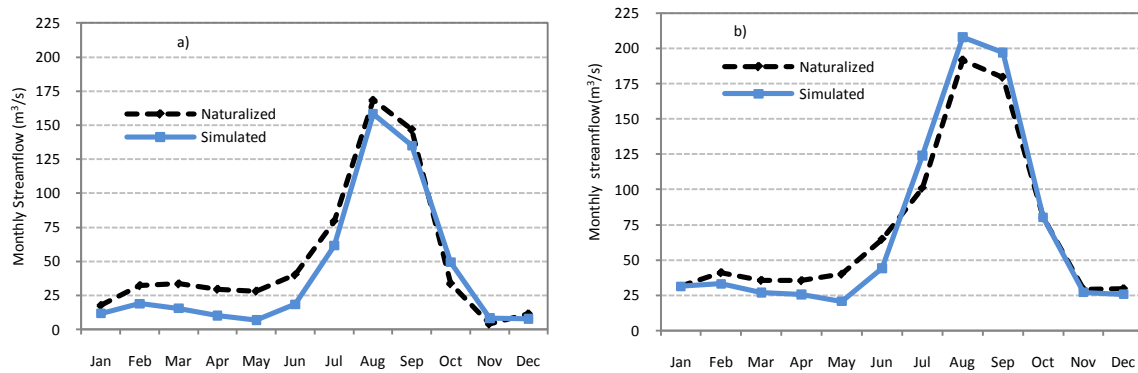


Figure 4-2: Monthly average naturalized and simulated streamflow for the calibration period: a) La Boquilla and b) Ojinaga.
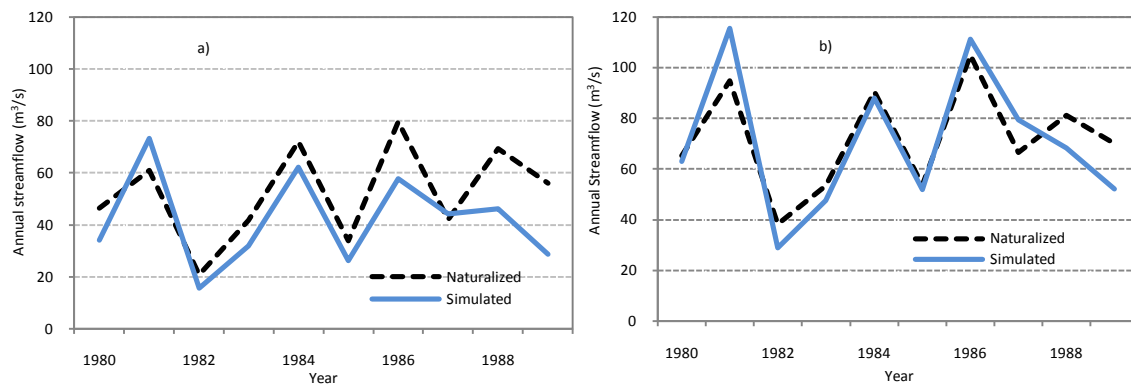


Figure 4-3: Annual naturalized and simulated streamflow for the calibration period: a) La Boquilla and b) Ojinaga.

87
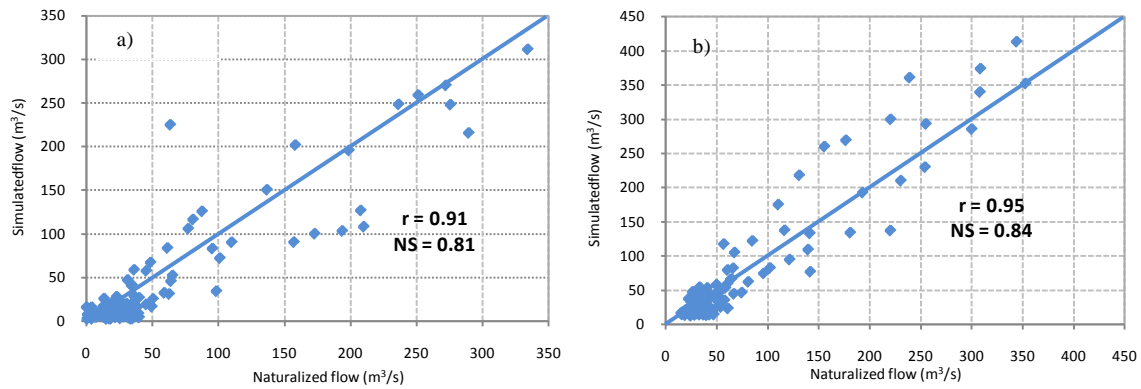
Figure 4-4: Relationship between monthly naturalized and simulated streamflow for the calibration period: a) La Boquilla and b) Ojinaga.

### 4.2.2 Validation Period

Figure 4-5 shows the validated monthly flow from 1990-1999. The model reproduced the drought conditions in the basin; estimation of the natural flow was much better than the calibration period, with errors less than 1% and 11% for Ojinaga and La Boquilla, respectively. Relationship between modeled and natural flows shows a strong correlation for the Ojinaga (0.94) and La Boquilla (0.84) stations (Figure 4-8). In general, the model exhibits good performance in reproducing the flows in all control stations; computing accurately the peak and low flow. In addition, average monthly flows for the ten years validation period (Figure 4-6) show an excellent model performance, with an exception in September where significant difference in magnitude is noted for La Boquilla. Similarly, naturalized annual flows are represented very adequately, with medium differences in 1997 and 1998 for Ojinaga, and 1991 and 1998 for La Boquilla (Figure 4-7).
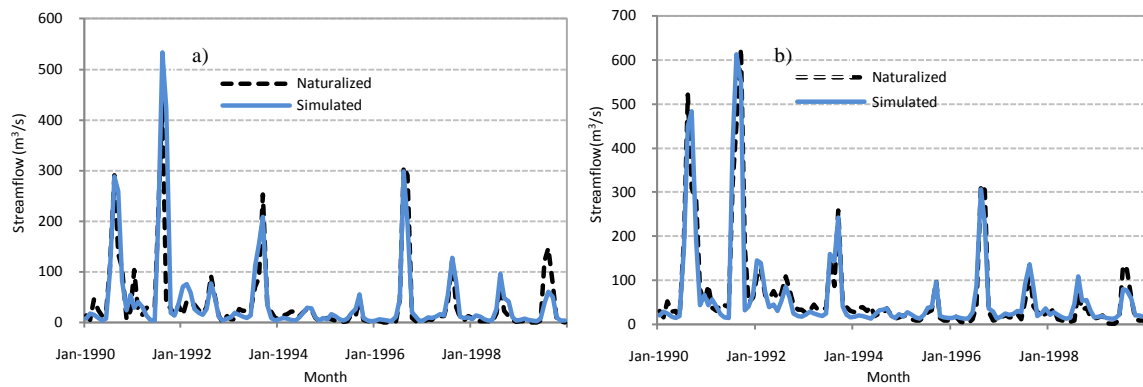
Figure 4-5: Monthly naturalized and simulated streamflow for the validation period: a) La Boquilla and b) Ojinaga.
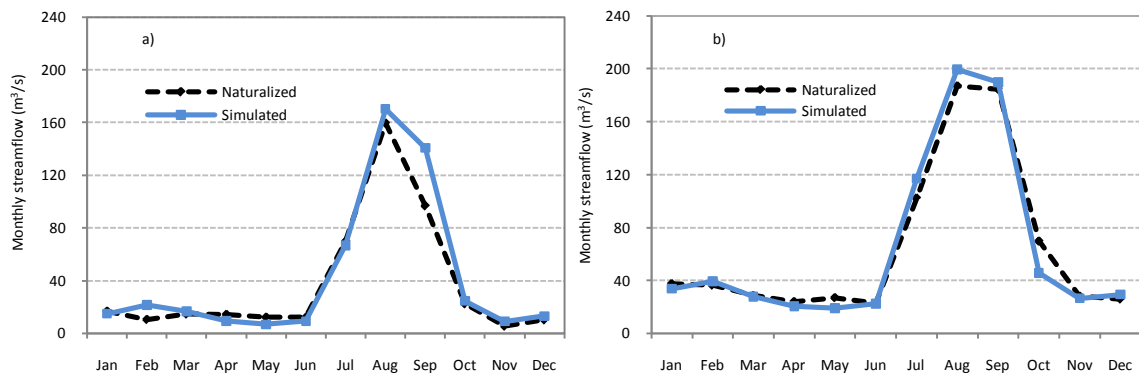


Figure 4-6: Monthly average naturalized and simulated streamflow for the validation period: a) La Boquilla and b) Ojinaga.
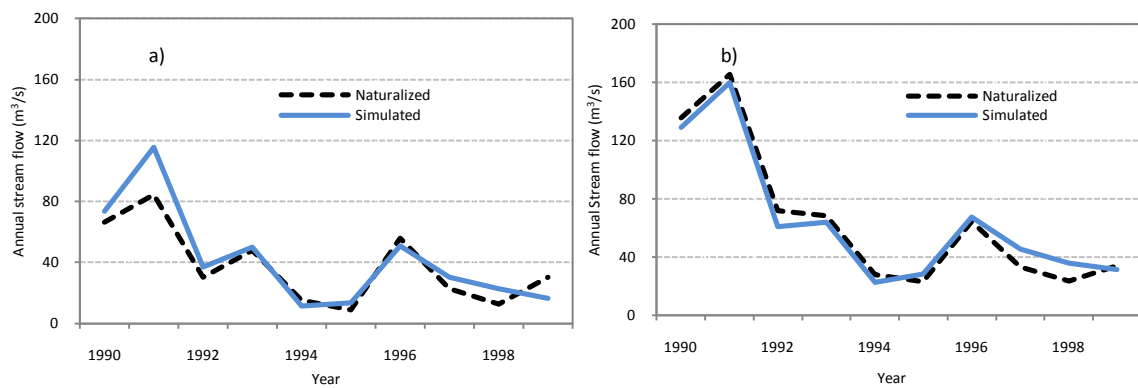


Figure 4-7: Annual naturalized and simulated streamflow for the validation period: a) La Boquilla and b) Ojinaga.
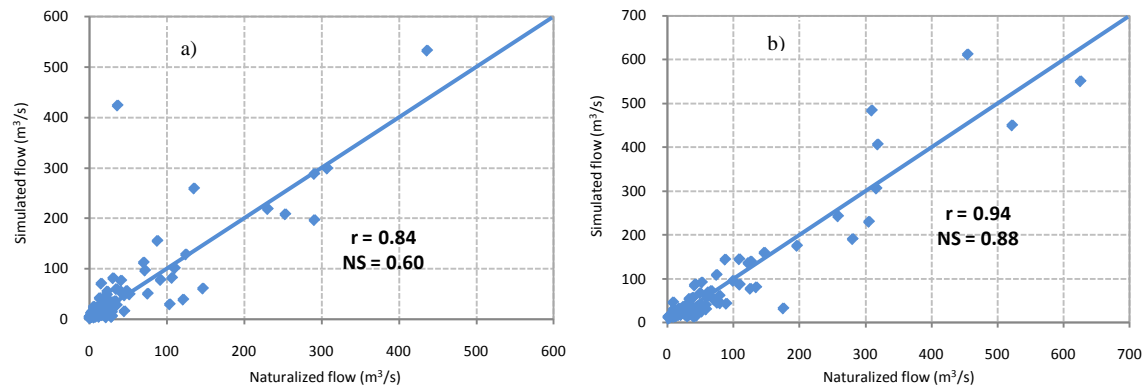
Figure 4-8: Relationship between monthly naturalized and simulated streamflow for the validation period: a) La Boquilla and b) Ojinaga.

## 4.3 STATISTICS

For the calibration and validation period, a statistical summary of the model performance is shown in Table 4-2. At most stations, the simulated monthly flow preserves the natural range of variability, depicted by the standard deviation. Likewise, the mean absolute error (MAE) and root mean square error (RMSE) were used to measure the deviation between the model outputs and the natural flows; MAE shows smaller deviation than the RMSE ($RMSE > MAE$). Annual flows show a small deviations; by contrast, the largest variance is found in monthly flows.

The volume error is small for Villalba, El Granero, and Ojinaga stations, with errors less than 6% for both periods. In all stations, most errors were less than 20%, except in the Rio Florido at Jimenez station where the error was greater than 30% in the calibration period. The biggest differences between flows are in La Boquilla and Las Burras, with volume errors of 19% and 14%, respectively; however, for the validation

90

period the errors decreased considerably (Table 4-2). The negative error indicates the model overestimates the flows in that station.

Likewise, Table 4-2 presents the Nash coefficients ($R$) for monthly flows ranging from 0.68 - 0.87 for the calibration period, and 0.60 - 0.88 for the validation period, indicating good model performance. According to the Table 3-4a, the model performance varies from good to very good. The Index of Agreement ($IA$) changes from 0.92 to 0.97 and from 0.91 to 0.97 for calibration and validation stages, respectively. In general, the model is more accurate in reproducing the flows in stations located in the middle and lower part of the basin, as shown by the Nash ($R$), Index of Agreement ($IA$), and correlation coefficients. Despite the good performance of the model, errors could be attributed to the uncertainty in estimating of natural flows and the average climatology data used for each sub catchment, groundwater interaction, as well as the complex hydrological characteristics of the upper basin (topography and size of catchments).

Table 4-2: Summary of statistical results for monthly simulated and naturalized flows

| Statistic | Calibration Period | | | | | |
|---|---|---|---|---|---|---|
| | Rio San Pedro at Villalba | Rio Conchos at La Boquilla | Rio Florido at Cd. Jimenez | Rio Conchos at Las Burras | Rio Conchos at El Granero | Rio Conchos at Ojinaga |
| Drainage Area (km$^2$) | 9556.2 | 20761.9 | 7468.2 | 52045.1 | 58679.3 | 67808.9 |
| Number months | 120 | 120 | 120 | 120 | 120 | 120 |
| Mean naturalized flow (m$^3$/s) | 11.45 | 52.13 | 5.46 | 81.45 | 78.32 | 71.66 |
| Mean simulated flow (m$^3$/s) | 11.31 | 41.87 | 7.28 | 69.86 | 75.52 | 70.36 |
| STDEV naturalized | 22.19 | 67.90 | 12.15 | 88.80 | 85.90 | 75.17 |
| STDEV simulated | 24.10 | 65.73 | 14.73 | 93.21 | 100.91 | 89.80 |
| Root Mean Square Error (m$^3$/s) | 12.57 | 29.72 | 7.15 | 31.54 | 33.70 | 30.07 |
| Mean Absolute Error (m$^3$/s) | 5.55 | 19.79 | 3.04 | 23.43 | 22.92 | 19.6 |
| Volume Error (%) | 1.19 | 19.50 | -33.44 | 14.12 | 3.34 | 1.70 |
| Nash-Sutcliffe Coefficient($E$) | 0.68 | 0.81 | 0.65 | 0.87 | 0.84 | 0.84 |
| Index of Agreement ($IA$) | 0.92 | 0.95 | 0.93 | 0.97 | 0.97 | 0.97 |
| Coefficient of correlation ($r$) | 0.85 | 0.91 | 0.88 | 0.95 | 0.95 | 0.95 |
| | Validation Period | | | | | |
| Number months | 120 | 120 | 120 | 120 | 120 | 120 |
| Mean naturalized flow (m$^3$/s) | 12.48 | 37.17 | 5.81 | 68.83 | 68.61 | 64.53 |
| Mean simulated flow (m$^3$/s) | 11.71 | 41.53 | 4.61 | 65.85 | 69.62 | 64.32 |
| STDEV naturalized | 29.23 | 69.59 | 15.13 | 104.23 | 99.07 | 101.56 |
| STDEV simulated | 29.52 | 80.64 | 11.78 | 109.87 | 116.57 | 105.17 |
| Root Mean Square Error (m$^3$/s) | 11.38 | 43.96 | 5.72 | 36.46 | 40.99 | 34.98 |
| Mean Absolute Error (m$^3$/s) | 4.99 | 17.44 | 2.32 | 21.89 | 23.66 | 20.72 |
| Volume Error (%) | 6.18 | -11.34 | 20.84 | 4.39 | -1.42 | 0.37 |
| Nash-Sutcliffe Coefficient ($E$) | 0.85 | 0.60 | 0.86 | 0.88 | 0.83 | 0.88 |
| Index of Agreement ($IA$) | 0.96 | 0.91 | 0.95 | 0.97 | 0.96 | 0.97 |
| Coefficient of correlation ($r$) | 0.92 | 0.84 | 0.94 | 0.94 | 0.94 | 0.94 |

## 4.4 LONG TIME PERIOD MODEL PERFORMANCE

Since that the hydrologic model will be used to assess future climate change effects on water availability each 20 years, the model performance was also evaluated for the entire period 1980-1999. Figure 4-9 shows the probability distribution function and confidence limits for naturalized and simulated annual flow. At Ojinaga (Figure 10 a),

small differences are noted between them, with errors less 1% on average. By contrast, the errors are higher at La Boquilla, less than 5%. Furthermore, the 95% confidence bounds for the lower, median, and upper quartiles are shown in Table 4-3. The largest flow difference is computed for the upper quartile (p=0.75) at La Boquilla. On average, small differences are computed for the median. Additionally, the model is very accurate in reproducing the maximum flows, with error less than 3% and 4% on average for the Ojinaga and La Boquilla.
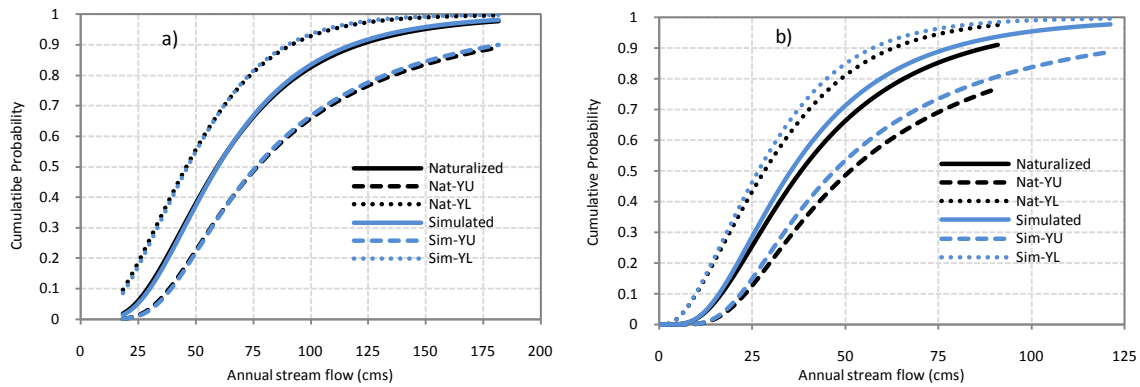


Figure 4-9: Cumulative probability and confidence limits (95% level) for the naturalized and simulated flow. Period 1980-1999. a) Ojinaga and b) La Boquilla.

Table 4-3: Upper (Up) and lower (Lw) limits computed by a 95% confidence level for annual flows

| Station | $P(X \leq x_n)$ | Period 1980-1999 | | | | | |
|---|---|---|---|---|---|---|---|
| | | Naturalized flow (cms) | | | Simulated flow (cms) | | |
| | | Up | Q | Lw | Up | Q | Lw |
| Ojinaga | 0.25 | 53 | 42 | 30 | 53 | 41 | 30 |
| | 0.50 | 77 | 60 | 46 | 76 | 59 | 47 |
| | 0.75 | 120 | 86 | 68 | 117 | 85 | 67 |
| La Boquilla | 0.25 | 32 | 25 | 17 | 31 | 24 | 16 |
| | 0.50 | 51 | 38 | 28 | 47 | 36 | 27 |
| | 0.75 | 86 | 58 | 44 | 78 | 54 | 41 |

**4.5 HISTORICAL CALIBRATION OF WATER PLANNING MODEL**

The planning model was calibrated using historical flows from four stream gages, historical storage volumes from five reservoirs, and historic water deliveries (including the flow requirement of the treaty at the Rio Grande confluence). Figure 4-10 shows a comparison between historical and simulated storage in La Boquilla reservoir for the period 1980-99. The performance of the model in simulating the monthly storages indicates a good agreement, with a coefficient Nash of 0.70 and a relative error less than 5%.

In addition, Figure 4-11 shows the simulated and historical total storages for five reservoirs located along to the Rio Conchos water system. Small differences are observed, except in the first and last year when the error is fairly significant. The initial and final conditions of the simulation period assumed in the hydrological planning model could be influencing this behavior. On overall, Nash–Sutcliffe coefficient of 0.67 is computed for the period 1980-1999.
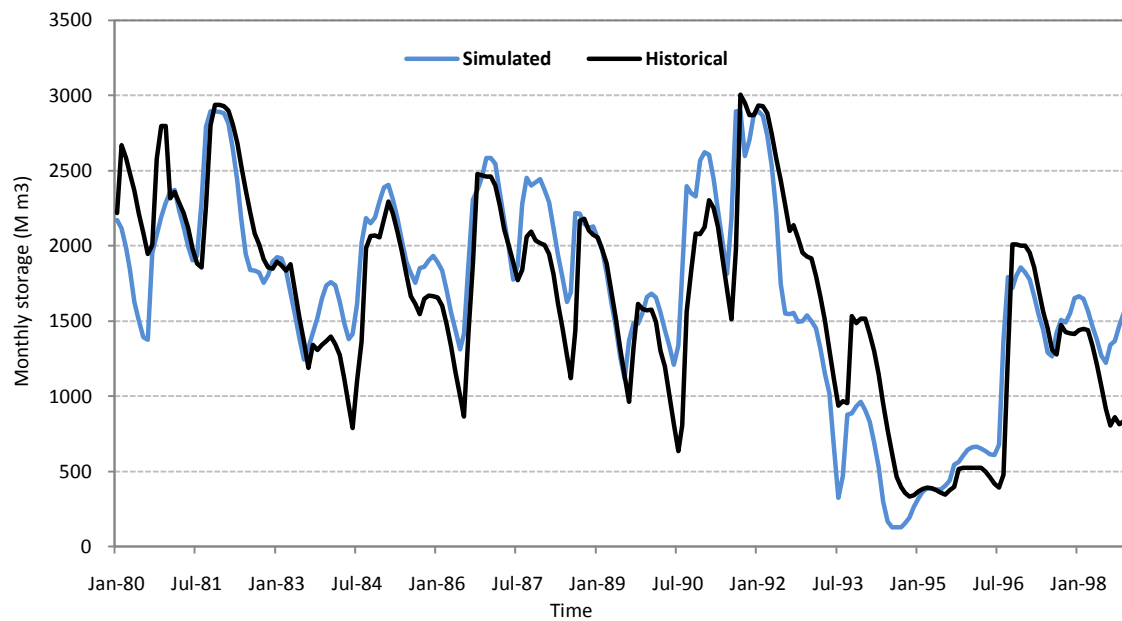
Figure 4-10: Comparison between historical and simulated storage for La Boquilla reservoir
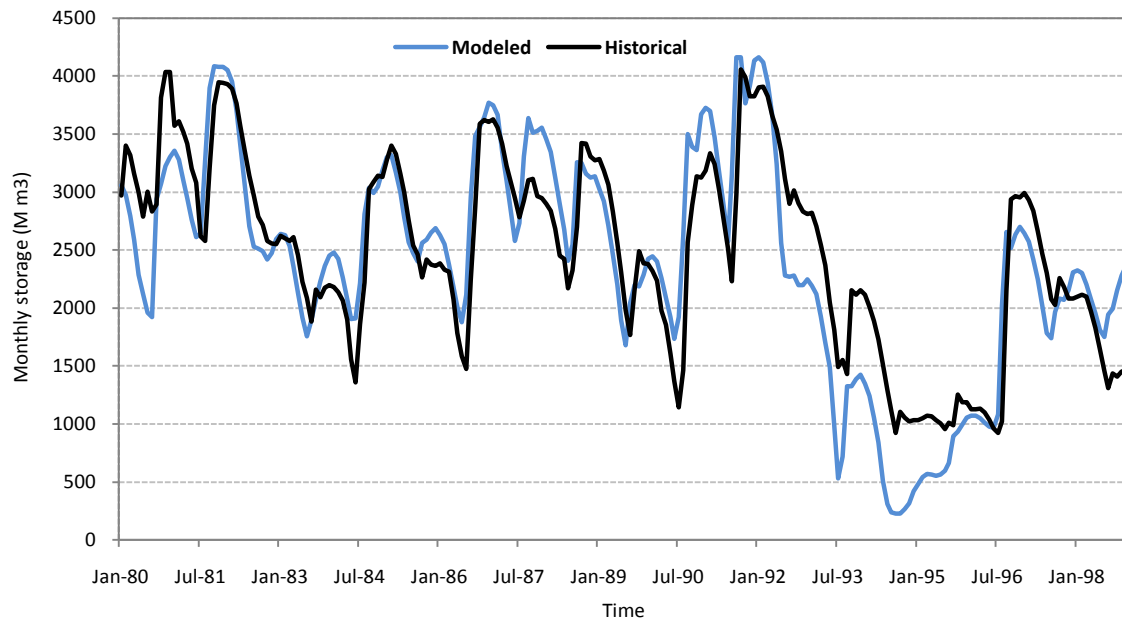


Figure 4-11: Comparison between historical and simulated total storage for five reservoirs in the Rio Conchos water system.

# Chapter 5: Climate Change Effects on Hydrologic Regimen of the Rio Conchos Basin

This section presents results of climate change impacts on Rio Conchos flow at Ojinaga, where Mexico delivers water to the US under the 1944 water treaty. The assessment includes an analysis of the performance of the GCMs for the main climate variables at the basin level, projections of temperature and precipitation for the Rio Conchos basin, streamflow under climate change (annual and monthly), wavelet analysis, and frequency analysis of maximum and minimum flows for the skill-weighted multi-model ensemble.

## 5.1 ANALYSIS OF HISTORICAL PERIOD CLIMATE DATA OF THE GENERAL CIRCULATION MODELS

Figure 5-1 shows the Cumulative Distribution Function (CDF) for annual temperature and precipitation (fitted using a log normal distribution model) simulated by 5 GCMs in the Rio Conchos basin, and for the reference period 1980-1999. Results indicate that the CGCM31 and Hadley models reproduce better the historical pattern of temperature for the Conchos basin, with a error less than 1% for P= 0.50.Nevertheless, the other models also follow the same trends but with less accuracy (Error range from 1-2%). In general, comparisons with annual precipitation indicate that the ECHAM5, CGCM31, and MIROC32 simulations represents better the historical conditions of the basin than HadCM3 and CCSM3 models (Figure 5-1 b). Although most models simulate the lower quartile well (Pr = 0.25), the ECHAM5 values are more close to the historical values, more rainfall is simulated by the CCSM3 and CGCM31 models, and less rainfall

for the MIROC32 and HadCM3 models, with differences ranging from 4% to -8%, respectively. For the upper quartile (Pr = 0.75), all models project less precipitation, but ECHAM5, CGCM31, and MIROC32 are more accurate; for instance, the average precipitation from these models at the 75th percentile is 490 mm compared to 525 mm in the historical data (an error of 6.6%), versus 440 mm for the CCSM3 and HadCM3 models.

The weighted multi model ensemble from GCM downscaled climate outputs suggests that annual temperature for the Rio Conchos basin is slightly underestimated by 0.20 degrees Celsius on average (Figure 5-1a). However, annual precipitation shows a larger error which represents around 7% being larger for values greater than 500 mm.
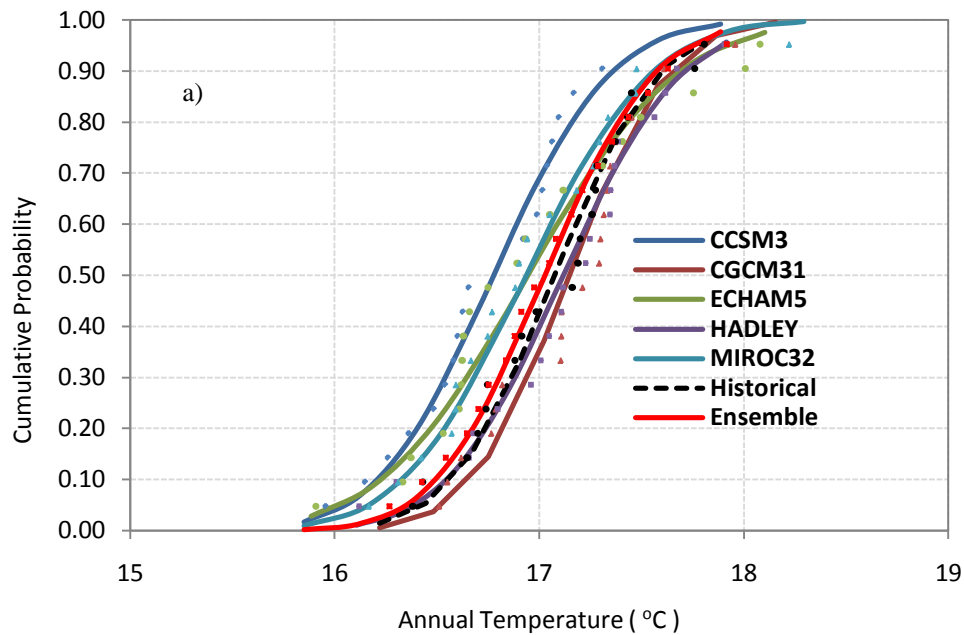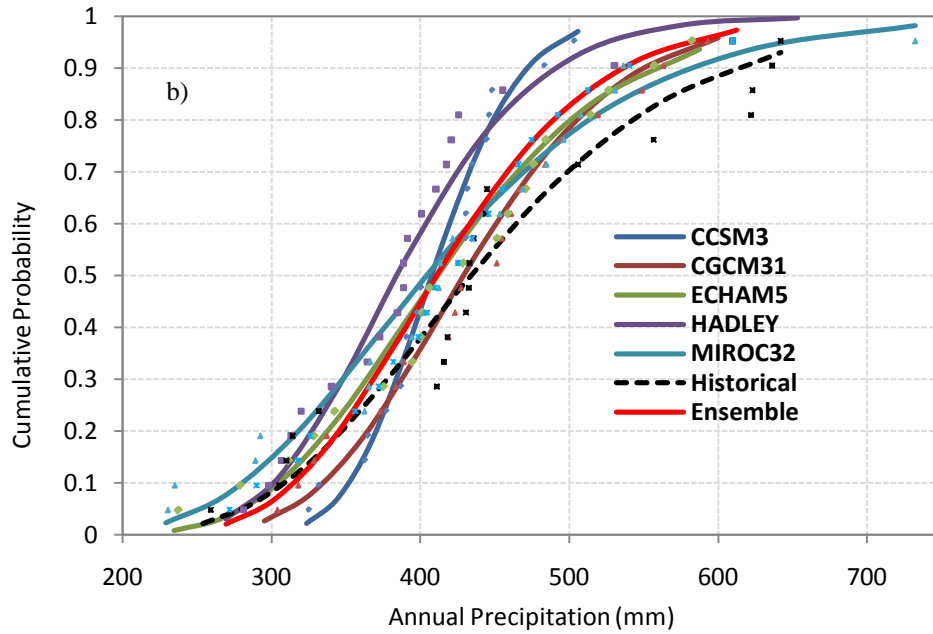
Figure 5-1: CDF Annual climate data simulated by 5 GCMs for the Rio Conchos. Period 1980-1999. The dotted line corresponds to historical values. a) Temperature and b) Precipitation

### 5.1.1 Average monthly GCM performance

Figure 5-2 (a) shows the seasonal temperature Bias in degrees Celsius computed on monthly average. The uncertainty range in the model prediction is given by ± $\sigma_{\Delta t}$ computed on the base of five GCMs and centered on the ensemble. This condition assumes that historical changes followed a Gaussian PDF. Maximum and minimum bias is also shown with dashed black lines. On the ensemble, monthly temperature is underestimated by 0.15 $^{o}$C, with a range from +0.20 $^{o}$C to -0.40 $^{o}$C which represent an error less than 2%. For August and September, GCMs overestimate the historical temperature by a range of 0.10-0.30 $^{o}$C.

Figure 5-2 (b) presents the monthly precipitation bias in percentage for the Rio Conchs basin. The ensemble average biases are generally varying between +5% and -

98

30%, with a clear predominance of negative biases, which means an underestimate of precipitation, especially in winter and spring seasons. However, these biases are not so important in terms of precipitation amount, since the rainfall period in the Rio Conchos basin is located from July to September. In these months, the ensemble biases are around within ±10% of observed precipitation.
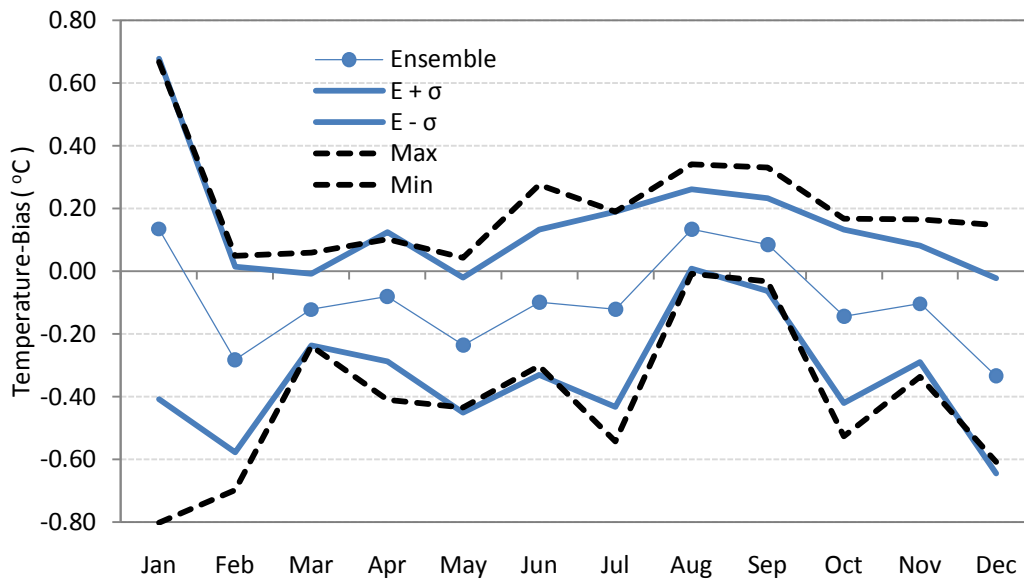


Figure 5-2a: Ensemble monthly temperature bias (%). Blue lines represent the ensemble ± the standard deviation of five GCMs predictions. Dashed black lines show the maximum and minimum values computed on average monthly.
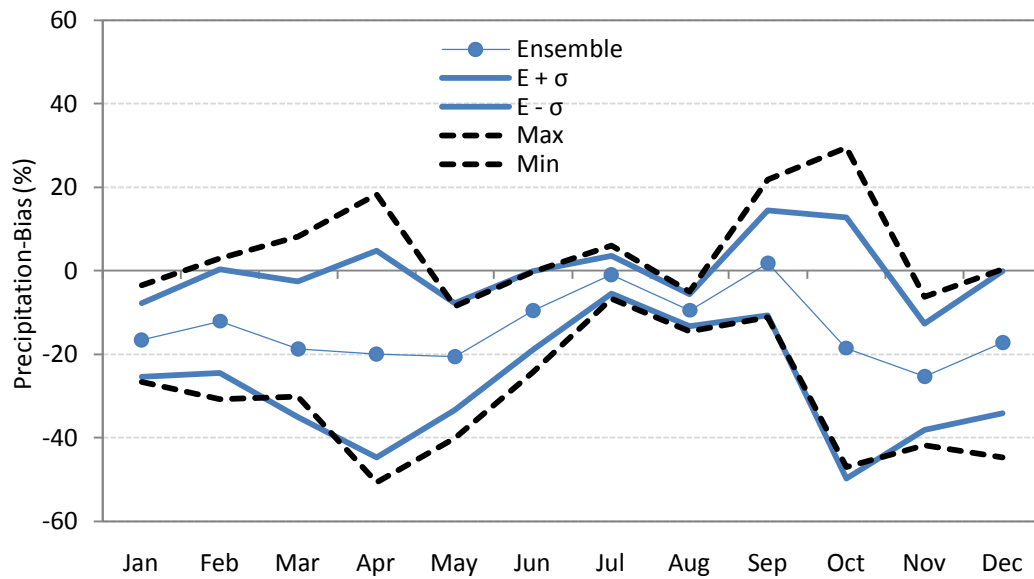
Figure 5-2b: Ensemble monthly precipitation bias (%). Blue lines represent the ensemble ± the standard deviation of five GCMs predictions. Dashed black lines show the maximum and minimum values computed on average monthly.

## 5.2 TEMPERATURE AND PRECIPITATION PROJECTIONS

### 5.2.1 Temperature

Projections for the middle (2040-2059) and end (2080-2099) of this century indicate that the annual temperature will increase by about 2.34 $C^o$ and 3.91 $C^o$ for scenario A1B and 2.24 $C^o$ and 4.89 $C^o$ for scenario A2 (Table 5-4). Figure 5-3 shows the annual temperature anomaly for the period 2040-99, relative to the period 1980-99, for both scenarios, including each of the five GCMs and the skill-weighted multi-model ensemble. A positive trend is indicated for the whole period. Both scenarios show similar behavior up to 2070; after which scenario A1B has less change than A2 (Figure 5-3). Likewise, Table 5-4 shows the projection of the annual change and Table 4-5 presents the

seasonal change of the temperature relative to 1980-99, at basin level for both climate scenarios.
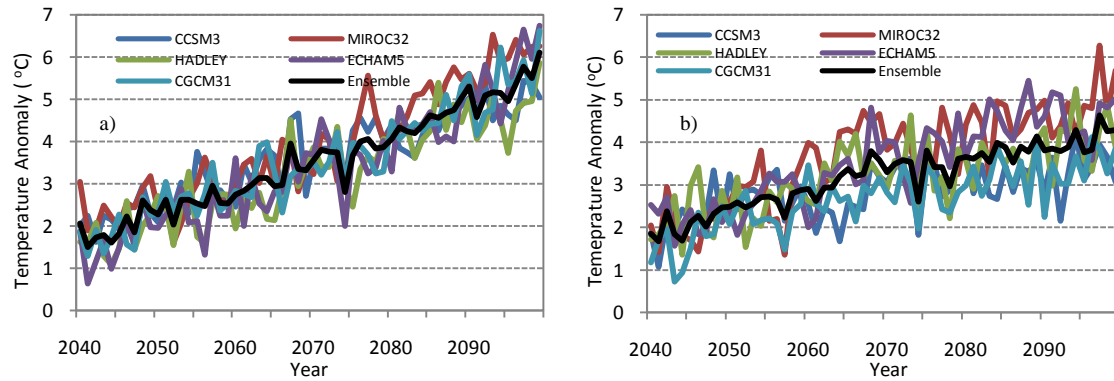


Figure 5-3: Annual temperature anomaly in the Rio Conchos basin for the period 2040-99 relative to 1980-99. a) Scenario A2, and b) Scenario A1B. The black line indicates the skill-weighted multi-model ensemble.

*Uncertainty range in temperature prediction*

Figure 5-4 shows the uncertainty range in the annual temperature prediction by GCMs during the period 2040-2099, under climate change scenarios A2 and A1B. The weighted ensemble with corresponding upper and lower uncertainty limits, which are computed adding or differentiating to the ensemble, the standard deviation of annual prediction from five general circulation models. The Maximum and minimum temperature limits are also shown. The range of uncertainty in the prediction is greater for A1B than A2. In general, average annual temperature for the period 2080-99 is projected by GCMs to increase by 4.89 $^{o}$C with an uncertainty range of $\pm$ 0.57 $^{o}$C, under scenario A2; and 3.9 $^{o}$C, with 0.81 $^{o}$C, under scenario A1B. Maximum and minimum

101

values simulated by five GCMs could be considered as a measure of the maximum uncertainty range that does not take into account the weighted ensemble time series. Highest and lowest values are close to upper and lower limits computed using the standard deviation.
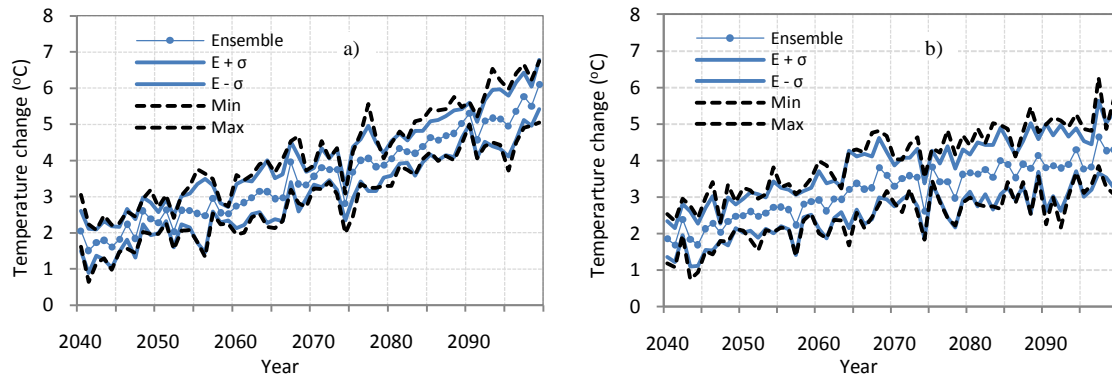


Figure 5-4: Uncertainty range in temperature prediction for the Rio Conchos basin. Weighted ensemble (blue circles), the upper and lower bound (continue blue lines, E ± σ), and the maximum and minimum changes simulated by individual GCMs (dashed black lines). a) Scenario A2 and b) Scenario A1B.

Table 5-4: Annual change ($^o$C) and uncertainty range of temperature relative to the 1980-99 period

| Period | A1B | A2 |
|---|---|---|
| 2040-59 | $2.34 \pm 0.53$ | $2.24 \pm 0.47$ |
| 2060-79 | $3.28 \pm 0.71$ | $3.42 \pm 0.57$ |
| 2080-99 | $3.91 \pm 0.81$ | $4.89 \pm 0.57$ |

Table 5-5: Seasonal change ($^o$C) and uncertainty range of temperature relative to the 1980-99 period

| Season | A1B | | | A2 | | |
|---|---|---|---|---|---|---|
| | 2040-59 | 2060-79 | 2080-99 | 2040-59 | 2060-79 | 2080-99 |
| Winter | $1.96 \pm 0.20$ | $2.72 \pm 0.44$ | $3.32 \pm 0.60$ | $1.81 \pm 0.24$ | $2.90 \pm 0.50$ | $4.36 \pm 0.45$ |
| Spring | $2.48 \pm 0.21$ | $3.41 \pm 0.34$ | $4.07 \pm 0.61$ | $2.36 \pm 0.22$ | $3.64 \pm 0.20$ | $5.02 \pm 0.35$ |
| Summer | $2.38 \pm 0.46$ | $3.64 \pm 1.05$ | $4.03 \pm 1.09$ | $2.29 \pm 0.61$ | $3.61 \pm 0.47$ | $4.90 \pm 0.89$ |
| Fall | $2.46 \pm 0.24$ | $3.33 \pm 0.38$ | $4.21 \pm 0.58$ | $2.45 \pm 0.45$ | $3.54 \pm 0.34$ | $5.28 \pm 0.53$ |

**5.2.2 Precipitation**

Figure 5-5 shows the projected precipitation anomalies computed for the same time period mentioned above, for both scenarios. Most models do not agree in estimating precipitation, while CCSM3 and Hadley Model show a positive trend, MIROC32, ECHAM31, and CGCM31 show a negative trend during the period of analysis. The skill-weighted multi-model ensemble indicates a slight negative trend for both scenarios, especially in the period 2060-79 when projected precipitation is reduced between 10 to 25mm/yr in both scenarios. For the end of the century, precipitation is reduced by more than 10% for scenario A2 and 7% for A1B (Table 5-6). Additionally, seasonal analysis indicates a major increment of temperature for winter, fall, and spring for scenarios A1B and A2. Precipitation is projected to be further reduced in winter and spring for both scenarios; with greater reductions in the periods 2060-2079 and 2080-2099 (Table 5-7).
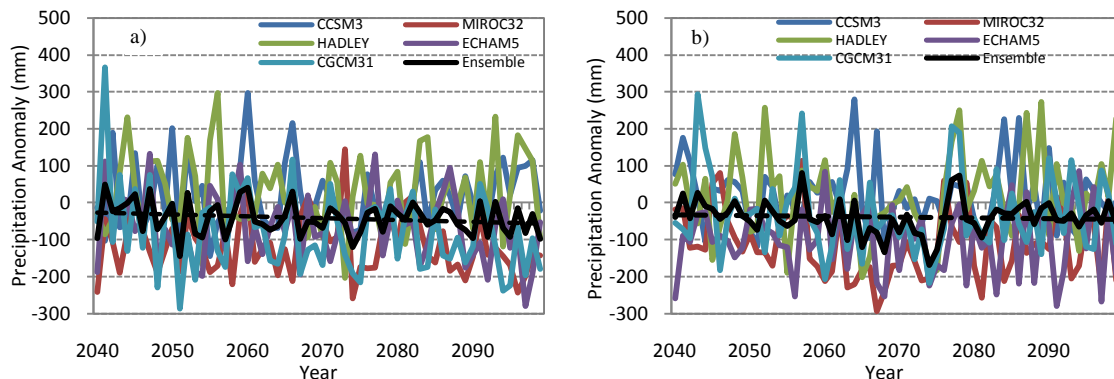


Figure 5-5: Annual precipitation anomaly for the Rio Conchos River basin for the period 2040-99 relative to 1980-99. a) Scenario A2, and b) Scenario A1B. The black line indicates the skill-weighted multi-model ensemble.

103

*Uncertainty range in precipitation prediction*

The range of precipitation prediction uncertainty by GCMs is presented in Figure 5-6 for climate change scenarios in the Rio Conchos basin. Under scenario A2 ( Figure 5-6a), precipitation changes are equally distributed between positive and negative values during the period 2065-2090; however, high variability during the period 2040-59 and 2090-2099 could be related to the ENSO frequency in the General Circulation Models. Likewise, it suggests the disagreement by GCMs in precipitation prediction; for instance, while Hadley and CCSM3 models project mostly positive changes in precipitation, MIROC32 and ECHAM5 predicts negative changes. In general, precipitation is projected to decrease by 7%, with an uncertainty range of ± 25% for the period 2040-59, and 11%, with ± 24% for the period 2080-99. The impact is similar under the scenario A1B but with more negative values during the period 2060-79, and with greater variability for the period 2080-2090.

Results show a high uncertainty level of general circulation models in predicting annual and season precipitation (Figure 5-6 and Table 5-7). Fundamentally, spatial resolution, numerical techniques, parameterization of local and regional climate processes (for instance precipitation), initial and boundary conditions used by each model, are the main uncertainty sources in GCMs (Karl 2002, Wood et al. 2004, Fowler et al. 2006, Ruiz-Barradas et. al, 2006).
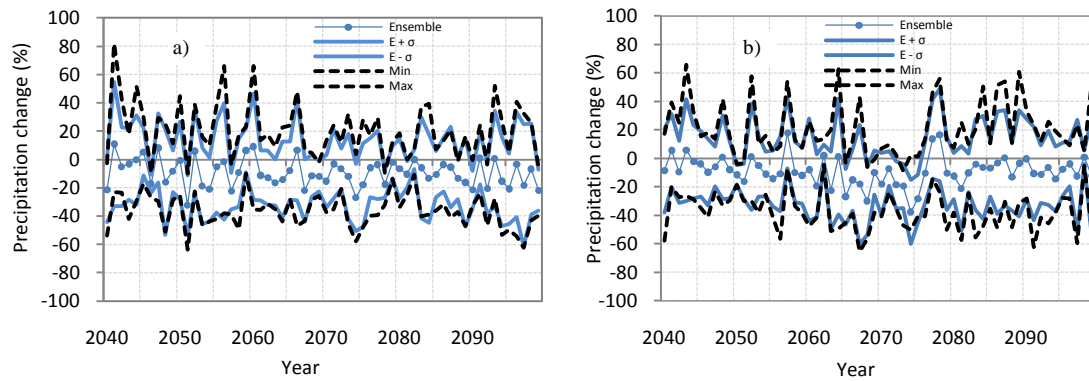
Figure 5-6: Uncertainty range in precipitation prediction for the Rio Conchos basin. Weighted ensemble (blue circles), the upper and lower bound (continue blue lines, E ± σ), and the maximum and minimum changes simulated by individual GCMs (dashed black lines). a) Scenario A2 and b) Scenario A1B.

Table 5-6: Annual change (%) and uncertainty range of precipitation relative to the 1980-99 period

| Period | A1B | A2 |
|---|---|---|
| 2040-59 | -5.4 ± 22 | -7.3 ± 25 |
| 2060-79 | -13.3 ± 23 | -10.2 ± 21 |
| 2080-99 | -7.9 ± 26 | -10.6 ± 24 |

Table 5-7: Seasonal change (%) and uncertainty range of precipitation relative to the 1980-99 period

| Season | A1B | | | A2 | | |
|---|---|---|---|---|---|---|
| | 2040-59 | 2060-79 | 2080-99 | 2040-59 | 2060-79 | 2080-99 |
| Winter | -30.5 ± 23 | -30.8 ± 27 | -33.28 ± 12 | -21.3 ± 25 | -31.58 ± 32 | -49.02 ± 25 |
| Spring | -28.9 ± 19 | -38.0 ± 28 | -35.02 ± 37 | -21.63 ± 11 | -29.88 ± 17 | -33.18 ±28 |
| Summer | -1.6 ± 15 | -10.3 ± 23 | -4.88 ± 18 | -4.28 ± 18 | -6.69 ± 15 | -6.27 ± 23 |
| Fall | 2.5 ± 25 | -7.3 ± 29 | 1.45 ± 41 | -6.43 ± 26 | -5.12 ± 21 | -0.65 ± 43 |

Percentage of annual change is computed on the historical annual average precipitation 1980-1999 which was around 448 mm. Seasonal changes are computed on

cumulated precipitation for each historical season, which are 43 mm for winter, 29 mm for spring, 256 mm for summer, and 120 mm for fall.

### 5.3 NATURALIZED STREAMFLOW

An analysis of streamflow changes for the period 1940-1999 at Ojinaga station was performed to determine how these are linked to naturally varying climatic patterns, such as El Niño-Southern Oscillation (ENSO) and the Pacific Decadal Oscillation (PDO). This consideration is important for water resources planning since in the next sections changes in streamflows under climate change and their connections to climate events are discussed. Figure 5-7 shows the naturalized annual streamflow for the period 1940-1999 (Brandes, 2003) at Ojinaga station in the Rio Conchos. By simple inspection, an oscillation of about 20 years is observed. In general, flow tends to be low from 1950 to 1970 and then high from 1970 to 1990. On average, negative and positive trends alternate in about 20-year cycles. The period from 1992 to 2003 is a notable drought in the basin.

Moving average reveals four long periods of flow variability. One from 1940-1958 characterized by a transition period with regular flows until 1948; from which, flows decreased significantly with regard to the average (extreme drought during 1948-1956). A second period from 1958-1968 is also characterized by low flows (severe drought from 1961-1965); a third period from 1968-1992 with high flows (above the average), and finally, a fourth period from 1992 -1999 with a marked drought, with flow rates below average. Current trends of annual flows can be analyzed using other

106

techniques such as the wavelet function to assess temporal oscillations of the flow and its

relation with climate patterns.
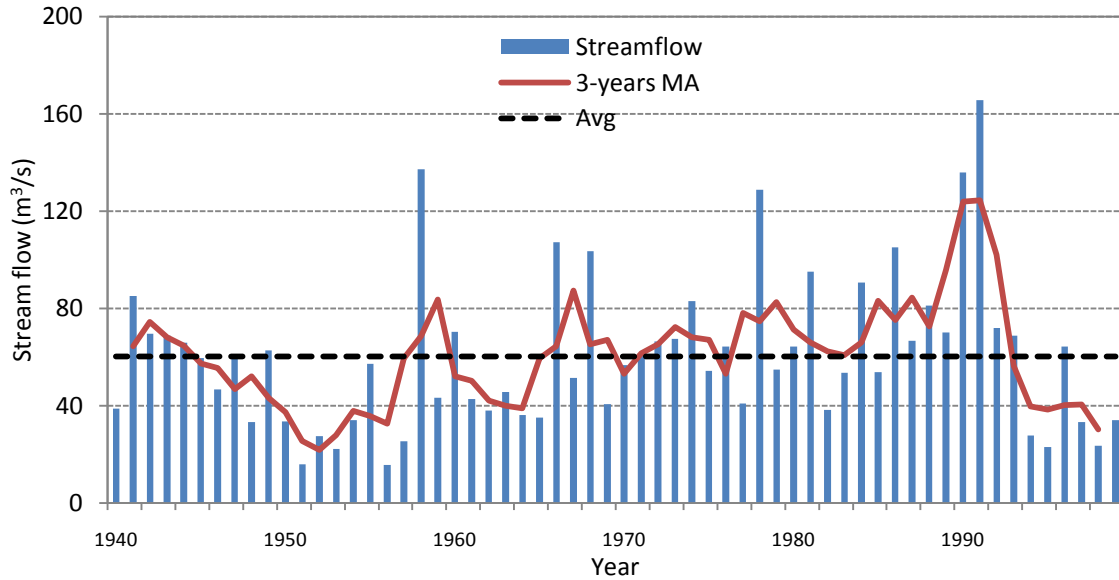


Figure 5-7: Naturalized historic annual flow (m3/s) at Ojinaga in the Rio Conchos (1940-1999). Source: Brandes (2003)

## 5.4 WAVELET ANALYSIS

### 5.4.1 Streamflow and its Relationship with El Niño-Southern Oscillation (ENSO)

Figure 5-8 shows the scale average wavelet power for the streamflow and ENSO

index, for the 2-3 year and 3-6 year bands, respectively. In general, the flow at Ojinaga

has a weak negative correlation to ENSO with oscillations of about 2-3 years (correlation

coefficient = -0.32 on average, Table 5-8). The 2-3 years band exhibits negative and

positive correlation alternating from 1940-1959, with a significant negative correlation of

-0.67 for the entire period. From 1960-1999, ENSO is negatively correlated to flows,

with an overall coefficient of -0.58. A weak positive correlation is computed for the period 1980-1984 (0.01).

For the 3-6 years band, a strong negative correlation (-0.70) is estimated for the period 1970-1984. However, ENSO is positively correlated to streamflow for the period 1940-1969 (0.34) with no significant correlation during 1955-1959 (0.04). A weak negative correlation (-0.05) is computed for the period 1985-1999. In general, 25% and 50% of the periods show a positive correlation for the 2-3 and 3-6 years bands, respectively. For the total analysis period (1940-1999), streamflow variation in the 2-3 and 3-6 years bands is correlated with ENSO, with correlation values of -0.32 and 0.28, respectively.
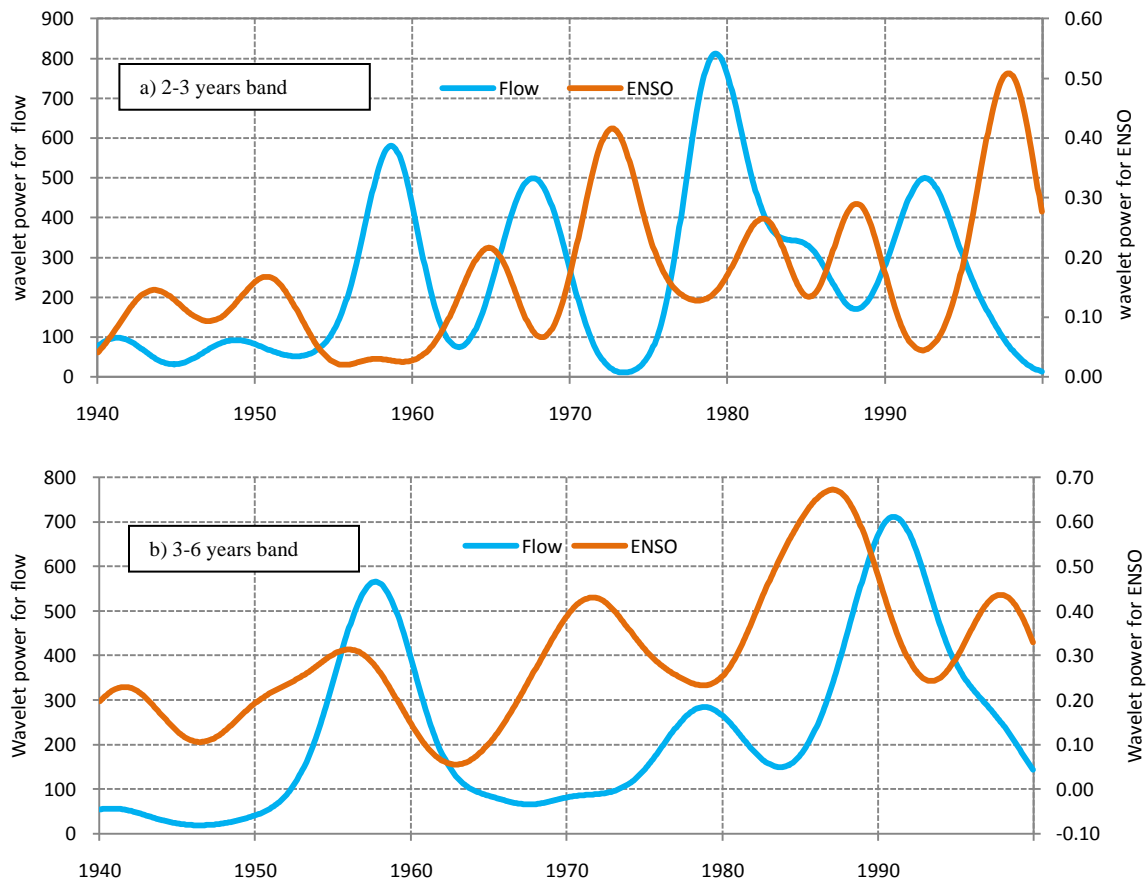
Figure 5-8:  Wavelet power for ENSO index and flows in the Rio Conchos at Ojinaga: a) 2-3 years bands, and b) 3-6 years band

### 5.4.2 Streamflow and its Relationship with the Pacific Decadal Oscillation (PDO)

The PDO climate pattern was analyzed for scale-average between streamflow periods of 5-10 and 8-15 years in order to show the oscillation whose persistence can last up to 30 years. Figure 5-9 shows the wavelet power for the PDO and streamflow at Ojinaga station. For the 5-10 years band, streamflow is positively correlated to the PDO for most periods (Table 5-8), with exceptions during 1955-1959 (-0.75) and 1975-1979 (-0.34). Similarly, the 8-15 years band shows a strong positive correlation between the

PDO index and streamflow; exceptionally, negative values are observed for the first ten years of the analysis period. By contrast, no significant dependence is noted for the period 1975-1979 (-0.05). Considering the complete analysis period (1940-1999), the streamflow in the 8-15 years band has a strong correlation (0.81) to the PDO index; in contrast, the 5-10 years band has a very weak correlation (0.1). Likewise, negative correlation for both bands could indicate some change points in the streamflow activity in study basin reflecting changes in intensity of the PDO index and changes in the dominant pattern of atmospheric circulation in this basin.

In general, these results show that streamflows in the Rio Conchos basin are negatively correlated to ENSO and positively correlated to PDO. This pattern can help explain the natural variability of the streamflow under potential climate change in the next decades. A comparison between the average wavelet power (8-15 year band) for the A2 and A1B emission scenarios with the historical period 1940-99 is discussed in the next section.

Other researchers have not studied this point for the Rio Conchos; however, the results are consistent with studies carried in other regions of North Mexico and the United States such Muñoz et al. (2009) and Englegart and Douglas (2002) who agree that ENSO and precipitation anomalies are negatively correlated. On the other hand, long term influences studied by Muñoz et al. 2009 in the Rio Yaqui Basin showed that warm PDO is related to high precipitation in northern Mexico during winter season. In addition,

a negative relationship between ENSO and streamflow in the Rio Conchos basin may be demonstrated by the El Niño phase occurrence in 1997-1998.
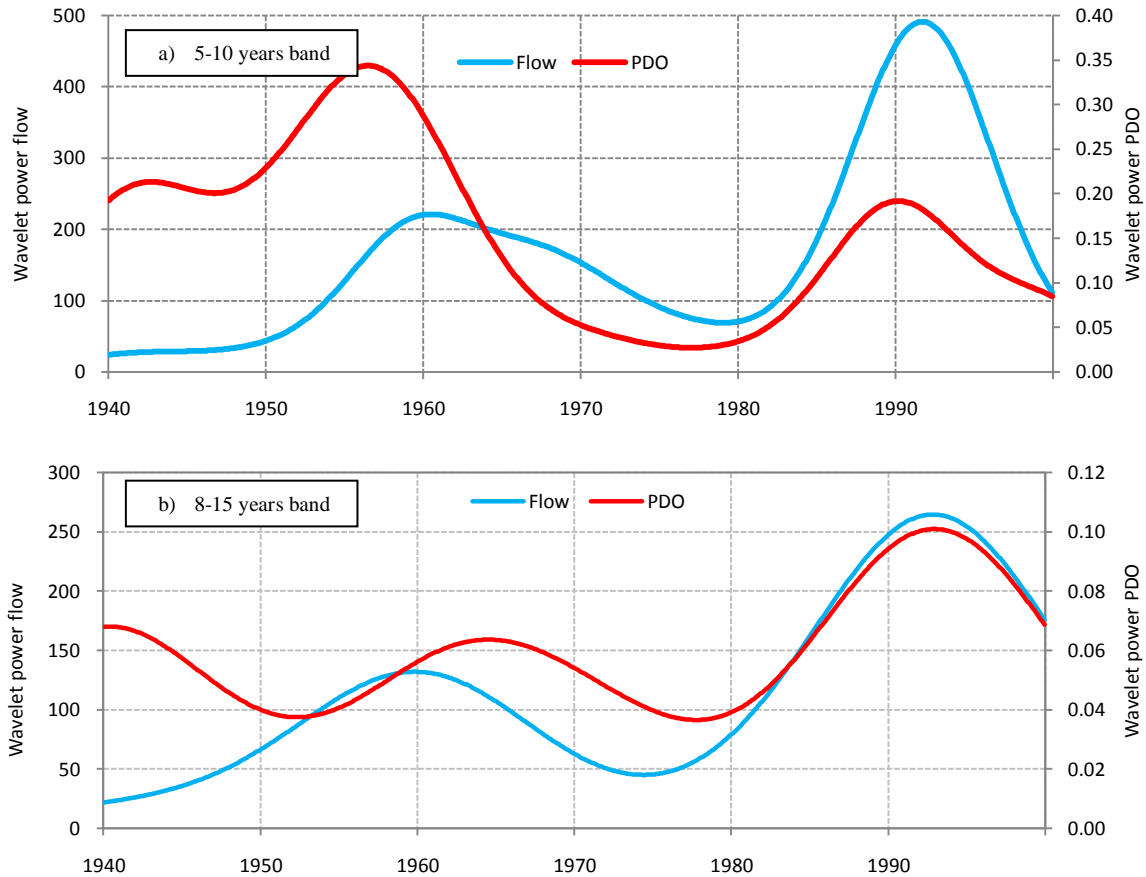


Figure 5-9: Wavelet power for PDO index and flows in the Rio Conchos at Ojinaga: a) 5-10 years bands, and b) 8-15 years band

Table 5-8: Correlation of naturalized historic flows with ENSO and PDO for each 5 years from 1940-1999

| Event | Band (yrs) | Period | | | | | | | | | | | |
|-------|------------|--------|-------|-------|-------|-------|-------|-------|-------|-------|-------|-------|-------|
| | | 40-44 | 45-49 | 50-54 | 55-59 | 60-64 | 65-69 | 70-74 | 75-79 | 80-84 | 85-89 | 90-94 | 95-99 |
| ENSO | 2-3 | -0.71 | 0.30 | -0.40 | 0.80 | -0.56 | -0.84 | -0.80 | -0.73 | 0.01 | -0.99 | -0.97 | -0.56 |
| | 3-6 | 0.92 | 1.00 | 0.97 | 0.04 | 0.78 | -0.15 | -0.93 | -0.99 | -0.90 | -0.71 | 0.64 | -0.36 |
| PDO | 5-10 | 0.72 | 0.93 | 0.98 | -0.75 | 0.98 | 0.97 | 0.99 | -0.34 | 0.99 | 0.99 | 0.87 | 0.99 |
| | 8-15 | -0.99 | -0.99 | 0.22 | 0.97 | -0.87 | 0.98 | 0.98 | -0.05 | 0.99 | 1.00 | 0.98 | 0.99 |

**5.5 STREAMFLOW UNDER CLIMATE CHANGE**

To evaluate potential climate change impacts on runoff in the Rio Conchos Basin an assessment was made of projected changes in precipitation and temperature including changes in the mean, coefficient of variation (CV), and cumulative distribution functions (CDFs) of flows. The Mann-Kendall method (Helsel and Hirsch 2002; Kahya and Kalayc 2004) was used to detect linear trends in the annual flow.

**5.5.1 Annual Streamflow**

Figure 5-10 shows the projected change in annual streamflow at Ojinaga, the confluence of the Rio Conchos with the Rio Grande, for the skill-weighted multi-model ensemble of five GCMs for scenarios A2 and A1B during the period 2040-2099 compared to average 1980-1999. The results indicate a greater reduction in flow for scenario A2 than scenario A1B relative to the period 1980-1999, with major differences for the period 2060-2079. In contrast, comparisons made between both climate scenarios indicate that while high differences are evident for the period 2080-2099, small differences are projected for the period 2060-2079. On average, the reduction of annual streamflow is 14% and 10% (2040-2059) 24% and 24% (2060-2079) and 21% and 14 (2080-2099) for emission scenarios A2 and A1B, respectively.

Likewise, in Figure 5-10, inter-annual variability of maximum flows for scenario A2 exhibits cycles of 3-6 years on average; a clear example can be seen in the period 2060-2066 which is bounded by big flows, with a recurrent drought period of about five years. This behavior could be related with the increase of future ENSO activity under this

112

emission scenario. The situation is similar for the scenario A1B with longer cycles for the periods 2065-2075; which could be related to ENSO and especially PDO activity. In addition, three long drought periods are detected under this scenario (2057-2064, 2064-2077, and 2078-2085). Table 5-9 shows the main characteristics of the annual flows at Ojinaga station in the Rio Conchos.

Figure 5-11 shows the cumulative probability (fitted using the General Extreme Value distribution) of the change of the ensemble mean annual streamflow for the period 2040-2099 relative to 1980–1999 for both scenarios A2 and A1B. The water treaty between the U.S. and Mexico was signed under historical conditions (up to 1944) with a mean annual flow of 65 $m^3$/s (Orive 1945) at Ojinaga, so the change characterizes the effect of climate change on the water availability in coming decades. Figure 5-11 also indicates that for scenario A2, six years out of the period 2040-2059 (30%) have a flow reduction of 30-40%; and for scenario A1B there may be five years. The impact is projected to be worse in the period 2060-2079, with ten years (50%) showing flow reductions of 30-40% for scenario A2; and eleven years (55%) in range of 35-50% for scenario A1B. In this time period, severe drought conditions would exist for both scenarios and only 20% of the values show increase in annual streamflow.

Similarly, for scenario A2 in the period 2080-2099, projections indicate that streamflow would be reduced between 30-48% for eight years (40%); in contrast, in scenario A1B, only five years (25%) show reduced flow in range 30-35%. Table 5-9 shows the main streamflow parameters at Ojinaga. The projected flows tend to be less

113

variable with respect to the naturalized flow of 1980-1999 for both climate scenarios. Peak flows tend to be reduced substantially, particularly in the period 2080-2099; by contrast, minimum flows tend to be more stable and larger than the historic flows. This behavior is related with the temporal variation of temperature and precipitation along the Rio Conchos basin; further analysis of this pattern is discussed in the section on annual extremes.
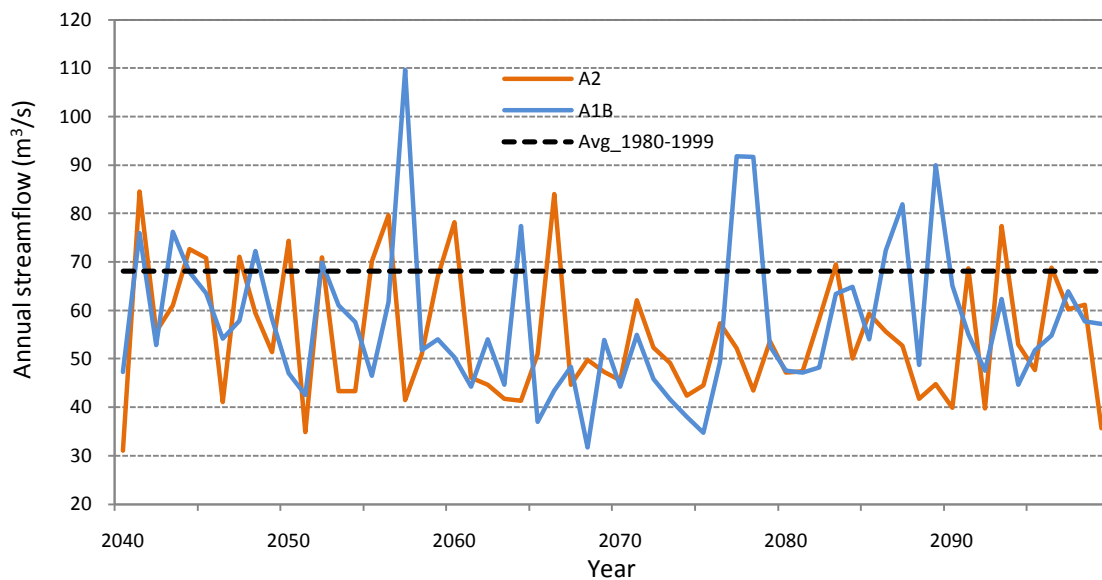


Figure 5-10: Skill-weighted multi-model ensemble annual flow projection at Ojinaga during 2040-99 for scenarios A2 and A1B.
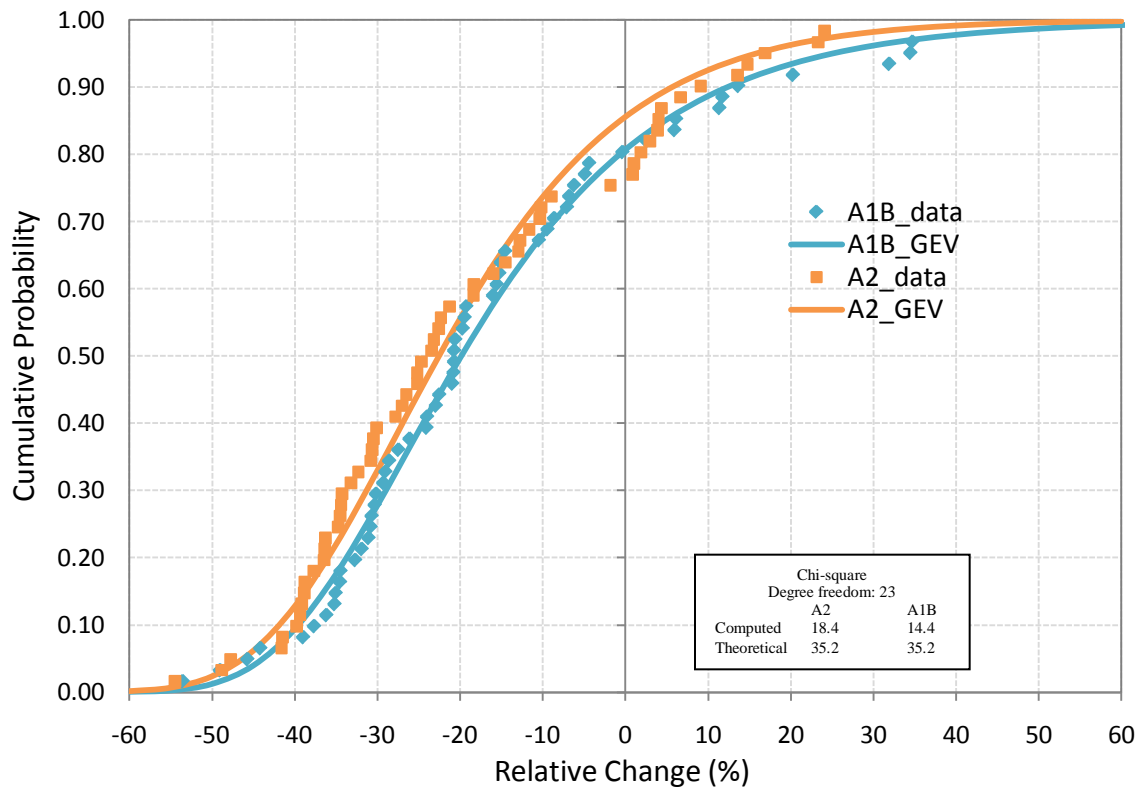
Figure 5-11:  Cumulative probability of the annual streamflow change (%) at Ojinaga for scenario A2 and A1B relative to average natural flow 1980-1999. Data was fitted to a General Extreme Value Distribution (GEV).

Table 5-9: Statistics of historic naturalized and skill-weighted ensemble annual flows under scenarios A1B and A2 at Ojinaga

| Statistic | 1940-99 Hist. | 1980-99 Hist. | 2040-59 A2 | 2040-59 A1B | 2060-79 A2 | 2060-79 A1B | 2080-99 A2 | 2080-99 A1B | 2040-99 A2 | 2040-99 A1B |
|---|---|---|---|---|---|---|---|---|---|---|
| Mean (m$^3$/s) | 60.3 | 68.3 | 58.7 | 61.4 | 51.6 | 51.5 | 53.9 | 58.9 | 54.7 | 57.3 |
| Median (m$^3$/s) | 57.1 | 66.5 | 60.3 | 58.1 | 48.2 | 47.1 | 52.8 | 56.2 | 51.7 | 54.0 |
| St. Dev. (m$^3$/s) | 31.3 | 37.2 | 15.8 | 15.0 | 11.5 | 16.8 | 11.4 | 12.0 | 13.2 | 15.1 |
| Max. (m$^3$/s) | 165.0 | 165.0 | 84.6 | 109.0 | 84.0 | 91.8 | 77.4 | 89.9 | 84.6 | 110 |
| Min. (m$^3$/s) | 15.7 | 23.0 | 31.0 | 42.5 | 41.3 | 31.7 | 35.6 | 44.6 | 31.0 | 31.7 |
| CV | 0.52 | 0.55 | 0.27 | 0.24 | 0.22 | 0.33 | 0.21 | 0.20 | 0.24 | 0.26 |
| Skew | 1.22 | 1.08 | -0.20 | 1.77 | 1.92 | 1.57 | 0.34 | 1.18 | 0.55 | 1.20 |

*5.5.1.1 Range of Variability in GCMs Prediction for Annual Flows*

Figure 5-12 and Figure 5-13 show the range of variation (for the period 2040-2099) of Maximum, 75th percentile, median, 25th percentile, and Minimum flows for each GCM and for the skill-weighted multi-model ensemble, under the emission scenarios A1B and A2, respectively. Each model prediction is compared with the naturalized flow for the period 1940-1999. Under the A1B scenario, the Hadley and CGCM31 models predict the highest flows and the MIROC31 and ECHAM5 models project the lowest flows at Ojinaga. Although the CGCM31 model shows a maximum flow higher than the naturalized flow, the median is reduced significantly (more than 20%). Strong reductions in flows are projected by MIRO32 and ECHAM5 (more than 40% on average). By contrast, CCSM3 and Hadley project increased flows (more than 15%).  The A2 scenario shows similar behavior. For the median, the lowest flows are projected by ECHAM and CGCM31. For both climate change scenarios, in general, three GCMs - MIROC32, ECHAM5, and CGCM31 - predict less water than the naturalized flows; by contrast, CCSM3 and Hadley project an increased streamflow at the Ojinaga station.
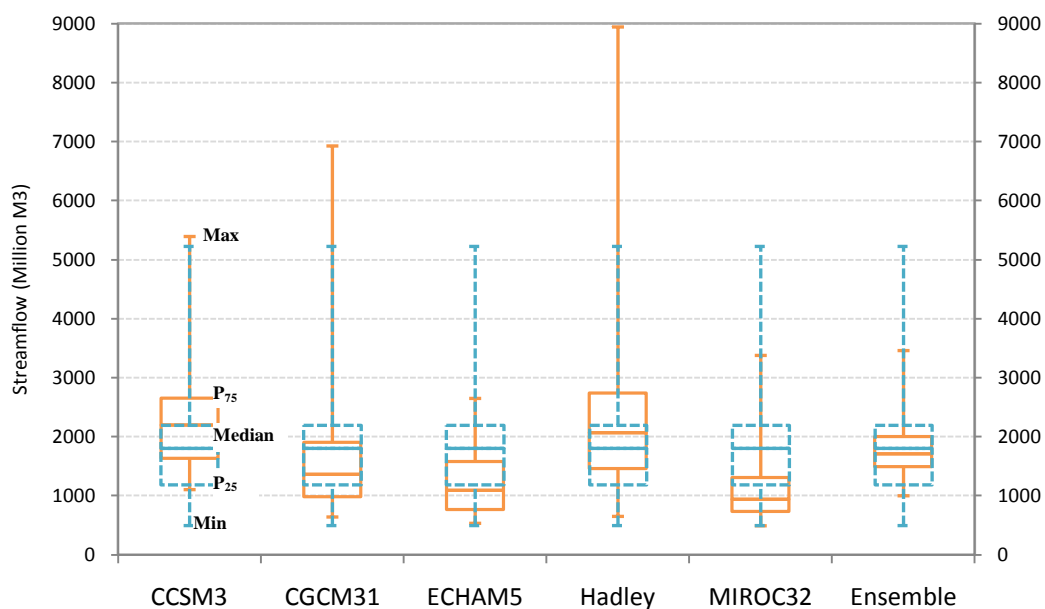
Figure 5-12: Box plot showing the variation range (Max, $P_{75}$, Median, Min, and $P_{25}$) for each GCM and Ensemble for the A1B scenario at Ojinaga. Dashed sky-blue line corresponds to the natural flow for the period 1940-1999.
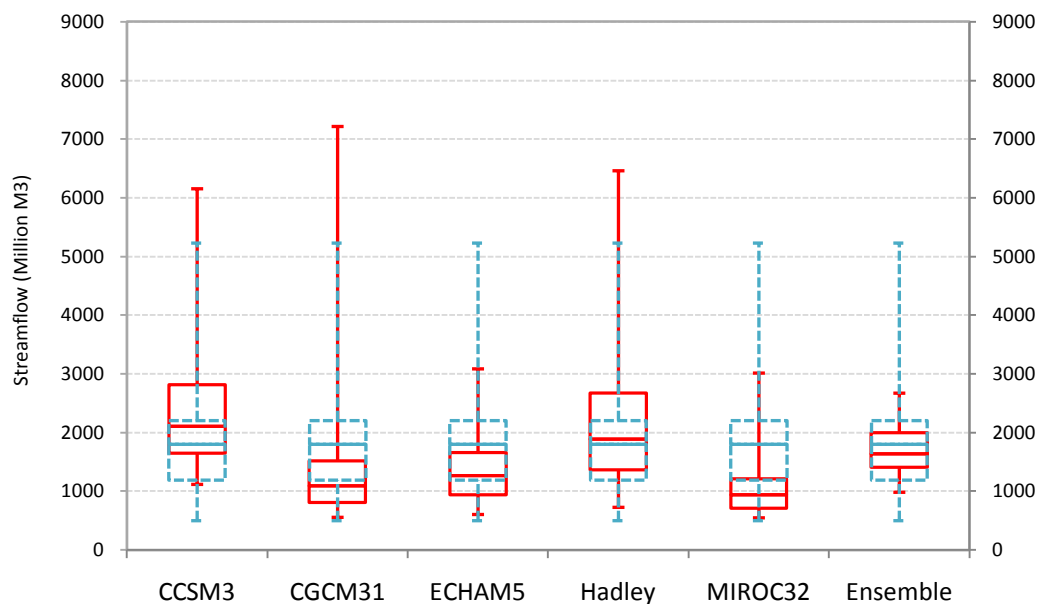


Figure 5-13: Box plot showing the variation range (Max, $P_{75}$, Median, Min, and $P_{25}$) for each GCM and Ensemble for the A2 scenario at Ojinaga. Dashed sky-blue line corresponds to the natural flow for the period 1940-1999.

**5.5.2 Monthly Average Streamflow**

Projected monthly average streamflows for the five GCMs and the multi-model ensemble are shown in Figure 5-14 for three different twenty-year periods for scenarios A2 and A1B, respectively. Overall, for both climate change scenarios, peak flows predicted by the CCSM3 and HADLEY models are larger than others for the whole time period. In contrast, the MIROC32 model predicts the lowest flows, with particular exception for scenario A1B in the period 2040-2059 (Figure 5-14b) where the lowest value was projected by the ECHAM5. The CGCM31 model predicts lower flows only in the periods 2060-2079 and 2080-2099 for scenario A2 (Figure 5-14c and e). There are small differences among the models in predicting the minimum flows (November-June). Larger summer flows are predicted by the CSSM3 model (as well as the Hadley model). Mostly, the GCMs project more water under scenario A1B than A2

Most of the models agree in predicting more water in the period 2080-2099 than 2060-2079 for scenario A1B. Most models agree in predicting the peak flow in September, a month later than historical conditions. Projected changes in the circulation patterns of atmosphere and oceans (Gulf of Mexico and Pacific Ocean) could be influencing this behavior.

There are important discrepancies among models in predicting precipitation as has been shown in other regions (e.g., Christensen et al., 2004). In order to reduce the uncertainties in the model predictions, the multi-model ensemble of five GCMs is used. The skill-weighted multi-model ensemble is also shown in Figure 5-14 denoted by a

118

black line. The ensemble indicates flows would be reduced more in the period 2060-2079 than in other periods.

Comparisons between the ensemble and naturalized flows indicate greater flow reductions in winter (30%) and spring (25%) for the periods 2040-2059 and 2080-2099; and winter (32%) and summer (29%) for the period 2060-2079, for both scenarios. On average, streamflow in August would be reduced by more than 20% for scenario A2 and 18% for A1B, in the period 2040-2059; in contrast, streamflow in September is projected to be increased in the range of 6-8%. For the period 2060-2079, August flow is reduced 29-32% for both A2 and A1B. Similarly, in the period 2080-2099, August is expected to be reduced by more than 25% for A2 and 20% for A1B.
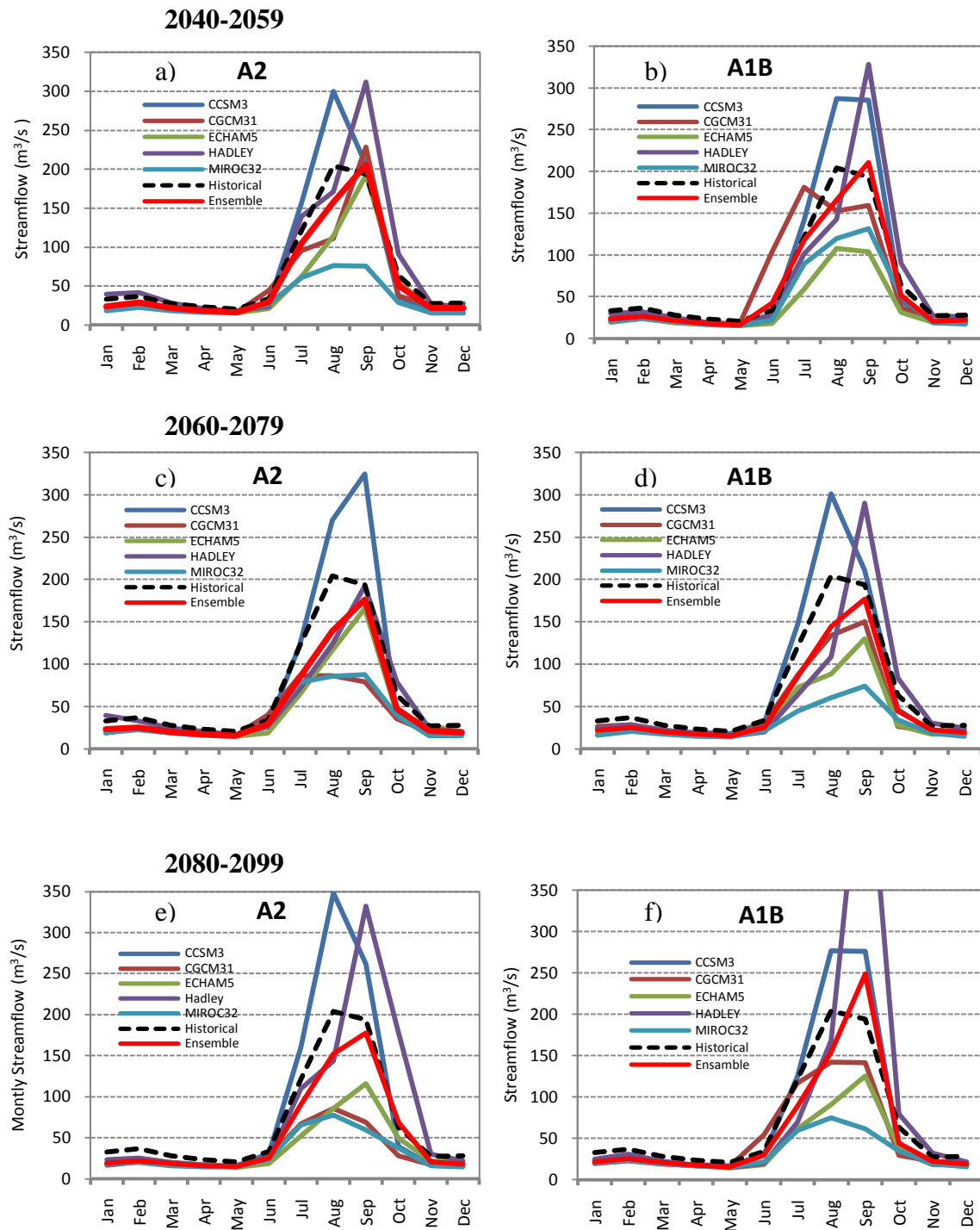
Figure 5-14: Monthly average flow at Ojinaga for each GCM and the multi-model ensemble under scenarios A2 and A1B. a) and b) for period 2040-59,  c) and d) for period 2060-79, and e) and f) for period 2080-99.

### 5.5.3 Trend Analysis

Multi-model ensemble annual streamflows at Ojinaga were analyzed for dispersion and trend using the Coefficient of Variation (CV) and the Mann-Kendall test. Figure 5-15a shows the CV computed from 2040-2099 (60 years) for scenarios A2 and A1B. The CV for scenario A2 ranges from 0.70-1.60 and from 0.6-2.10 for scenario A1B, on average, with most values greater than 1. This high variability is due to the irregular monthly distribution during the year where the maximum flows in the basin are usually produced in August and September (more than 45% of the total runoff). Scenario A1B shows large variability in the period from 2075-2090, for which scenario A1B projects greater flow than A2. The skill-weighted multi-model ensemble annual flows were tested for linear trend using a ten-year Mann-Kendall test (see Fig. 5-15b) with a significance level of 0.05. In general, scenario A2 shows no significant trend for the period 2040-99. Scenario A1B shows an increasing trend in the period 2080-90.
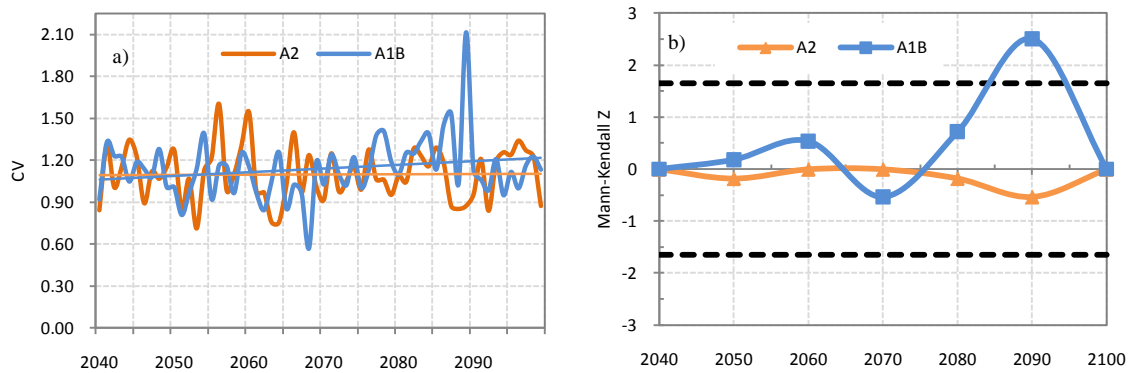


Figure 5-15:  Trend of annual flow at Ojinaga. a) Coefficient Variation (CV) where dashed lines denote the linear trend of each time series, b) Ten-year Mann-Kendall test using the multi-model ensemble time series, where dashed lines denote the limit of significance at 95% confidence level (z = 1.645).

### 5.5.4 Concentration Degree (CD)

Change in concentration degree was explored to assess the streamflow distribution at Ojinaga station.  Concentration degree (CD) can range from 0 to 1; a value of 0 indicates that monthly runoff is equal for all months, and a value of 1 indicates runoff in a year will be produced in 1 month.  Figure 5-16 shows the CD computed for the multi-model ensemble time series for both climate scenarios. CD varies from 0.20-0.48, with an average of 0.30 for scenario A2, and 0.18-0.63, with average 0.31 for scenario A1B.  Here one can note two interesting things; while, the concentration degree shows a positive trend over all periods for scenario A1B, a slight negative trend is shown for scenario A2. Meaning that streamflow would tend to be more concentrated in a month for scenario A1B and a little bit more distributed during a year for the scenario A2.
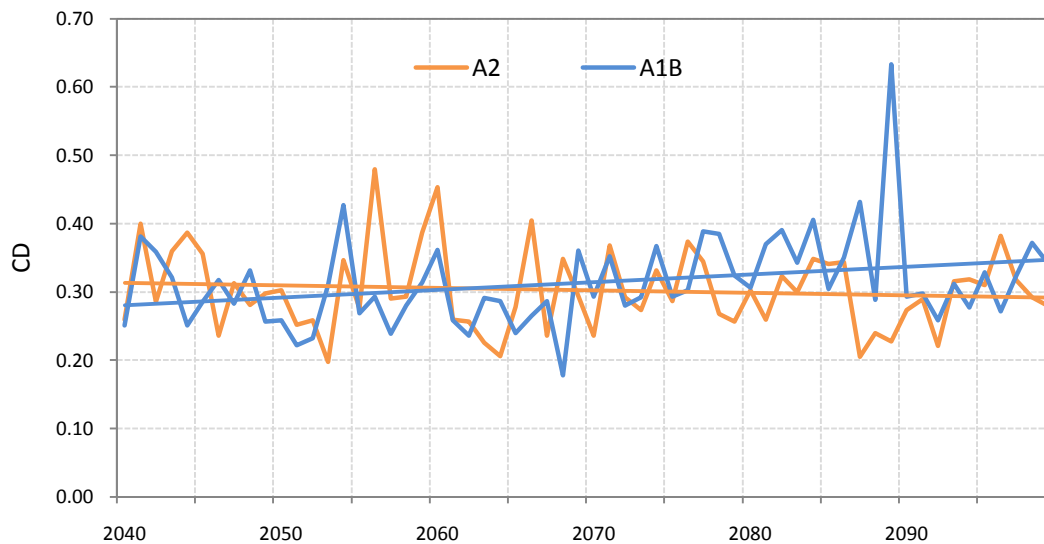


Figure 5-16:  Change in concentration degree of streamflow at Ojinaga for the skill multi-model Ensemble time series.

122

**5.5.5 Changes in Oscillation of Flows under Climate Change**

Although the time period (60 years) used for the PDO analysis by 8-15 year bands is relatively short, it gives us a clear idea about the relationship between future flows and PDO under potential climate change. The wavelet power (8-15 year band) for the historic and skill-weighted scenario A2 and A1B flows at Ojinaga are shown in Figs. 5-17b and 5-17c, respectively. Flow under scenario A2 follows the same pattern as those of the historical flows (correlation coefficient 0.78), with 30-years cycles coinciding with the PDO phase. Under scenario A1B, flows exhibit similar behavior but with cycle peaks 5-8 years earlier (correlation coefficient 0.30).

As in previous section, we discussed that PDO is positively correlated to natural flows in the Rio Conchos basin at Ojinaga, then, the high relationship between historical natural flow and climate change flow suggests that cold and warm phase PDO climate pattern probably will match with high and low flows under a changing climate for the scenario A2. Similarly, under scenario A1B but as we mentioned above, the frequency of flow peaks are expected to occur earlier than historical climate conditions. Such climate-flow relationship may be useful to improve the long- term forecasting in the Rio Conchos basin, which is essential to develop optimal reservoir planning and operation policies for water supply and flood control in the study area.

123
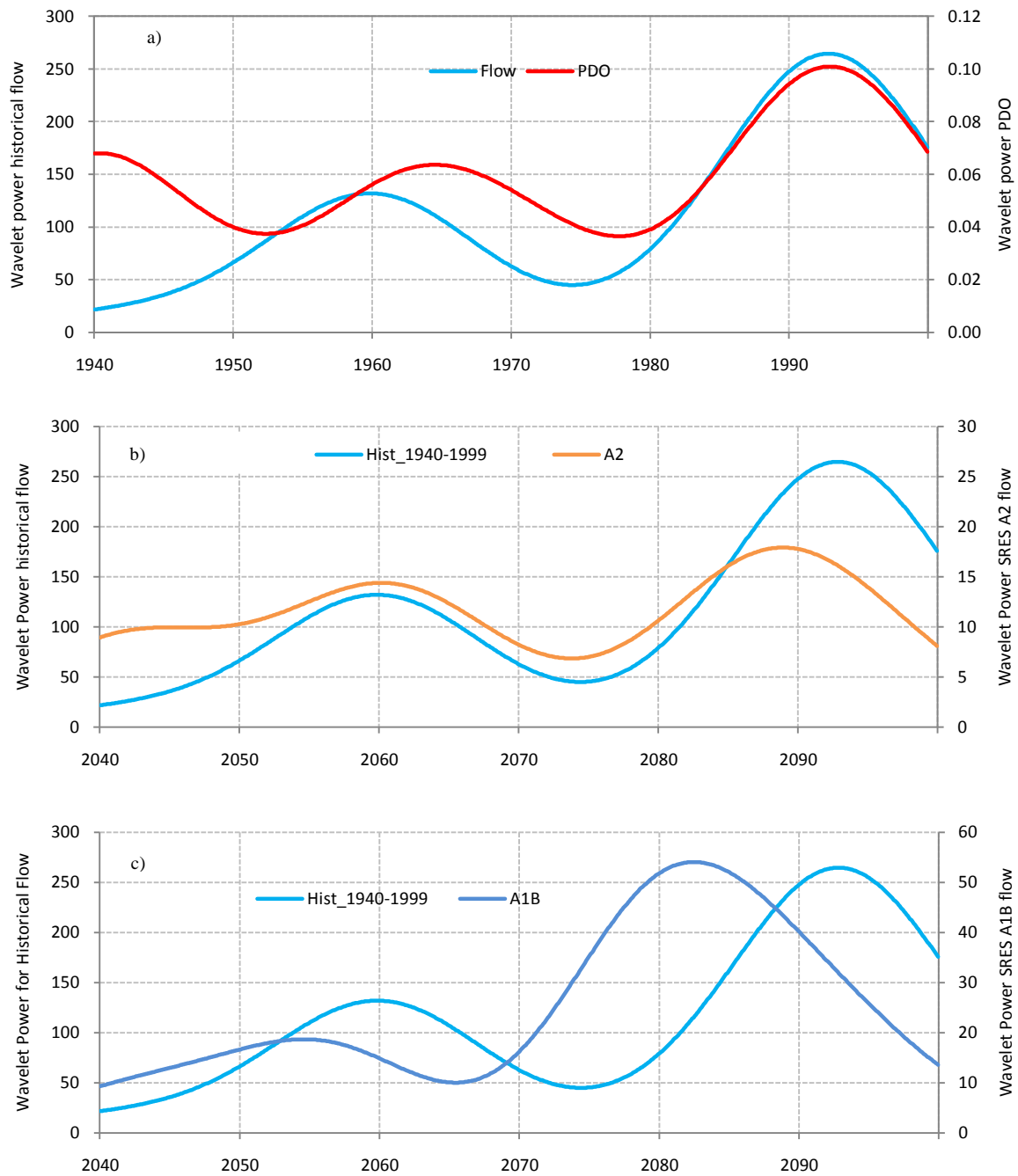
Figure 5-17:  Wavelet power (8-15 year band) for Rio Conchos at Ojinaga: a) Naturalized
historic flow and PDO index, and b) Historic flow and scenario A2 flow, and c) Historic
flow and scenario A1B flow.

124

**5.6 FREQUENCY ANALYSIS**

**5.6.1 Annual Streamflow**

Log-Normal distributions were fit to the multi-model ensemble annual flows at Ojinaga. This was done for 20-year periods from 2040 to 2099 for scenarios A2 and A1B.

For scenario A2, in general for flows above the median, a decrease is evident over the whole period, but the reduction is greatest during 2060-79 (Figure 5-18a), which probably coincides with a low period in the future PDO cycle. For the lower quartile (Pr = 0.25), flows tend to be above the historic value and there is a modest difference across the time periods, with $Q_{25}$ = 45 m$^3$/s compared to 38.5 m$^3$/s in the historic period, a 14% increase over the historic period. For the upper quartile (Pr = 0.75), the runoff in 2040-59 is projected to be $Q_{75}$ = 70 m$^3$/s (compared to the historic value of 80 m$^3$/s), and 57 m$^3$/s for 2060-79, a reduction of 18% over the historic period. Similar trends are seen in scenario A1B (Fig. 5-18b), with increments of more than 25% for the lower quartile for 2040-59 and 2080-99 and decreased flow in the upper quartile by as much as 25%. Distribution parameters and goodness-of-fit statistics are shown in Table 5-10.
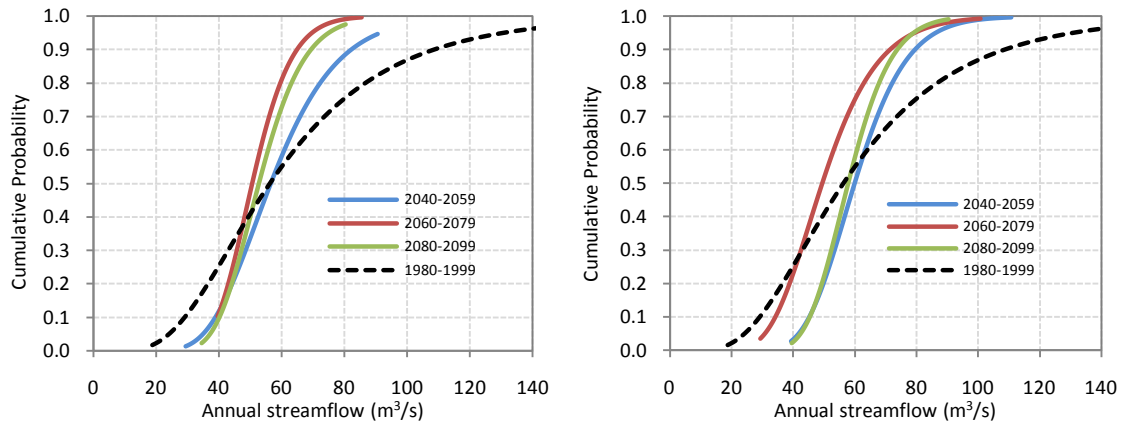
Figure 5-18: Cumulative distribution functions for historic (dashed line) and skill-weighted multi-model ensemble annual flow at Ojinaga for scenarios A2 (left) and A1B (right).

Table 5-10: Parameters of Log-Normal Distribution and Goodness-of-Fit Tests for annual flows at Ojinaga (95% Confidence Level)

| Statistic | | Scenario A2 | | | Scenario A1B | | |
|---|---|---|---|---|---|---|---|
| | | 2040-59 | 2060-79 | 2080-99 | 2040-59 | 2060-79 | 2080-99 |
| Parameters | Mean | 4.03 | 3.92 | 3.97 | 4.09 | 3.90 | 4.06 |
| | St. Dev. | 0.29 | 0.19 | 0.21 | 0.22 | 0.29 | 0.19 |
| Chi-Square | Degrees of freedom | 8.00 | 7.00 | 7.00 | 8.00 | 8.00 | 8.00 |
| | Computed | 8.83 | 13.11 | 5.83 | 13.65 | 7.03 | 8.27 |
| | Theoretical* | 15.51 | 14.07 | 14.07 | 15.51 | 15.51 | 15.51 |

* Statistic for 95% Confidence Level

126

**5.6.2 Extreme Event Analysis**

*5.6.2.1 Annual Maximum*

Exceedance probabilities for annual maximum flows using the Log Pearson Type III distribution are shown in Figure 5-19 for the scenarios A2 and A1B. In addition, the historic period (1980-1999) flows are shown in order to compare how maximum streamflows might change with regard to recent events. For scenario A2, maximum flows show a marked decrease in all periods with 2040-59 being somewhat less reduced than the other periods. The 10% flows decrease from the historic value of $Q_{10}$ = 475 m$^3$/s to 278 m$^3$/s (2080-2099). Scenario A1B shows similar results (Figure 5-16), but the reductions in the flows are not as great as Scenario A2, as is expected. Lower annual maximum flows under climate change in the Rio Conchos basin mean that it may be easier to manage flooding events, since they will be not as large.   However, it could make delivering future environmental flows more difficult.

Likewise, comparisons between time periods indicate that most annual maximum flows will be lower in the period 2060-79 for scenario A2. The same is true for scenario A1B, but with some exceptions for exceedance probabilities less than 10%. In addition, scenario A2 shows that maximum flows are expected to be greater for the period 2040-59 than in later periods. Nevertheless, for scenario A1B, the annual maximum flow is projected to be greater for the period 2080-99 than those in previous periods (2040-2059 and 2060-2079). Table 5-11 shows the parameters and goodness-of-fit test statistics for the LP3 distribution for the flows in the Rio Conchos at Ojinaga. The same analysis was

127

performed for the historical period of 1980-99 to assess how future extremes under climate change may differ from historical extremes. Figure 5-11a shows the exceedance probability values for maximum annual flows, as well as, return periods for natural flows and flows under climate change.
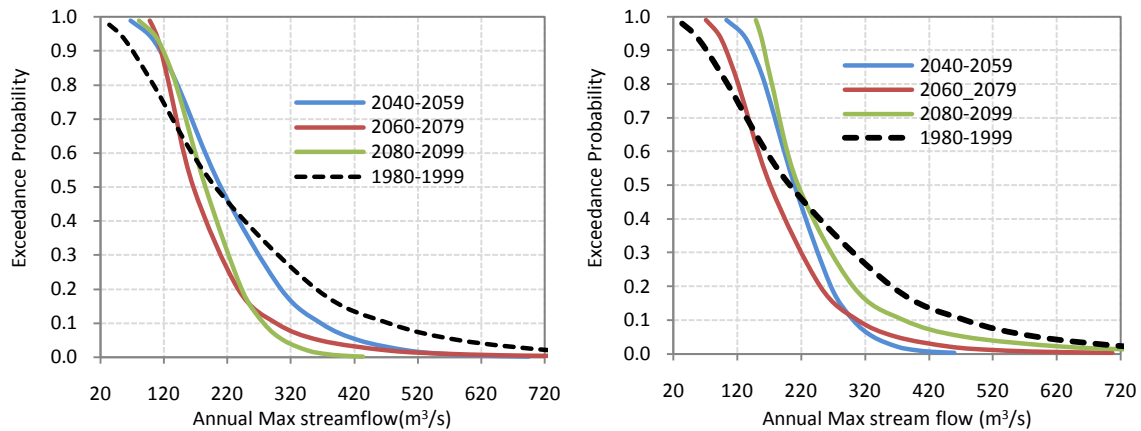


Figure 5-19: Exceedance probability for the annual maximum flow at Ojinaga, estimated using Log Pearson III distribution, for scenarios A2 (left) and A1B (right). Dashed lines are the historic period.

Table 5-11: Parameters of Log Pearson III Distribution and Goodness-of-Fit Tests (95% confidence level) for maximum flows at Ojinaga

| Scenario/Statistic | | Hist. 1940-99 | A2 | | | | A1B | | | |
|---|---|---|---|---|---|---|---|---|---|---|
| | | | 2040-59 | 2060-79 | 2080-99 | 2040-99 | 2040-59 | 2060-79 | 2080-99 | 2040-99 |
| Parameters | Mean | 2.26 | 2.32 | 2.25 | 2.26 | 2.27 | 2.32 | 2.24 | 2.37 | 2.31 |
| | St. Dev. | 0.30 | 0.20 | 0.17 | 0.14 | 0.17 | 0.13 | 0.19 | 0.16 | 0.15 |
| | Station Skew | -0.22 | -0.18 | 1.04 | -0.22 | 0.28 | -0.13 | 0.31 | 1.50 | 0.81 |
| Chi-Square | Degree of Freedom | 8.00 | 8.00 | 8.00 | 8.00 | 8.00 | 8.00 | 8.00 | 8.00 | 8.00 |
| | Computed | 1.61 | 2.18 | 6.01 | 7.09 | 4.64 | 2.01 | 8.59 | 6.43 | 8.99 |
| | Theoretical | 15.51 | 15.51 | 15.51 | 15.51 | 15.51 | 15.51 | 15.51 | 15.51 | 15.51 |

Table 5-11a: Annual maximum flows (m$^3$/s), return period (TR), and exceedance probabilities at Ojinaga for scenarios A2 and A1B.

| Scenario | P(X $\geq$ x$_n$) | 1940-99 | 1980-99 | 2040-59 | 2060-79 | 2080-99 | 2040-99 | TR (years) |
|---|---|---|---|---|---|---|---|---|
| A2 | 0.50 | 188 | 202 | 210 | 166 | 186 | 186 | 2 |
| | 0.20 | 334 | 361 | 305 | 237 | 243 | 261 | 5 |
| | 0.10 | 443 | 475 | 368 | 297 | 278 | 316 | 10 |
| | 0.05 | 556 | 587 | 427 | 366 | 309 | 371 | 20 |
| | 0.02 | 713 | 733 | 504 | 474 | 347 | 448 | 50 |
| | 0.01 | 838 | 842 | 562 | 572 | 374 | 510 | 100 |
| | 0.005 | 968 | 951 | 619 | 686 | 400 | 575 | 200 |
| | 0.002 | 1149 | 1,094 | 695 | 867 | 434 | 668 | 500 |
| A1B | 0.50 | 188 | 202 | 209 | 172 | 215 | 197 | 2 |
| | 0.20 | 334 | 361 | 266 | 250 | 301 | 272 | 5 |
| | 0.10 | 443 | 475 | 301 | 308 | 379 | 332 | 10 |
| | 0.05 | 556 | 587 | 332 | 368 | 474 | 397 | 20 |
| | 0.02 | 713 | 733 | 370 | 453 | 631 | 493 | 50 |
| | 0.01 | 838 | 842 | 398 | 523 | 780 | 576 | 100 |
| | 0.005 | 968 | 951 | 425 | 599 | 962 | 670 | 200 |
| | 0.002 | 1149 | 1,094 | 459 | 707 | 1,264 | 811 | 500 |

*5.6.2.2 Annual Minimum*

The Generalized Extreme Value (GEV) distribution was used to describe annual minimum flows at Ojinaga for scenarios A2 and A1B. The flows do not show significant changes (at most 2 m$^3$/s – 63 million m$^3$ per year - over the entire 21$^{st}$ century) under both emission scenarios A2 and A1B. Results indicate that annual minimum flow will be lower in the period 2080-99 for the scenario A2. By contrast, lower minimum flow is projected for the period 2060-79 for the scenario A1B (see Figure 5-20). In general, lower minimum flows tend to be greater than those computed for the historical period. Although there is significant uncertainty in predictions, minimum flow projections could help water planners establish minimum environmental flow requirements in the next decades to protect the aquatic environment in the Rio Conchos basin and in the Big Bend

reach of the Rio Grande. Table 5-12 shows the parameters and goodness-of-fit test statistics for the GEV distribution, for the flows in the Rio Conchos at Ojinaga.
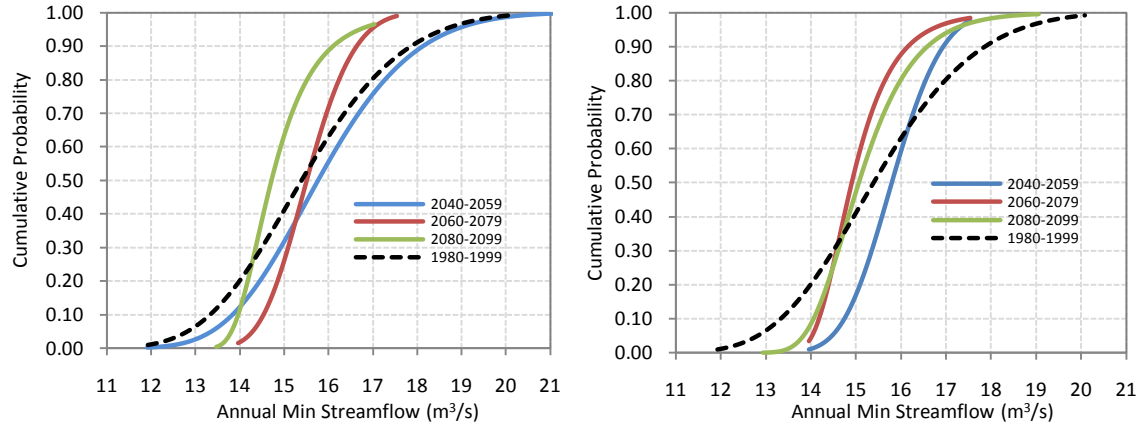


Figure 5-20: Cumulative probability for the minimum annual flow at Ojinaga, estimated using GEV distribution, for scenarios A2 (left) and A1B (right). Dashed lines are the historic period.

Table 5-12: Parameters of GEV Distribution and Goodness-of-Fit Tests (95% confidence level) for minimum flows at Ojinaga

| Scenario/Statistic | | Hist. | A2 | | | | A1B | | | |
|---|---|---|---|---|---|---|---|---|---|---|
| | | 1940 -99 | 2040- 59 | 2060- 79 | 2080- 99 | 2040- 99 | 2040- 59 | 2060- 79 | 2080- 99 | 2040- 99 |
| Parameters | K | - 0.04 | -0.16 | -0.20 | 0.11 | - 0.09 | -0.24 | 0.06 | -0.02 | - 0.06 |
| | Mu | 15.6 9 | 15.21 | 15.24 | 14.47 | 14.9 3 | 15.51 | 14.69 | 14.76 | 14.9 5 |
| | Sigma | 4.45 4 | 1.54 | 0.77 | 0.64 | 1.09 | 0.82 | 0.61 | 0.83 | 0.82 |
| Chi- Square | Degree of Freedom | 7.00 | 5.00 | 7.00 | 4.00 | 7.00 | 3.00 | 4.00 | 4.00 | 7.00 |
| | Computed | 17.1 2 | 6.25 | 1.53 | 2.18 | 6.38 | 0.42 | 2.30 | 4.79 | 1.23 |
| | Theoretical | 14.0 7 | 11.07 | 14.07 | 9.49 | 14.0 7 | 7.81 | 9.49 | 9.49 | 14.0 7 |

## 5.7 UNCERTAINTY RANGE IN STREAMFLOW PREDICTION

### 5.7.1 Annual streamflow

Figure 5-21 shows the annual flow uncertainty range in the Rio Conchos at Ojinaga, under scenario A2. Upper and lower bounds (Ensemble E ± standard deviation σ) computed around the ensemble using the GCM variability in predicting annual flows, and the maximum and minimum are shown in cubic meter per second. A box plot representing the natural variability during 1980-99 is shown in order to compare potential changes in streamflow. The high uncertainty range in predicting maximum annual flows is depicted by 5-year cycles during the period 2040-70; which could be related to ENSO frequency. Furthermore, streamflows are more reduced and distributed between positive and negative uncertainty ranges (E ± σ and max and min) during the period 2070-2090. The cold phase of the Pacific Decadal Oscillation may be influencing this behavior as shown in Figure 5-17b. For the ensemble, annual streamflow may be reduced by 14%, with an uncertainty range of ± 50% for the period 2040-59, 25% with ± 37% for 2060-79, and 20%, with ± 45% during 2080-99.

Under scenario A1B (Figure 5-22), the behavior is similar but with cycles a little bit greater than scenario A2. The biggest uncertainty range in annual flow prediction is located in the last twenty years of this century. On the ensemble, average annual flow is expected to decrease by 10%, with range of uncertainty of ± 47% for the period 2040-59, 25% with ± 39% for 2060-79, and 12%, with ± 53% during 2080-99.
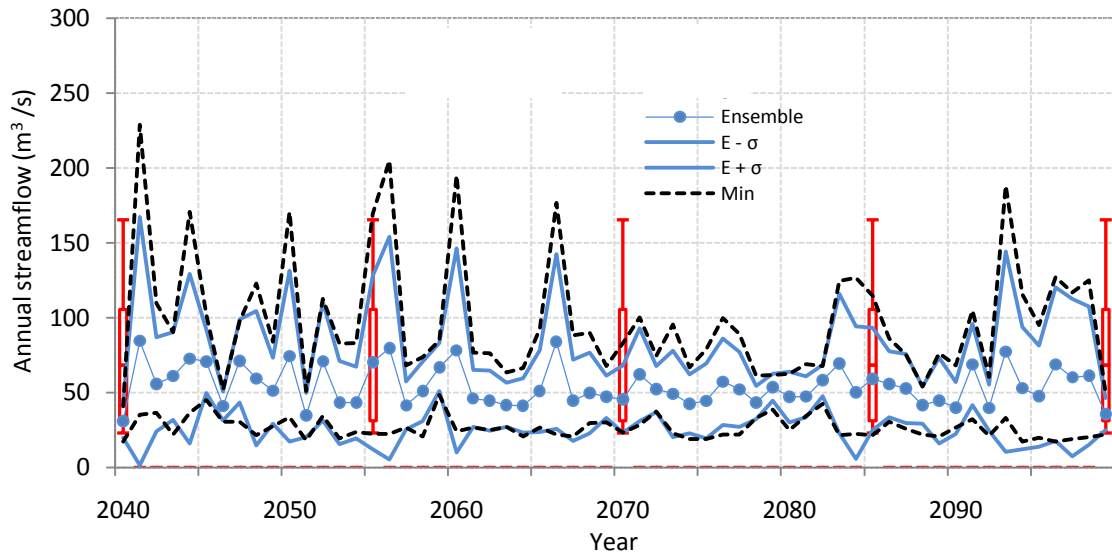
Figure 5-21: Uncertainty range in annual flow prediction in the Rio Conchos at Ojinaga. Weighted ensemble (blue circles), the upper and lower bound (continue blue lines, E ± σ), and the maximum and minimum changes simulated by individual GCMs (dashed black lines). Scenario A2.
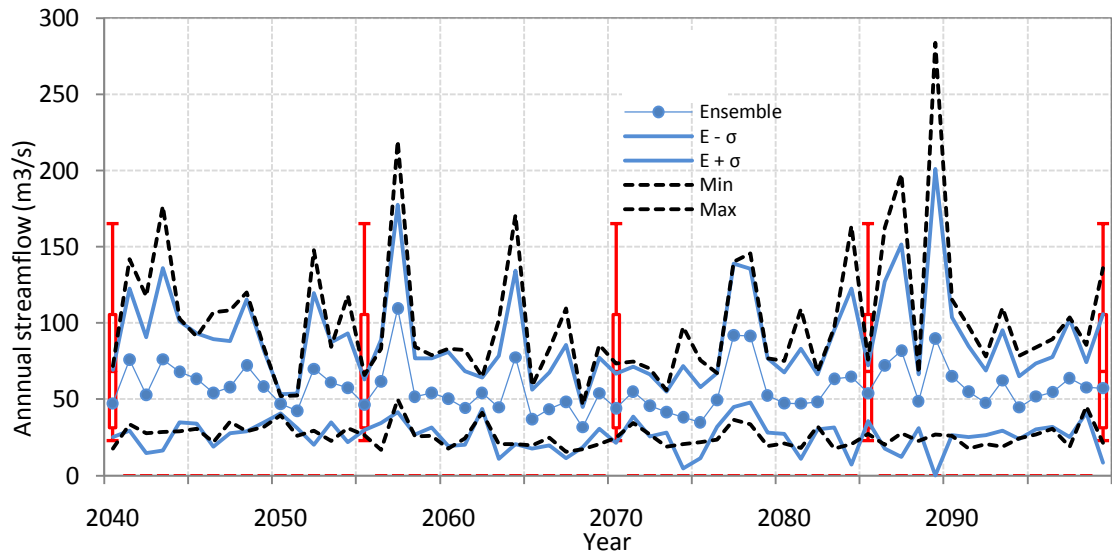


Figure 5-22: Uncertainty range in annual flow prediction in the Rio Conchos at Ojinaga. Weighted ensemble (blue circles), the upper and lower bound (continue blue lines, E ± σ), and the maximum and minimum changes simulated by individual GCMs (dashed black lines). Scenario A1B.

132

## 5.7.2 Average monthly streamflow

Figure 5-23 presents the uncertainty range in the prediction of monthly average streamflow (20-years periods) under scenarios A2 (left) and A1B (right). For both climate change scenarios, general circulation models project a high range of variability in predicting the North American monsoon (July-September) season, however, the historical natural flow lies well within the uncertainty range. Since monsoon period is a complex process located in small-scales that involves atmosphere and ocean interactions, land elevation, vegetation (Warren and Parkinson 2005), etc., it is difficult to catch this climate pattern due to the coarse resolution grids and parameterization schemes (fundamentally to represent precipitation) in GCMs. Here results are congruent with studies focused in evaluating the ability of GCMs for North American Monson (Lin et al; 2008).

In general results indicate that the variability range in predicting the monsoon season increases over time for both scenarios. For instance, streamflow in September will increase by 6%, with a variability range of ± 44% for the period 2040-2059, while streamflow will reduce by 8% with ± 63% for the period 2080-2099, under scenario A2. Similarly, scenario A1B shows a high range of variability for the period June-September. While the uncertainty range for September (period 2040-59) is around ± 51% centered on the ensemble, it is ± 100% in the last 20 years of this century. It suggests that predicting the monsoon season in a changing climate where several driving forces are considered is even more complicated for current GCMs.

133
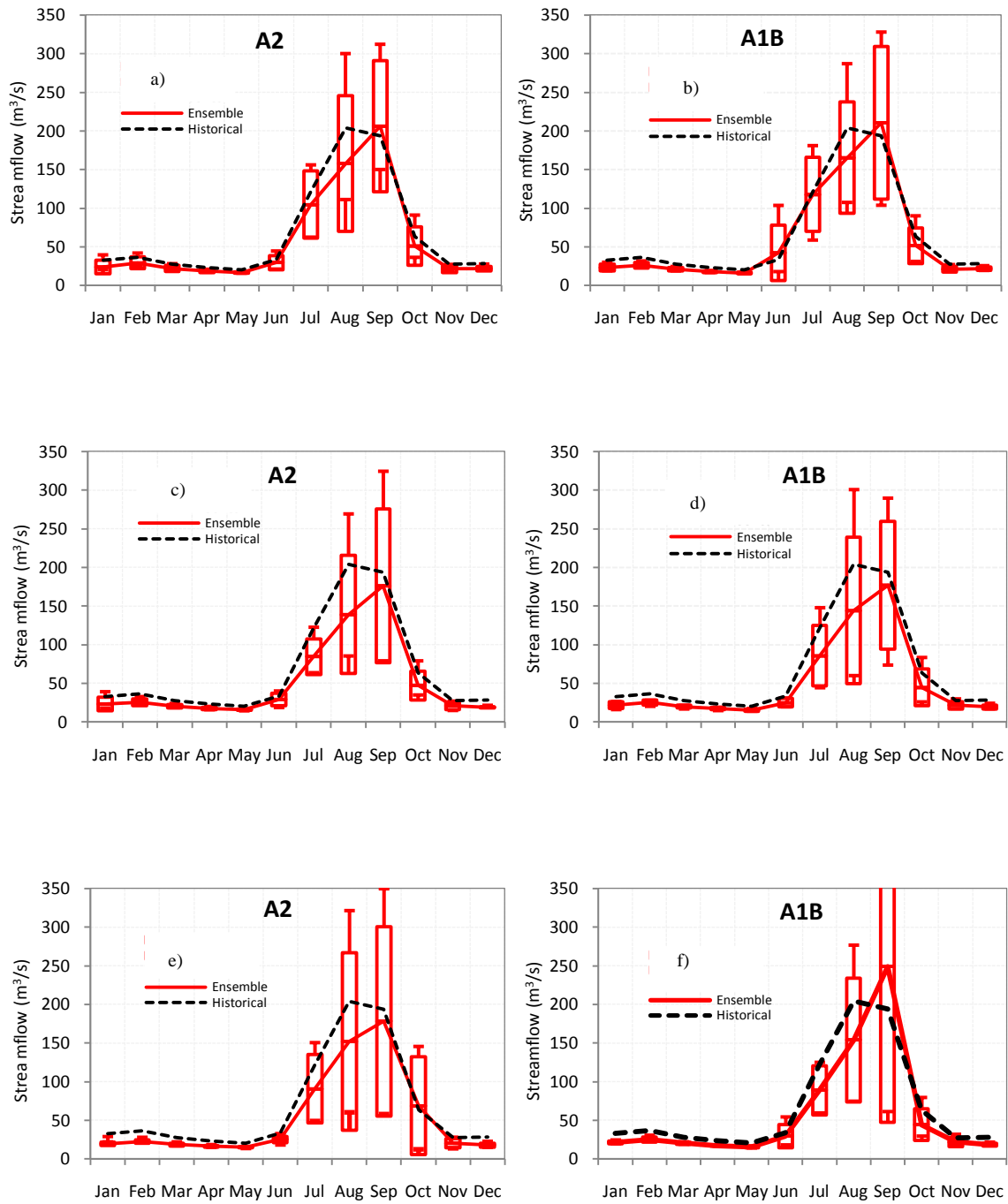
Figure 5-23: Uncertainty range in the prediction of monthly average flow at Ojinaga under scenarios A2 and A1B. a) and b) period 2040-59, c) and d) period 2060-79, and e) and f) period 2080-99.

134

# Chapter 6: Climate Change Effects on Water Availability

This section presents results of the Rio Conchos water system performance to potential climate change under emission scenarios A1B and A2. The impacts are evaluated in terms of changes in the reliability, resiliency, and vulnerability of water users relative to the baseline scenario 1980-99 which represents historical conditions in the basin. The assessment considers the period 2040-99 and 20-year periods. Additionally, changes in the sustainability index are evaluated.

## 6.1 BASELINE PERIOD 1980-99

Under current climate conditions, the reliability of the main water users in the basin is generally high, except in the 103 Rio Florido irrigation district (where the index is less than 25%). This water demand also shows the lowest ability of the system to recover from an unsatisfactory condition (resiliency), and the highest vulnerability, which is directly related to the low flows in the Rio Florido as result of an important deficit of precipitation in this part of the basin. In general, groundwater, irrigation, municipal users, and the 1944 water treaty show high reliability, but a significant maximum deficit of more than 40% was estimated for irrigation during the period 1980-99. An interesting aspect can be noted in the performance of Labores Viejas irrigation district. Although the reliability is high, it shows a low resiliency, which means during failures, the system does not recover efficiently.

**6.2 WATER SYSTEM PERFORMANCE FOR 2040-2099**

The performance of the water system was evaluated for the period 2040-2099 relative to the historical period 1980-99. Figure 6-1 shows the change in reliability, resiliency, and vulnerability for water users in the Rio Conchos Basin under the emission scenario A1B. Results indicate that the reliability of water supply to most demands is reduced more than 15% on average. Reliability will be reduced in the range of 10-25% for irrigation and groundwater users. Municipal users have only a slight reduction in performance since they are the highest priority users in the system. However, it will be more severe when we consider increasing municipal demand over time. Only, ID_103 Rio Florido shows an improved reliability for both scenarios of emission. Since these indicators are negatively correlated, increased vulnerability is observed. The change from the baseline scenario shows an increased annual maximum deficit by more than 14% for irrigation demands. On average, there is a slight reduction in vulnerability for groundwater users that could be related to drought duration and magnitude in the Rio Conchos Basin. Under the emission scenario A2 (Figure 6-2), the impact is similar. Reliability and resiliency for the water treaty will be reduced by more 13% for A1B scenario, with greater impact under the A2 scenario. Table 6-1 and Table 6-2 also show the values of the performance for climate change scenarios, for the period 2040-99.
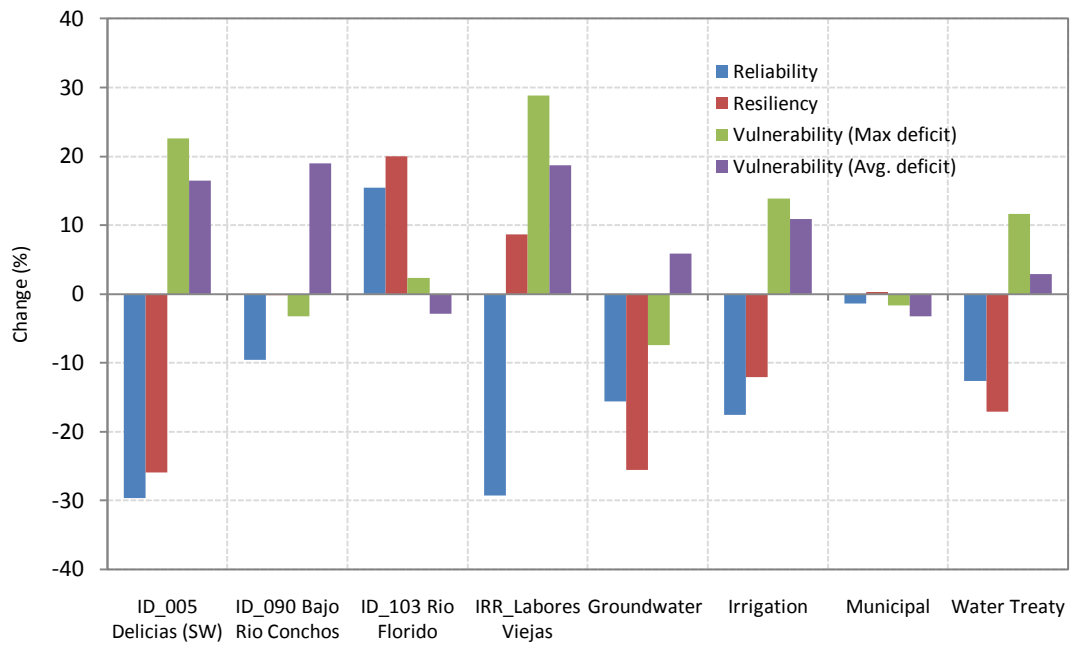
Figure 6-1: Water system performance under scenario A1B as percentage of change from the baseline scenario 1980-1999. Period 2040-2099.
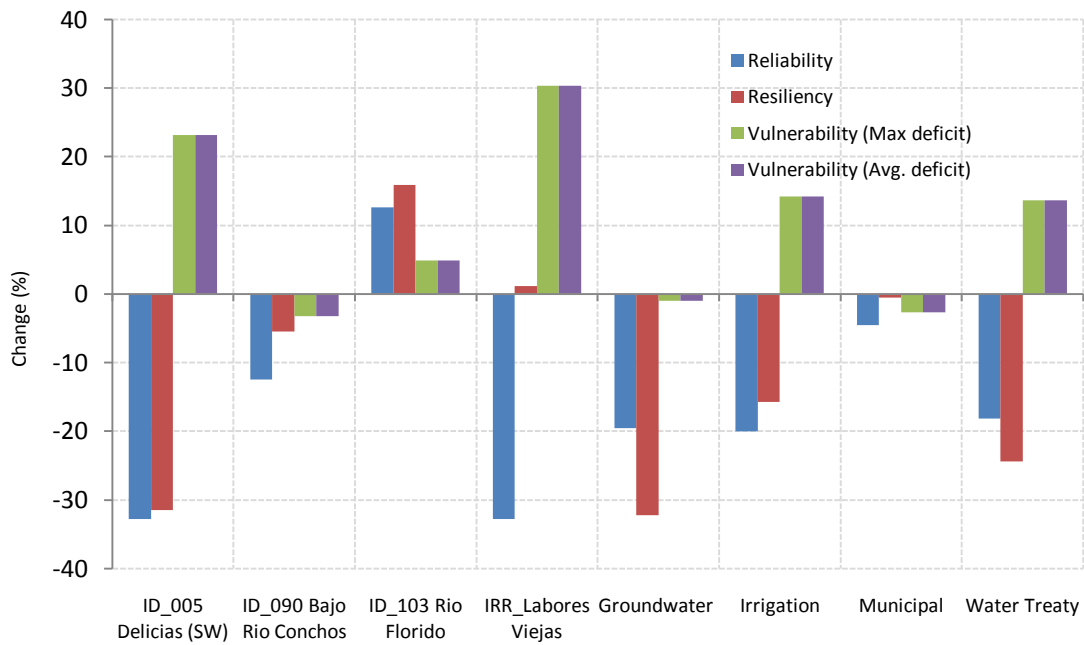


Figure 6-2: Water system performance under scenario A2 as percentage of change from the baseline scenario 1980-1999. Period 2040-2099.

Table 6-1: Water resources system performance results as percentage of change from the baseline scenario 1980-1999, under emission scenario A1B.

| Index | Period | Main users | | | | Total performance | | | |
|---|---|---|---|---|---|---|---|---|---|
| | | ID 005 Delicias (SW) | ID 090 Bajo Rio Conchos | ID 103 Rio Florido | IRR Labores Viejas | Ground water | Irriga tion | Muni cipal | Water Treaty |
| Reliability | 2040-59 | -20 | -5 | 18 | -20 | -9 | -11 | -1 | -8 |
| | 2060-79 | -39 | -21 | 7 | -39 | -24 | -26 | -4 | -28 |
| | 2080-99 | -30 | -3 | 21 | -29 | -14 | -16 | 1 | -2 |
| | 2040-99 | -30 | -10 | 15 | -29 | -16 | -18 | -1 | -13 |
| Resiliency | 2040-59 | -6 | 14 | 25 | 28 | -16 | 2 | 1 | 5 |
| | 2060-79 | -29 | -1 | 16 | 4 | -28 | -14 | -2 | -26 |
| | 2080-99 | -13 | 22 | 23 | 16 | -9 | -2 | 6 | -2 |
| | 2040-99 | -26 | 0 | 20 | 9 | -26 | -12 | 0 | -17 |
| Vulnerability (Max deficit) | 2040-59 | 1 | -23 | -4 | 7 | -20 | -2 | -5 | 4 |
| | 2060-79 | 23 | -3 | -1 | 28 | -7 | 13 | -5 | 11 |
| | 2080-99 | 5 | -46 | -8 | 12 | -22 | -2 | -12 | 2 |
| | 2040-99 | 23 | -3 | 2 | 29 | -7 | 14 | -2 | 12 |
| Vulnerability (Average deficit) | 2040-59 | 6 | 3 | -7 | 10 | 2 | 3 | -4 | 1 |
| | 2060-79 | 21 | 20 | 1 | 24 | 7 | 14 | -2 | 5 |
| | 2080-99 | 7 | -20 | -4 | 11 | 1 | 2 | -7 | 0 |
| | 2040-99 | 16 | 19 | -3 | 19 | 6 | 11 | -3 | 3 |
| Average supply efficiency | 2040-59 | -11 | -12 | 12 | -11 | -2 | -11 | 2 | -4 |
| | 2060-79 | -25 | -26 | -2 | -25 | -9 | -24 | -1 | -11 |
| | 2080-99 | -17 | -9 | 11 | -17 | -5 | -16 | 3 | -7 |
| | 2040-99 | -17 | -16 | 7 | -18 | -6 | -17 | 2 | -7 |

Table 6-2: Water resources system performance results as percentage of change from the baseline scenario 1980-1999, under emission scenario A2.

| Index | Period | Main users | | | | Total performance | | | |
|---|---|---|---|---|---|---|---|---|---|
| | | ID 005 Delicias (SW) | ID 090 Bajo Rio Conchos | ID 103 Rio Florido | IRR Labores Viejas | Ground water | Irriga tion | Muni cipal | Water Treaty |
| Reliability | 2040-59 | -28 | -8 | 16 | -28 | -10 | -16 | -6 | -7 |
| | 2060-79 | -35 | -14 | 8 | -34 | -21 | -22 | -6 | -19 |
| | 2080-99 | -36 | -15 | 13 | -37 | -28 | -22 | -2 | -28 |
| | 2040-99 | -33 | -12 | 13 | -33 | -20 | -20 | -4 | -18 |
| Resiliency | 2040-59 | -30 | -6 | 26 | 3 | -20 | -14 | 1 | -11 |
| | 2060-79 | -32 | 0 | 9 | 2 | -20 | -16 | -2 | -21 |
| | 2080-99 | -21 | 4 | 21 | 2 | -26 | -9 | 4 | -27 |
| | 2040-99 | -31 | -5 | 16 | 1 | -32 | -16 | -1 | -24 |
| Vulnerability (Max deficit) | 2040-59 | 16 | -3 | 5 | 22 | -10 | 9 | -3 | 8 |
| | 2060-79 | 17 | -8 | 1 | 23 | -16 | 9 | -4 | 6 |
| | 2080-99 | 15 | -23 | -9 | 22 | -11 | 6 | -10 | 14 |
| | 2040-99 | 23 | -3 | 5 | 30 | -1 | 14 | -3 | 14 |
| Vulnerability (Average deficit) | 2040-59 | 14 | 19 | -5 | 17 | 8 | 9 | -3 | 4 |
| | 2060-79 | 17 | 3 | -4 | 21 | 1 | 10 | -4 | 4 |
| | 2080-99 | 19 | 3 | 1 | 22 | 6 | 11 | -5 | 6 |
| | 2040-99 | 18 | 13 | -3 | 21 | 9 | 11 | -4 | 5 |
| Average supply efficiency | 2040-59 | -16 | -16 | 9 | -16 | -3 | -15 | 0 | -6 |
| | 2060-79 | -20 | -15 | 3 | -21 | -6 | -20 | 0 | -8 |
| | 2080-99 | -26 | -21 | 1 | -27 | -11 | -25 | 1 | -14 |
| | 2040-99 | -21 | -18 | 4 | -21 | -7 | -19 | 1 | -5 |

## 6.3 WATER SYSTEM PERFORMANCE FOR 20-YEAR PERIODS

Table 6-1 and Table 6-2 show the reliability, resiliency, and vulnerability indicators for water users, as well as the global performance of the system as percentage of change from the baseline scenario 1980-1999, for the emission scenarios, A1B and A2, respectively. The assessment is carried out for 20-year periods. Additionally, the supplied average efficiency and the sustainability index are included.

**6.3.1 Period 2040-59**

*Scenario A1B*

Under the emission scenario A1B, simulations suggest that the reliability of supplying most water demands decreases by more than 10% over the baseline scenario, and only for one case (ID 103 Rio Florido), it increases significantly as result of a greater amount of precipitation projected in the southeast of the Rio Conchos basin. Furthermore, resiliency is increased in some water demands as result of a reduction in the magnitude in the maximum deficit, allowing the system to recover faster from a failure (relative to the baseline) during this period. The maximum deficit is projected to be reduced for most water users (Table 6-1); however, the average deficit (vulnerability) is increased due to increased drought duration, as shown in the 005 Delicias Irrigation District and the Labores Viejas irrigation district. In general, results indicate that the average deficit will increase around 3% for irrigation surface water users. Groundwater users also show a reduction in reliability and a slight increase in vulnerability.

*Scenario A2*

Under the emission scenario A2 (Table 6-2), results indicate that the reliability of supplying users will be reduced about 10-15% over the baseline scenario. Similarly, the resilience of most users is reduced due to increased drought duration and magnitude. As in the scenario A1B, the 103 Rio Florido Irrigation District shows a significant increase in both reliability and resiliency; however, although the average deficit is reduced for this user, the maximum deficit vulnerability is increased 5%. Most water users will

140

experience an increased vulnerability of average deficit during 2040-2059. The total performance of the water system indicates that irrigation users will be more constrained (16%).

## 6.3.2 Period 2060-79

*Scenario A1B*

Under emission scenario A1B, results indicate that reliability of supplying water all users is substantially reduced-more than 25% over the baseline scenario. Although there is an increase in reliability for the 103 Rio Florido irrigation district, it decreases with respect to 2040-59. Municipal users have the lowest impact-less than 5% relative to the baseline-because of its high priority. Unlike the previous period, the resiliency decreases more than 10% because of the increases in drought duration and magnitude. The maximum and average deficit vulnerability tends to increase over time. As discussed above, municipal users are less negatively impacted than irrigation users under this scenario.

*Scenario A2*

Results show that the reliability of supplying water users decreases by more 15% relative to 1980-99. Similarly, reduced resiliency is projected during this period. The vulnerability of water supplies is markedly increased for almost all users. On average, the irrigation deficit is increased by 20% over the baseline scenario, and it is reduced by 6% for municipal users. As in the previous period, the reliability of the Rio Florido improves; consequently, the vulnerability is slightly reduced. However, reliability and resiliency of

this sub-system tend to decrease with respect to 2040-59. Comparisons of the results for both climate change scenarios indicate that the impact of scenario A1B is greater than A2, and the magnitude of failure is substantially greater than the period 2040-2059. However, the failure for scenario A2 is similar to that of 2040-2059.

**6.3.3 Period 2080-99**

*Scenario A1B*

For the end of the century (2080-2099), the reliability of supplies in the Rio Conchos basin is reduced by more than 10% over the baseline scenario, but it is increased with respect to the period 2060-2079. Some irrigation users show an increased resiliency because of reservoir regulation and greater precipitation projected in the Rio Florido sub-basin. This behavior makes the system less vulnerable to the maximum deficit; however, drought duration is increased as indicated by the average deficit vulnerability. Municipal users have a vulnerability greater than 7%.

*ScenarioA2*

Reliability of supply to all water users decreases by more than 19% on average, but it is expected to increase by 13% over the baseline in the 103 Rio Florido Irrigation District. Despite this increase, the reliability remains low. Similarly, resiliency tends to be reduced for most water users; consequently, the vulnerability increases. Irrigation District 005 Delicias, the main water user in the Rio Conchos basin, shows a marked reduction in performance; by contrast, municipal users have a negative impact less than 10%; under the assumption that its demand remains constant during the next decades. At

142

system level, reliability of groundwater and irrigation users are reduced by more than 22%; nevertheless, municipal users only show a marginal reduction of 2%. Similar impact is expected for the resiliency of the system during the period 2080-2099. The average deficit vulnerability increases by more than 6% for groundwater users and by 11% for surface water irrigation users over the baseline scenario.

**6.4 COMPARISONS BETWEEN SCENARIOS AND TIME PERIODS.**

Comparisons between both climate change scenarios indicate, in general, that water supplies under scenario A2 will be more constrained than under A1B, with a significant impact on groundwater and irrigation users. Although, municipal users show a low impact, this could be affected significantly if a changing demand over time is considered, as shown in next sections. Under scenario A1B, comparisons among time periods suggest that reliability and resiliency of water supply to all users will be more reduced in 2060-79 than 2040-59 and 2080-99. Therefore, the vulnerability of the water system is expected to be greater because of the increment in drought magnitude and duration during this time period. Under scenario A2, reliability and resiliency are significantly reduced; consequently, the vulnerability tends to be increased over time. Municipal users have a slightly reduced reliability and resiliency, with vulnerability less than 5% on average. Likewise, during the period 2060-79, scenario A1B shows a greater impact on the system performance than scenario A2.

## 6.5 IMPACT ON THE 1944 WATER TREATY

Table 6-1 and Table 6-2 also show the impact of climate change on water supply to the 1944 treaty computed as a percent change from the baseline scenario, for the scenarios A1B and A2, respectively. Under scenario A1B, results indicate that the reliability will decrease by more than 8% for 2040-59, 25% for 2060-79, and a slight impact for 2080-99. Similar impact is expected on the resiliency for 2060-79; however, an increased resiliency by 5% is expected for 2040-59. For the end of this century, in general, resiliency is reduced by more than 15%. Consequently, the water treaty signed between U.S and Mexico becomes more vulnerable to potential climate change, with a significant impact during the period 2060-79.

Under scenario A2, the impact on reliability of water delivery to the treaty for 2040-59 is similar to scenario A1B. A reduced reliability, more than 15% and 25% for 2060-79 and 2080-99, respectively, is projected. Resiliency of the treaty deliveries is similarly reduced over time. Thus, the vulnerability is increased for the three periods of time. For the end of this century, maximum deficit vulnerability is increased by more than 10%.

The sustainability index (SI) for the water treaty is shown in Tables 6-3 and 6-4. SI decreases more than 20% for the period 2060-79. Small changes are projected for 2050-2059 and 2080-2099, under scenario A1B. The reduction is more significant under scenario A2, with more than 10% for 2040-59, increasing by more than double for the period 2060-79 and almost three times for 2080-99.

144

**6.6 CHANGE OF SUSTAINABILITY INDEX**

A combination of performance indicators discussed above can be used to explain the total performance of the water system. Figures 6-3 and 6-4 show the sustainability index (SI) as percentage of change from the baseline scenario (1980-1999) computed on the basis of reliability, resiliency, and average deficit vulnerability. In general, most water users have a reduction in sustainability index, except for Rio Florido Irrigation District 103 where the SI increases significantly. Under the scenario A1B (Table 6-3), groundwater and irrigation (surface water) users show the highest values, with a deeper impact on the Irrigation District 005 Delicias. The most negative impact is projected for the period 2060-79. Similarly, simulations for scenario A2 suggest a slightly larger reduction. For the period 2060-79, A1B decreases more than A2. For both climate change scenarios, SI is marginally reduced for municipal uses. Table 6-4 also shows the change in SI values for scenario A2. Note that the Irrigation District 005 Delicias uses around 55% of the total surface water in the Rio Conchos basin. Irrigation District 090 Bajo Rio Conchos, Irrigation District 103 Rio Florido, and Labores Viejas Irrigation District consume around 21% of the total surface water.
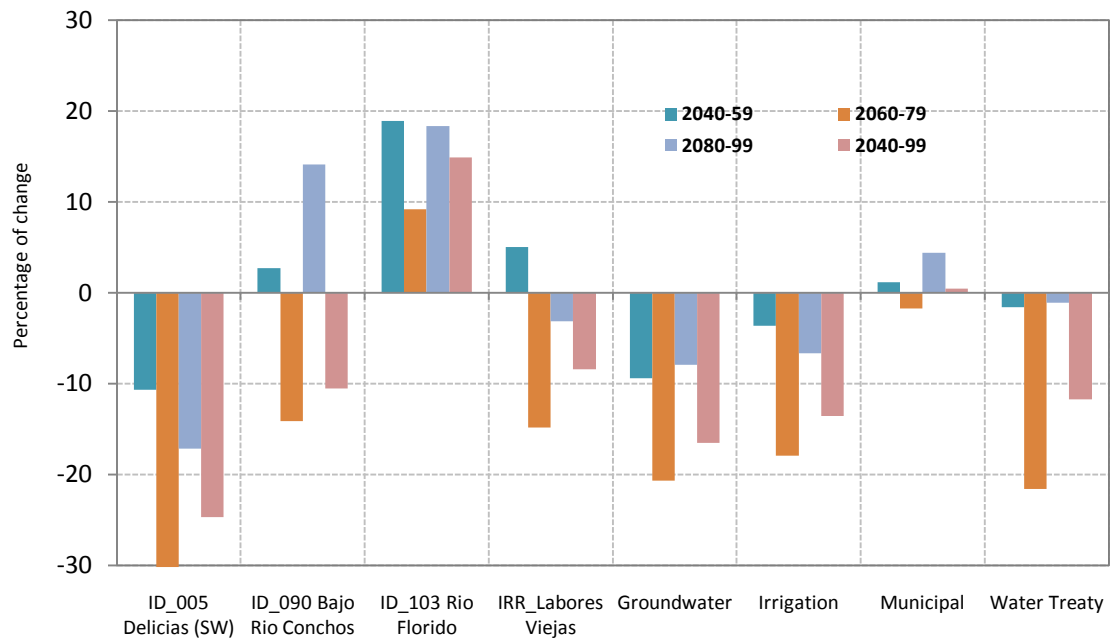
Figure 6-3: Sustainability index as percentage of change from the baseline scenario (1980-199). Scenario A1B.



Figure 6-4: Sustainability index as percentage of change from the baseline scenario (1980-199).  Scenario A2.

146

Table 6-3: Change (%) of sustainability index from the baseline scenario (1980-1999), under Scenario A1B.

| Period | Main users | | | | System level | | | |
|---|---|---|---|---|---|---|---|---|
| | ID 005 Delicias (SW) | ID 090 Bajo Rio Conchos | ID 103 Rio Florido | IRR Labores Viejas | Groundwater | Irrigation | Municipal | Water Treaty |
| 2040-59 | -11 | 3 | 19 | 5 | -9 | -4 | 1 | -2 |
| 2060-79 | -30 | -14 | 9 | -15 | -21 | -18 | -2 | -22 |
| 2080-99 | -17 | 14 | 18 | -3 | -8 | -7 | 4 | -1 |
| 2040-99 | -25 | -11 | 15 | -8 | -17 | -14 | 0 | -12 |

SW: Surface Water
ID: Irrigation District

Table 6-4: Change (%) of sustainability index from the baseline scenario (1980-1999), under Scenario A2

| Period | Main users | | | | System level | | | |
|---|---|---|---|---|---|---|---|---|
| | ID 005 Delicias (SW) | ID 090 Bajo Rio Conchos | ID 103 Rio Florido | IRR Labores Viejas | Groundwater | Irrigation | Municipal | Water Treaty |
| 2040-59 | -25 | -13 | 18 | -10 | -13 | -13 | -1 | -8 |
| 2060-79 | -29 | -4 | 8 | -13 | -15 | -16 | -2 | -16 |
| 2080-99 | -25 | -4 | 14 | -15 | -21 | -14 | 2 | -22 |
| 2040-99 | -28 | -10 | 12 | -13 | -21 | -16 | -1 | -17 |

# Chapter 7: Adaptive Water Management Alternatives to Mitigate Potential Climate Change Effects

One of the main challenges is how the water system could be managed and what kind of strategies could be implemented to adapt to future climate conditions. This section presents results of simulating four adaptive water management alternatives to reduce the effect of climate change on the Rio Conchos system under emission scenarios A1B and A2. The effectiveness of each alternative is computed using the performance indicators discussed in previous section.

## 7.1 GLOBAL WATER SYSTEM PERFORMANCE UNDER ADAPTIVE MEASUREMENTS

Figure 7-1 presents the system performance in a critical case (Alternative I) and adaption measures as a percentage of change from the emission scenario A1B. As was addressed in the methodology section, Alternative I (SI) considers a substantial increase in the municipal demands for the next decades. Under this condition, the Rio Conchos system water supply is less reliable and more vulnerable; with a strong impact on the municipal users. However, with the water management policy stated in Alternative II (SII), which includes relevant improvements to the hydraulic infrastructure, change of crops, and groundwater use for drought periods, the system reliability increases; consequently, the vulnerability may be reduced considerably.

Under emission scenario A1B, results indicate an increase in reliability and resiliency by more than 20% for irrigation and 5% for municipal users (Alternative II), with a substantial reduction of the maximum deficit vulnerability (19% for irrigation and

14% for municipal). Furthermore, it should be noted for groundwater users, the reliability and resiliency decrease more than 10% because of the system improvement, which is translated in an increase of the efficiency of water use; consequently, the groundwater recharge is reduced significantly.

Alternative III (SIII), which considers a reduction of water demands by 25% and a global efficiency of 44% for a constant municipal demand, the system performance increases; thus, the vulnerability decreases significantly. Similarly, the simulation for Alternative IV (SIV) shows a notable improvement in reliability and resiliency for municipal and irrigation users, and reduced vulnerability; however, groundwater users, as also shown for Alternative II, have reduced performance. Because of municipal water demand was also considered constant; Alternative IV is more reliable than other ones. Table 7-1 also presents the water system performance under these adaptive strategies as percentage of change, for the 2040-2099.

Under emission scenario A2 (Figure 7-2), reliability and resiliency for groundwater and irrigation users decrease slightly for Alternative I; by contrast, municipal users show significant reduction in performance similar to scenario A1B, with a strong increase in maximum deficit vulnerability of more than 25%. With Alternative II, both irrigation and municipal users improve their performance significantly; even better than under emission scenario A1B, which means that this strategy may further increase the system reliability, with a substantial increase in water efficiency and an important use of groundwater resources for drought periods.

149

Under the assumptions described in previous sections, simulations for Alternatives III and IV also suggest an increased reliability and resiliency, but municipal vulnerability is not reduced. For all adaptive strategies, the performance for groundwater users decreases but vulnerability increases marginally due to recharge reduction as result of hydraulic system improvement. Table 7-2 also presents the water system performance to adaptive strategies as a percentage of change for 2040-2099.

*Water treaty*

An increase in the municipal water demands over the next decades may affect 1944 water treaty commitments under climate change. Results indicate that reliability of the water treaty could be reduced by more than 10% for Alternative I (Table 7-1). With the adaptive measurements, water supply for the treaty improves respect to Alternative I; nevertheless, it may not become more reliable than scenario A1B and A2, with one exception for Alternative IV where a small increase of the performance is projected (Table 7-2).

In general, treaty vulnerability increases by not more than 8% for both climate change scenarios. One of the reasons why the treaty does not improve substantially is because the Rio Conchos tributary has as a main priority meeting demands of water users under a changing climate in the next decades. However, the treaty performance could be improved by increasing the priority to meet treaty deliveries and setting special operation rules to release water from La Boquilla and Luis L. Leon reservoirs. This would represent a major change in Mexican water management policy.

150

Figure 7-1:  Water system performance to adaptive strategies as percentage of change from the A1B scenario. Period 2040-2099.

Table 7-1: Summary of water system performance results under adaptive strategies, expressed as percentage change from the A1B scenario.

| Index | Groundwater user | | | | Irrigation | | | | Municipal | | | | Water Treaty | | | |
|---|---|---|---|---|---|---|---|---|---|---|---|---|---|---|---|---|
| | SI | SII | SIII | SIV | SI | SII | SIII | SIV | SI | SII | SIII | SIV | SI | SII | SIII | SIV |
| Reliability | -2 | -11 | -3 | -16 | -1 | 23 | 16 | 30 | -16 | 7 | 4 | 26 | -11 | -11 | -3 | 0 |
| Resiliency | 3 | -11 | -4 | -15 | 1 | 26 | 12 | 30 | -11 | 7 | 1 | 27 | -4 | -4 | 5 | 9 |
| Vulnerability (Max deficit) | 0 | 9 | 3 | 10 | 1 | -19 | -12 | -34 | 6 | -14 | -2 | -25 | 5 | 8 | 3 | 2 |
| Vulnerability (Avg deficit) | -2 | 4 | 2 | 5 | 0 | -9 | -8 | -22 | 5 | -8 | -1 | -13 | 3 | 7 | 2 | 1 |
| Avg supply efficiency | 0 | -3 | 0 | -5 | -1 | 12 | 8 | 15 | -7 | 6 | 1 | 10 | -2 | -4 | -1 | -1 |

151
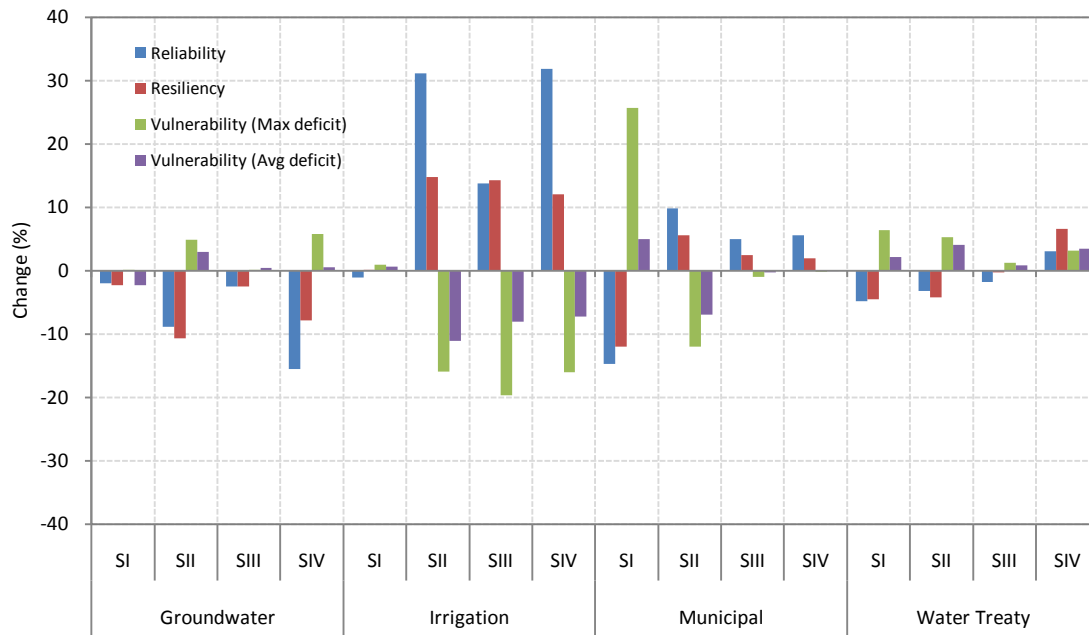
Figure 7-2: Water system performance to adaptive strategies as percentage of change
from the A2 scenario. Period 2040-2099.

Table 7-2: Summary of water system performance results under adaptive strategies,
expressed as percentage change from the A2 scenario.

| Index | Groundwater | | | | Irrigation | | | | Municipal | | | | Water Treaty | | | |
|---|---|---|---|---|---|---|---|---|---|---|---|---|---|---|---|---|
| | SI | SII | SIII | SIV | SI | SII | SIII | SIV | SI | SII | SIII | SIV | SI | SII | SIII | SIV |
| Reliability | -2 | -9 | -3 | -16 | -1 | 31 | 14 | 32 | -15 | 10 | 5 | 6 | -5 | -3 | -2 | 3 |
| Resiliency | -2 | -11 | -2 | -8 | 0 | 15 | 14 | 12 | -12 | 6 | 2 | 2 | -5 | -4 | 0 | 7 |
| Vulnerability (Max deficit) | 0 | 5 | 0 | 6 | 1 | -16 | -20 | -16 | 26 | -12 | -1 | 0 | 6 | 5 | 1 | 3 |
| Vulnerability (Avg deficit) | -2 | 3 | 0 | 0 | 1 | -11 | -8 | -7 | 5 | -7 | 0 | 0 | 2 | 4 | 1 | 3 |
| Avg supply efficiency | 0 | -3 | 0 | -4 | -1 | 13 | 9 | 13 | -6 | 7 | 1 | 2 | -3 | -4 | 0 | 0 |

152

**7.2 PERFORMANCE OF MAIN USERS UNDER ADAPTIVE STRATEGIES**

Figures 7-3 and 7-4 show results of the performance of the adaptive strategies of main irrigation users in the Rio Conchos basin. Under scenario A1B (Figure 7-3 and Table 7-3), results indicate that main irrigation users (surface water) such as ID-005 Delicias, IRR-Labores Viejas, and ID-103 Rio Florido, which represent around 70% of the surface water consumption in the basin, probably will not be affected significantly by Alternative I (SI). However, a reliability reduction of about 4% is shown for ID-090 Bajo Rio Conchos. Despite of the reservoir releases from Luis L. Leon to this irrigation district, the performance tends to decrease due to its location in the lower basin.

Under Alternative II (SII), a substantial increase of more than 15% in reliability and resiliency is projected for the main irrigation users, noting a higher improvement in the ID-005 Delicias and IRR- Labores Viejas due to the effect of this alternative on La Boquilla reservoir operation. Similarly, the ID-103 Rio Florido, which is regulated by the San Gabriel and Pico del Aguila reservoirs, and uses groundwater from the Jimenez-Camargo aquifer during drought years, displays an improved performance. Although, the reliability does not improve substantially for ID-090, the vulnerability is reduced considerably. Likewise, under Alternatives III (SIII) and IV (SIV), reliability and resiliency are increased greatly; in consequence, the vulnerability for the irrigation users decreases substantially.

Figure 7-4 and Table 7-4 show the performance of the adaptive strategies as a percent change from scenario A2. SI impacts negatively on the reliability of ID-090 Bajo

Rio Conchos by less than 5%; and by less than 1% for the ID-005 Delicias. However, with adaptive measures, the reliability and resiliency improve significantly. Maximum and average deficit vulnerability diminishes markedly.

As expected, alternatives perform less well under A2 than A1B. For SII, the reliability and resiliency increase by more than 20%, and the vulnerability decreases in the range of 14% to 40%. Although, reliability and resiliency for ID-090 do not show improvement, these increase with respect to Alternative I; in consequence, the average and maximum deficit are reduced markedly. Groundwater from Bajo Rio Conchos aquifer is a complement to surface water in drought periods in the ID-090.

Similarly, with the adaptive strategies SIII and SIV, simulations suggest an increased performance for irrigation users and an important reduction in water deficit, which could help mitigate the effects of climate change. For ID-090, the reliability and resiliency show a slight improvement over Alternative I; however, the average deficit increases by 5% with SIV. Adaptive strategies for scenario A2 do not perform as well as under scenario A1B. The performance of ID-005 Delicias and IRR-Labores Viejas are almost similar. Since these two users are close spatially and are using water from La Boquilla reservoir, the effect of the operation rules set in the water planning model is similar for both users. In general, simulations suggest that water management measures to adapt to climate change in the Rio Conchos contribute to improving system performance, making it more reliable and less vulnerable.
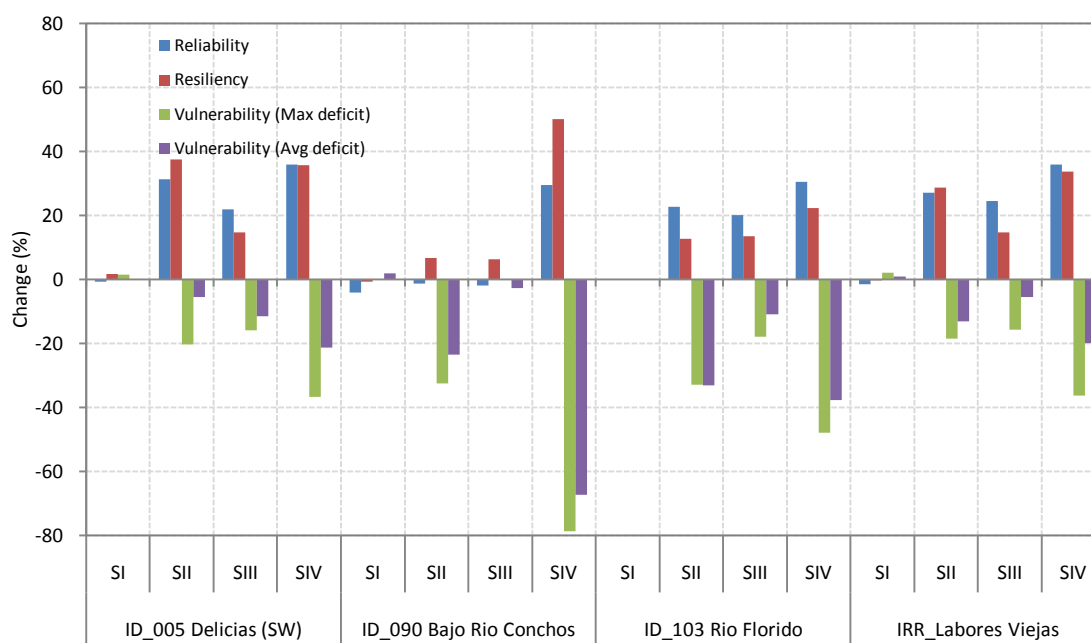
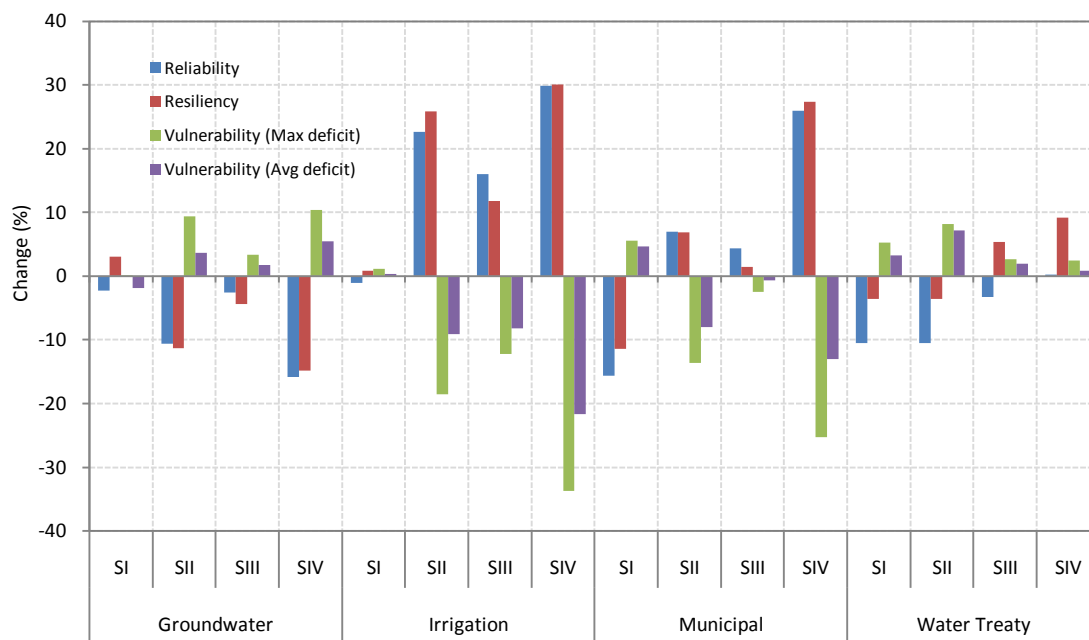Figure 7-3: Performance of main irrigation users under adaptive strategies as percentage of change from the A1B scenario. Period 2040-2099.

Table 7-3: Summary of the performance main irrigation users under adaptive strategies, expressed as percentage change from the A1B scenario.

| Index | ID_005 Delicias (SW) | | | | ID_090 Bajo Rio Conchos | | | | ID_103 Rio Florido | | | | IRR_Labores Viejas | | | |
|---|---|---|---|---|---|---|---|---|---|---|---|---|---|---|---|---|
| | SI | SII | SIII | SIV | SI | SII | SIII | SIV | SI | SII | SIII | SIV | SI | SII | SIII | SIV |
| Reliability | -1 | 31 | 22 | 36 | -4 | -1 | -2 | 30 | 0 | 23 | 20 | 31 | -1 | 27 | 25 | 36 |
| Resiliency | 2 | 38 | 15 | 36 | -1 | 7 | 6 | 50 | 0 | 13 | 14 | 22 | 0 | 29 | 15 | 34 |
| Vulnerability (Max deficit) | 2 | -20 | -16 | -37 | 0 | -32 | 0 | -79 | 0 | -33 | -18 | -48 | 2 | -18 | -16 | -36 |
| Vulnerability (Avg. deficit) | 0 | -5 | -12 | -21 | 2 | -24 | -3 | -67 | 0 | -33 | -11 | -38 | 1 | -13 | -5 | -20 |
| Avg. supply efficiency | -1 | 14 | 11 | 17 | -4 | 11 | -2 | 25 | 0 | 25 | 13 | 30 | -1 | 14 | 11 | 16 |

155
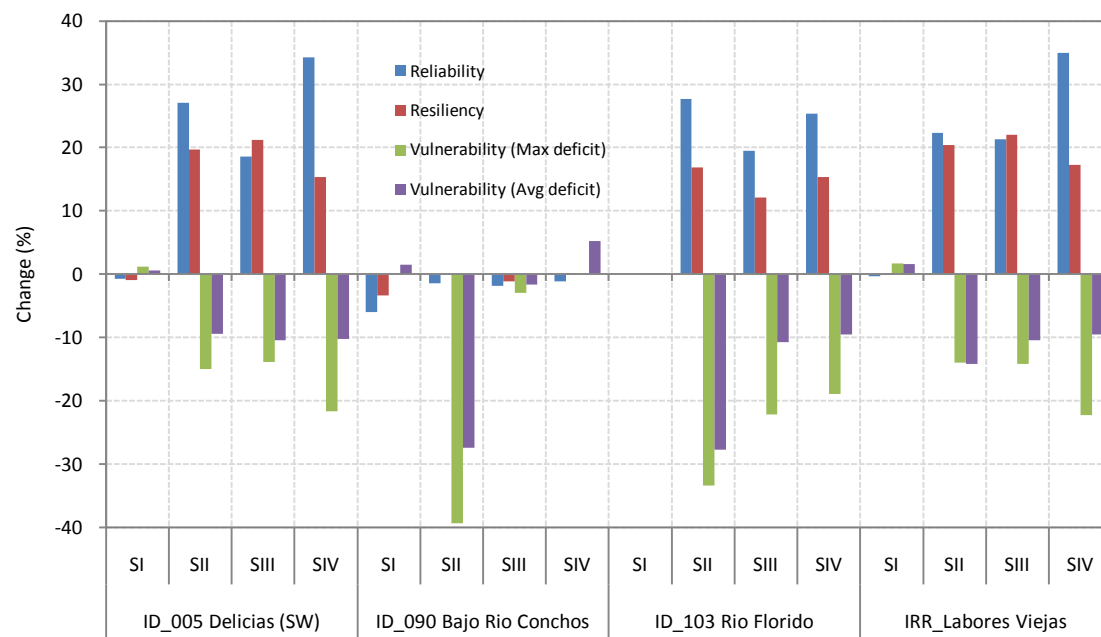
Figure 7-4:  Performance of main irrigation users under adaptive strategies as percentage of change from the A2 scenario. Period 2040-2099.

Table 7-4: Summary of the performance main irrigation users under adaptive strategies, expressed as percentage change from the A2 scenario.

| Index | ID_005 Delicias (SW) | | | | ID_090 Bajo Rio Conchos | | | | ID_103 Rio Florido | | | | IRR_Labores Viejas | | | |
|---|---|---|---|---|---|---|---|---|---|---|---|---|---|---|---|---|
| | SI | SII | SIII | SIV | SI | SII | SIII | SIV | SI | SII | SIII | SIV | SI | SII | SIII | SIV |
| Reliability | -1 | 27 | 19 | 34 | -6 | -1 | -2 | -1 | 0 | 28 | 19 | 25 | 0 | 22 | 21 | 35 |
| Resiliency | -1 | 20 | 21 | 15 | -3 | 0 | -1 | 0 | 0 | 17 | 12 | 15 | 0 | 20 | 22 | 17 |
| Vulnerability (Max deficit) | 1 | -15 | -14 | -22 | 0 | -39 | -3 | 0 | 0 | -33 | -22 | -19 | 2 | -14 | -14 | -22 |
| Vulnerability (Avg. deficit) | 1 | -9 | -10 | -10 | 1 | -27 | -2 | 5 | 0 | -28 | -11 | -9 | 2 | -14 | -10 | -10 |
| Avg. supply efficiency | -1 | 15 | 11 | 18 | -6 | 11 | -1 | -2 | 0 | 26 | 13 | 16 | -1 | 14 | 12 | 18 |

156

**7.3 SUSTAINABILITY IMPROVEMENT OF THE RIO CONCHOS WATER SYSTEM**

The combined performance of the water system in meeting water demands in the Rio Conchos basin and the treaty under adaptive management alternatives is shown in Figure 7-5 and Table 7-5. These results are computed on the basis of reliability, resiliency, and average deficit vulnerability. Values are expressed as percent change from the A1B and A2 scenarios for the period 2040-2099. Under both emission scenarios, the sustainability index for municipal users is reduced under Alternative I (increasing municipal demand over time without adaptive measures).

The adaptive measures of Alternative II increase the sustainability for municipal and irrigation users; however, it decreases (more than 8%) for groundwater users due to the reduction of aquifer recharge. Furthermore, water delivery to the treaty shows a 5% decrease in performance because of its low priority.

Figure 7-5 shows the sustainability indicator for irrigation users in the Rio Conchos basin. It should be noted that Alternative I does not reduce the sustainability for irrigation, as also discussed in previous section, except for ID-090 where a slight decrease is shown. For Alternative II, the index improves by more than 20% for ID-005 Delicias, IRR-Labores Viejas, and ID-103 Rio Florido, but it only increases 10% for ID-090 Bajo Rio Conchos, for both climate scenarios. Similarly, this indicator improves substantially under Alternatives III and IV. In general, results suggest that the water system of Rio Conchos could be more sustainable under climate change conditions, if adaptive measures are implemented in the next decades.

157
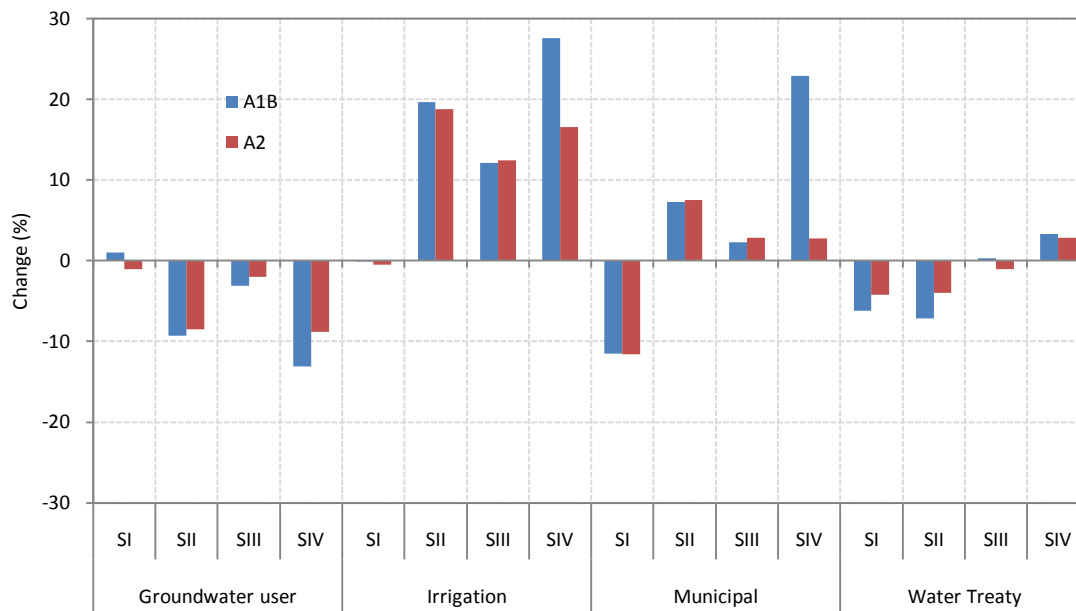
Figure 7-5: Sustainability Index of Rio Conchos water system under adaptive strategies as percentage of change from the A1B and A2 scenarios. Period 2040-2099.

Table 7-5: Sustainability Index for the Rio Conchos Basin under adaptive strategies, stated as percentage change from the A1B and A2 scenarios.

| SCENARIO | Groundwater user | | | | Irrigation | | | | Municipal | | | | Water Treaty | | | |
|---|---|---|---|---|---|---|---|---|---|---|---|---|---|---|---|---|
| | SI | SII | SIII | SIV | SI | SII | SIII | SIV | SI | SII | SIII | SIV | SI | SII | SIII | SIV |
| A1B | 1 | -9 | -3 | -13 | 0 | 20 | 12 | 28 | -12 | 7 | 2 | 23 | -6 | -7 | 0 | 3 |
| A2 | -1 | -8 | -2 | -9 | 0 | 19 | 12 | 17 | -12 | 8 | 3 | 3 | -4 | -4 | -1 | 3 |
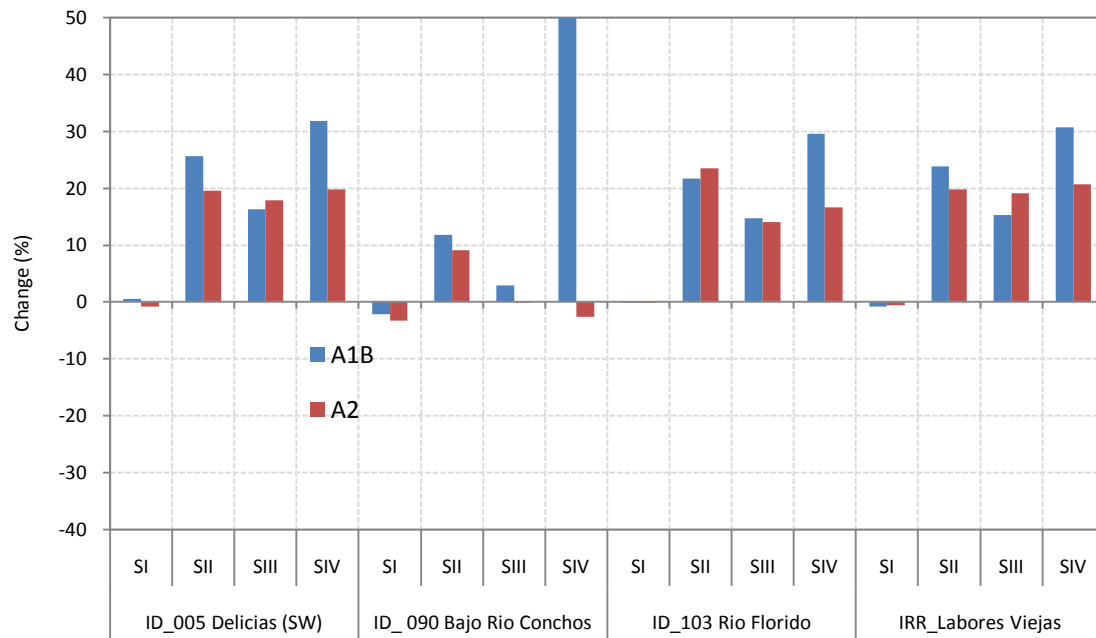
Figure 7-6: Sustainability Index of irrigation users under adaptive strategies as percentage of change from the A1B and A2 scenarios. Period 2040-2099.

Table 7-6: Sustainability Index for irrigation users in the Rio Conchos Basin under adaptive strategies, stated as percentage change from the A1B and A2 scenarios.

| Alternative | ID_005 Delicias (SW) | | | | ID_090 Bajo Rio Conchos | | | | ID_103 Rio Florido | | | | IRR_Labores Viejas | | | |
|---|---|---|---|---|---|---|---|---|---|---|---|---|---|---|---|---|
| | SI | SII | SIII | SIV | SI | SII | SIII | SIV | SI | SII | SIII | SIV | SI | SII | SIII | SIV |
| A1B | 1 | 26 | 16 | 32 | -2 | 12 | 3 | 51 | 0 | 22 | 15 | 30 | -1 | 24 | 15 | 31 |
| A2 | -1 | 20 | 18 | 20 | -3 | 9 | 0 | -3 | 0 | 24 | 14 | 17 | -1 | 20 | 19 | 21 |

# Chapter 8: Conclusions

## 8.1 RESEARCH SUMMARY

A hydrologic model has been developed using the one-dimensional, 2 layer soil moisture accounting scheme embedded in the Water Evaluation and Planning (WEAP) model. A ten year period was used to calibrate the model, which was achieved by a trial-and-error method for the adjustment of the model parameters. Calibrating the model involved both quantitative and qualitative evaluation of the hydrologic response of each sub-catchment. This was carried out using historical observed data, such as, precipitation, temperature, relative humidity, wind velocity, and soil parameters to produce streamflow output from each sub-catchment. Some empirical equations were used to calibrate the model to match, as closely as possible, the monthly and annual historical flows. The calibration parameters considered in each sub-catchment were the water storage capacity, hydraulic conductivity, initial storage and flow direction for each of the two model layers. A validation data set for a drought period in the basin was used to assess the performance of the model.

After developing the hydrologic representation of the basin described above, this model was used to simulate future climate change scenarios from five General Circulation Models. The methodology included: (1) analyzing multiple, downscaled General Circulation Model (GCM) outputs under two emission scenarios, A2 and A1B; (2) simulating the response of the basin hydrologic system to the resulting climate change; (3) deriving skill-weighted multi-model ensemble outputs describing the basin

response to climate change; and (4) assessing climate change impacts on hydrology in the basin. Flows produced by using the downscaled data from the five GCMs in a hydrologic model form an ensemble response of the basin. A weighted method was developed for the model ensemble which gives preference to the GCMs that present greater skill with respect to reproducing historic runoff values. Although this approach has some limitations, for example, correcting errors in magnitude, the method is much better than a simple average. Weights were assigned according to the performance or skill of reproducing the monthly flow of a historical period using the GCMs in the hydrologic model. Several techniques were used to evaluate the impacts of climate variability and change on hydrology for annual, maximum, and minimum flows, such as probability density functions, wavelet analysis, and trend analysis. The wavelet analysis was used to examine the connections of the historical monthly flows with long- and short-term climatologic pattern variability, such as the Pacific Decadal Oscillation (PDO) and El Niño/Southern Oscillation (ENSO) and their influence on the hydrology of the Rio Conchos, and how they are correlated to future flows under climate change. Likewise, wavelet analysis was applied to the flow time series under the climate change scenarios.

A water resources planning model has been developed for the Rio Conchos Basin. The model integrates two parts: the hydrologic model described above and water management modeling. Five main reservoirs, operation rules, municipal and irrigation water demands, aquifers, water distribution policies, return flows, stream gages, and transmission links are represented in the water planning model. A yearly demand with

161

monthly variation was used to represent water demands; priorities and consumptive use are set in the model. Constraints were defined for maximum flow in transmission links for demand points that use water from reservoirs, which are linked to special operation rules. The model was calibrated using historical streamflow, storage reservoir volumes, irrigation and municipal water deliveries, water distribution rules, and priorities. For groundwater modeling, a combination of the deep soil layer of the WEAP soil moisture method and groundwater-surface water flow method was used. Climate change impacts on the performance of the water system were evaluated using the reliability, resiliency, and vulnerability to meet the user demands. Finally, four adaptive water management strategies to mitigate the impact of climate change in the study basin were designed and simulated for each emission scenario.

## 8.2 RESEARCH QUESTIONS AND OBJECTIVES

The research developed here answers the following questions:

1. *What will the hydrologic response of the Rio Conchos basin be under the potential effects of climate change?*

2. *What will happen to water availability in the basin over the coming decades taking account the climate change impacts in the basin?*

3. *What will happen to the water treaty between Mexico and the US under the potential effects of climate change?*

4. *How can the water infrastructure, such as dams and channels for irrigations districts, be operated to reliably adapt to climate change in the basin?*

5. *What kind of management strategies could be implemented in order to face future drought periods?*

In order to answer the research questions, the research objectives pursued are described below:

1. Model the hydrological behavior of the Rio Conchos basin (rainfall – runoff) using the soil moisture method;

2. Process and analyze statistically downscaled climate outputs from 5 General Circulation Models (GCMs) for emission scenarios A2 (high emission path) and A1B (middle emission path);

3. Simulate and assess the result of climate change on the hydrology system of the Rio Conchos;

4. Assess climate change impacts on water resources management in basin and its effect on the 1944 Treaty between the US and Mexico; and

5. Simulate and evaluate water management scenarios to adapt to the climate change effects in the next decades.

## 8.3 CONCLUSIONS

The conclusions achieved in this study address the objectives outlined and described in the introduction and research objective sections.

**8.3.1 Hydrologic Modeling**

This part satisfies the first objective and generates the necessary tool to answer the research questions stated in previous section:

*Question 1.  What will the hydrologic response of the Rio Conchos basin be under the potential effects of climate change?*

Objective 1. Model the hydrological behavior of the Rio Conchos basin (rainfall – runoff) using the soil moisture method;


The hydrologic model developed in WEAP reproduces the response of the Rio Conchos Basin. The model was calibrated using a trial-and-error method over a ten-year period and validated for an independent ten-year period. Empirical equations were used to estimate initial values for the conductivities of the model layers in the sub-catchments for the calibration process.

Final parameters from the calibration process included the initial storage, hydraulic conductivity, water holding capacities, and the preferred flow direction, for both layers. High values of water capacity estimated for the lower layer indicate the presence of deep aquifers especially in the middle and lower basin. Average monthly and annual flows were accurately estimated by the model.

Comparisons between simulated and naturalized streamflows, for both monthly and annual showed an error less than 10%. The error in reproducing the naturalized flows was less than 5% for the basin outlet (Ojinaga station) for the calibration period; and

these errors decreased significantly in the validation period. Statistical parameters indicate good model performance (Nash Coefficient, and Index of Agreement). The model computes smaller low flows in some stations compared with naturalized flow, and this behavior could be improved by considering the interaction between surface runoff and shallow aquifers in the study basin.

### 8.3.2 Climate Change Impacts on Hydrology

Conclusions addressed here meet the second and third research objectives in order to answer questions one and two of this investigation.

*Question 1. What will the hydrologic response of the Rio Conchos basin be under the potential effects of climate change?*

*Question 2. What will happen to water availability in the basin over the coming decades taking account the climate change impacts in the basin?*

Objective 2. Process and analyze statistically downscaled climate outputs from 5 General Circulation Models (GCMs) for emission scenarios A2 (high emission path) and A1B (middle emission path);

Objective 3. Simulate and assess the result of climate change on the hydrology system of the Rio Conchos;

*Climate data analysis from the multi-model ensemble*

The analysis of temperature and precipitation projections from five GGMs for the Rio Conchos basin suggests that the models agree in predicting temperature trends for

165

both the A2 and A1B emission scenarios. By contrast, the models differ in estimating the precipitation. For instance, MIROC32 and EACHM5 are the models that better represent the historical precipitation, as shown in the results section, however, these models predict very low precipitation for the period 2040-2099, with a reduction by more than 50-60%, which will be impossible for the hydrological conditions of the study basin.

Essentially, as pointed out in the literature review section, the main uncertainty sources in the GCM precipitation prediction come from the spatial resolution, parameterization of local and regional climate processes, model structures, and numerical methods used in each GCM. For the ensemble average, historical monthly temperature is underestimated by 0.15 $^{o}$C with an uncertainty level that oscillates from +0.20 $^{o}$C to -0.40 $^{o}$C. In general, the GCMs underestimate historical precipitation, with average biases varying between +5% and -30%.

A multi-model ensemble of five General Circulation Models was developed using the mean square error weighting approach. The method was applied for temperature, precipitation, and streamflow time series. The weighted multi-model ensemble indicates that annual temperature in the basin may increase by 4.8 $^{o}$C ± 0.57 $^{o}$C by the end of the period 2080-2099 under scenario A2, and 3.9 $^{o}$C ± 0.81 $^{o}$C for under scenario A1B. For the ensemble, annual precipitation shows a negative trend over the century, with an average annual change around -11% ± 24% for the period 2080-99 under scenario A2, and -8% ± 26% under scenario A1B. In addition, some seasonal changes are expected with less precipitation occurring in winter and spring.

166

*Natural variability of streamflow*

An analysis of the natural variability of streamflow and its connection with climate patterns was also explored. A three-year moving average for the period 1940-1999 indicates strong negative and positive trends alternating on 5-10 years cycles. Wavelet technique was used to evaluate inter-annual and temporal viability of annual streamflows in the Rio Conchos at Ojinaga. The analysis shows that ENSO has a weak negative correlation to streamflow in the Rio Conchos at Ojinaga. By contrast, PDO index has a strong positive correlation for the 5-10 and 8-15 years bands indicating that the decadal oscillations tend to coincide with natural variations in streamflows.

Under scenarios A2 and A1B, flows show a strong positive correlation with historical flows (for the 8-15 year wavelet band); consequently, they may be correlated to PDO phases. This flow-climate relationship may be useful to improve the long-term forecasting in the Rio Conchos basin, which is essential to developing optimal reservoir planning and operation policies for water supply and flood control. Further analysis is needed in other river locations in order to investigate the interconnection between flows and climate patterns.

*Impacts of climate change on streamflow*

As mentioned above, there is uncertainty in the precipitation predicted by the GCMs. The uncertainty range is high, causing a wide range of variability in streamflow projections. Even more, if the uncertainty in the hydrological modeling calibration

process is taken into account, the flow predictions for water resources applications are difficult and uncertain. Under this consideration, streamflow in the Rio Conchos basin is expected to be negatively affected by climate change in the coming decades. According to the multi-model ensemble, annual streamflows at Ojinaga are projected to decrease by 20%, with an uncertainty range of $\pm$ 45% under scenario A2 and 12% $\pm$ 53% under scenario A1B by the last twenty years of this century. Greater reductions in streamflow are predicted for the period 2060-2079 under both emission scenarios, and this may be related to a PDO phase.

Analysis indicates that peak flows may be reduced substantially, with a notable effect in the period 2080-2099 under scenario A2; by contrast, minimum flows may tend to be more stable and larger that the historic flows (1980-1999). Despite the discrepancies in predicted monthly streamflow among the GCMs, the results agree in projecting that peak annual flow will occur in September, a month later than historical conditions. An analysis of streamflow variability for both climatic scenarios shows a positive trend indicating increased variability over time. There is a negative streamflow trend over the whole time period under scenario A2; by contrast, there is a slight increase for scenario A1B, with significant variability for both scenarios after 2065. The results indicate that annual runoff will be reduced more in 2060-2079 than in 2040-2059 or 2080-2099 for both emissions scenarios. Comparisons with the historic period indicate that maximum flows will be reduced, while minimum flows tend to be larger.

While the uncertainty range is expected to be ±40%, maximum flows are predicted to increase more than 15% in 2080-2099 under scenario A1B; by contrast, a small reduction of 5% is projected under scenario A2. Probabilistic analysis indicates a significant increase of more than 15% in the period 2080-2099 under the scenario A1B; by contrast, a reduction by more than 5% is projected under scenario A2.

For both climate change scenarios, predicted maximum flows show an increased in the 75$^{th}$ percentile flow and a decrease in the 25$^{th}$ percentile flows. Although, there are not large changes in terms of magnitude, minimum flows tend to be decreased for the upper quartile and increased for the lower quartile.

For monthly average flow, the GCM results show a high range of variability in predicting the North American monsoon (July-September) season. The main problem here is that GCMs can't simulate this complex (small scale) climate pattern due to the coarse resolution grids and parameterization schemes used in each GCM to represent the precipitation process at the local scale. For this reason, the range of variability in flow prediction is from ± 35% to ± 100%. Likewise, results show that the variability range in predicting the monsoon season increases over time for both scenarios. For instance, streamflow in September may increase by 6% ± 44% for the period 2040-2059, while streamflow may decrease by 8% with an uncertainty range ± 63% for the period 2080-2099, under scenario A2.

**8.3.3 Water System Performance under Climate Change**

In this section, conclusions meet the fourth objective in order to answer research questions two and three.

*Question 2. What will happen to water availability in the basin over the coming decades taking account the climate change impacts in the basin?*

*Question 3. What will happen to the water treaty between Mexico and the US under the potential effects of climate change?*

Objective 4. Assess climate change impacts on water resources management in basin and its effect on the 1944 Treaty between the US and Mexico; and

Conclusions arrived here must be interpreted carefully, considering the high uncertainty range in the flow predictions. In addition, in this study, uncertainties are introduced at each step and propagated through a modeling chain, including: GCMs (discussed in previous sections), driving forces in the emission scenario formulation, downscaling technique, hydrological modeling (calibration process), ensemble method, and, finally, the water management model.

This research demonstrates that the water availability in the Rio Conchos Basin will likely become more vulnerable to future drought events under climate change; however, adaptive strategies may play an important role in reducing the negative effects on the system. Using a weighted multi-model ensemble of results from five GCMs for emission scenarios A1B and A2 in a hydrologic water management model shows that the

reliability and resiliency of water supplies to meet demands will decrease significantly for most users; even more, this condition is projected to be more critical if an increased municipal demand due to population growth is considered.

The vulnerability (deficit) for irrigation, municipal, and water treaty deliveries increases substantially over time, which could exacerbate even more the competition for water resources on both sides of the border. The impact is less for emission scenario A1B, as expected. In general, the reliability of water supply to meet most demands is reduced by more than 15% on average for the period 2040-99. The ability to meet municipal demands is only slightly reduced due to the highest priority set in the water planning model in meet this requirement. The change, expressed as percentage from the baseline scenario, suggests an increase of the annual maximum deficit by more than 14% for irrigation demands. The impact is similar under emission scenario A2.

The 20-year period analysis suggests that the reliability and resiliency of water supplies to meet demands will be more reduced in 2060-79 than 2040-59 and 2080-99, under the emission scenario A1B. As a consequence, the vulnerability of the water system is expected to increase because of the likely increase in magnitude and duration of droughts during this time period. Under emission scenario A2, reliability and resiliency are significantly reduced; therefore, the vulnerability tends to increase. Municipal demands showed a slightly reduced reliability and resiliency, with increased deficit of 5% on average. In general, scenario A1B predicts a greater impact on the system performance than the scenario A2 during the period 2060-79.

171

Since the 1944 water treaty was signed under historical conditions, a negative impact on the ability of water supplies to meet the demands of the treaty is expected. Reliability and resiliency for the water treaty will be reduced by more than 13% for the A1B scenario. These are are further reduced in 2060-79 and 2080-99. Consequently, the water treaty may become increasingly vulnerable to potential climate change, with a significant impact during the period 2060-79. The effect is slightly more significant under the scenario A2.

Despite the uncertainty in the GCM predictions and hydrologic modeling, the effect of climate change in the Rio Conchos Basin suggests a negative impact on water availability and management of the basin. This situation indicates the need for considering adaptive strategies to mitigate this problem in the coming decades.

## 8.3.4 Adaptive Strategies to Mitigate Climate Change Effects

Conclusions expressed here meet the fifth objective in order to answer research questions four and five.

*Question 4. How can the water infrastructure, such as dams and channels for irrigations districts, be operated to reliably adapt to climate change in the basin?*

*Question 5. What kind of management strategies could be implemented in order to face future drought periods?*

Objective 5. Simulate and evaluate water management scenarios to adapt to the climate change effects in the next decades.

Four water management alternatives were simulated and evaluated for each emission scenario. For each alternative, special reservoir operation rules of were programmed to meet water demands for irrigation, municipal, groundwater, and the water treaty.

The simulation of the adaptive measures shows that it is possible to improve the performance of the system, making it more reliable, less vulnerable, and more sustainable. The overall performance of the system, expressed in terms of a sustainability index, indicates that the system will probably be less sustainable under climate change; nevertheless, substantial performance improvement is indicated with the implementation of adaptation measures.

In general, under the condition of Scenario I, the system is less reliable and more vulnerable; with a strong impact on municipal users. However, for Scenario II, which includes relevant improvement on the hydraulic infrastructure, change of crops, and groundwater use for drought periods, the system reliability increases; consequently, the vulnerability may be reduced significantly. Similar behavior, but with a different magnitude, occurs for Scenarios III and IV. However, performance is reduced for groundwater users, due to the recharge reduction as result of the improvement efficiency of the water system.

The performance of the water treaty does not improve significantly under the proposed strategies. Under climate change, increasing demand for municipal water in the next decades may affect even more the ability to meet treaty commitments. One of the

reasons why treaty performance does not improve substantially is the high priority on meeting the in-basin water demands in the Rio Conchos. Nevertheless, treaty performance could be improved by increasing the priority of meeting this water demand and setting special operating rules to release water from La Boquilla and Luis L. Leon reservoirs.

Finally, this methodology can be replicated in other basins, however, it is somewhat difficult and has quite a lot uncertainty as discussed in previous sections.

## 8.4 RECOMMENDATIONS AND FUTURE WORK

Some recommendations and future work are derived from this research in order to improve future climate change studies for water resources in the Rio Conchos basin, as well as other basins. As shown in the results, the hydrologic model computes lower low flows in some stations than the historic record, e.g., La Boquilla station. This performance could be improved by including the groundwater – surface water interaction for shallow aquifers located in this area. Moreover, including simple routing flow in the model could be useful in the hydrologic modeling for climate change.

Future work should consider an economic analysis to evaluate the feasibility of proposed water strategies under climate change. On the other hand, further groundwater and surface water studies are required to evaluate water management strategies based on improvements to the hydraulic system, considering thresholds of water efficiency that don't significantly diminish groundwater recharge. Likewise, future studies in the Rio Conchos should consider the impact of climate change on potential evapotranspiration,

174

since it is important to design and develop new water irrigation schemes to face the changing climate.

The proposed strategies have been evaluated through simulation approach. Future work is recommended to develop and derive optimal water policies under climate change using optimization methods on the basis of the multi-model ensemble.

Unchanging land use in the next decades is one of the main assumptions of this research. Changes in land use and how they could affect the hydrology of the basin, exacerbating even more the competition for water resources, under climate change are recommended to be explored in future investigations.

The improvement of spatial resolution and climate feedbacks in GCMs is important to reduce the modeling uncertainty. Perhaps, also, the use of an increased number of GCMs could reduce the range of uncertainty. However, the need for close communication is suggested between water resources researchers and the IPCC in order to incorporate relevant local climate aspects through use of regional climate models (RCM), perform sensitivity analyses based on RCMs for specific regions, before simulating future emission scenarios. Furthermore, many investigators agree that stationary conditions may not exist now or in the future; therefore, the development of new probabilistic methods and uncertainty analysis under nonstationary conditions including future flow variability is recommended.

Finally, the development of reservoir operating schemes, adaptive water management strategies, decision support systems, and mathematical programming tools

175

for the management of the water resource system, reservoir planning, flood control, irrigation, hydropower, wastewater management, and the interaction between groundwater and surface water under changing climate and demands need further studies.

# References

Ajami, N.K; Hornberger, G.M; and Sunding, D.L. (2008). "Sustainable water resources management under hydrological uncertainty". Water Resour. Res; 44, W11406, doi:10.1029/2007WR006736, 1-10.

Akhtar, M., Ahmad, N., and Booij, M.J. (2008). "The impact of climate change on the water resources of Hindukush–Karakorum–Himalaya region under different glacier coverage scenarios". Journal of Hydrology, 355, 148– 163.

Amato, Ch.C., McKinney, D.C., Ingol-Blanco, E., and Teasley, R.L. (2006). "WEAP Hydrology model applied: The Rio Conchos Basin". Center for Research in Water Resources.  The University of Texas at Austin.  Online Report 06-12.

Barbaro, J.R., and Zarriello, P.J. (2006). "A precipitation–runoff model for the Blackstone River basin, Massachusetts and Rhode Island". Scientific Investigations Report 2006-5213. U.S. Department of the Interior, U.S Geological Survey, 92 pp.

Benaman, J., Shoemaker, C.A. and Haith, D.A. (2005). "Calibration and validation of soils and water assessment tool on an agricultural watershed in upstate New York". J. Hydrol. Eng., 10(5):363-374.

Bayazit, M, Onoz, B, and Aksoy, H. (2001). "Nonparametric flow simulation by wavelet of Fourier analysis". Hydrologic Science, 46(4):623-634.

Beyene, T., Lettenmaier, D.P., and Kabat, P. (2008). "Hydrologic impacts of climate change on the Nile River basin. Implications of the 2007 IPCC climate scenarios". Department of Civil and Environmental Engineering, University of Washington. 46 pp. www.hydro.washington.edu/.../Publications/Tazebe_**Nile**_Aug07.pdf

Brandes, R.J. (2003). "Water availability modeling for the Rio Grande Basin, naturalized streamflow data". Texas Commission on Environmental Quality. Final Report

Brinkmann W.A.R. (2000). "Modification of a correlation–based circulation pattern classification to reduce within–type variability of temperature and precipitation". International Journal of Climatology 20: 839-852.

Canadell, J., Jackson, R.B., Ehleringer, J.R., Mooney, H.A., Sala, O.E., and Schulze, E.D. (1996). "Maximum rooting depth of vegetation types at the global scale". Oecologia. 108:583-595.

Chong–Yu, X. (1999). From GCMs to River Flow: A Review of Downscaling Methods and Hydrologic Modeling Approach. Progress in Physical Geography 23, 2: 229-249.

Chow, V., Maidment, D., and Mays, L. (1988). "Applied Hydrology". McGraw-Hill, New York.

Christensen, N.S., Wood, A.W., Voisin, N., Lettenmaier, D.P., and Palmer, R.N. (2004). "The effects of climate change on the hydrology and water resources of the Colorado river basin". Climatic Change, 62(1–3), 337–363.

Chu, J.T., Xia, J., Xu, C.Y., and Singh, V.P. (2009). "Statistical downscaling of daily mean temperature, pan evaporation and precipitation for climate change scenarios in Haihe River, China". Theoretical and Applied Climatology, DOI 10.1007/s00704-009-0129-6.

Chu, X., and Steinman, A. (2009). "Event and continuous hydrologic modeling with HEC-HMS". *J. Hydrol. Eng*. 135(1):119-124.

Collado, J. (2002). "Criterios de distribución del agua en la Cuenca del Rio Bravo." Instituto Mexicano de Tecnología del Agua (IMTA). Cuernavaca, Morelos, México.

Conway D. and Jones P.D. (1998). "The use of weather types and air flow indices for GCM downscaling". Journal of Hydrology 212–213, 348–361.

CONAGUA – Comisión Nacional del Agua. (2004). "Registro Público de Derechos de Agua." México, D.F.

CONAGUA – Comisión Nacional del Agua. (2008.b). "Acuerdo por el que se da a conocer el resultado de los estudios de disponibilidad media anual de las aguas superficiales en la cuenca del Rio Bravo" Diario Oficial de la Federación. 29 de Septiembre de 2008. México D.F.

CONAGUA – Comisión Nacional del Agua. (2009). "Estadísticas Agrícolas de los Distritos de Riego. Año Agrícola 2007-2008" Gobierno Federal – Secretaria del Medio Ambiente y Recursos Naturales. Mayo 2009. México D.F.

Danner, C.L., McKinney, D.C., Teasley, R.L., and Sandoval, S. (2006). Documentation and Testing of the WEAP Model for the Rio Grande/Bravo Basin. Center for Research in Water Resources, The University of Texas at Austin, Online Report 06-08.

El-Adlouni, S, Ouarda, T.B, Zhang, X, Roy, R, and Bobee, B. (2007). "Generalized maximum likelihood estimators for the nonstationary generalized extreme model". Water Resources Research 43(W03410):14pp.

Collins, W.D., Bitz, C.M., Blackmon, M.L., Bonan, G.B., Bretherton, C.S., Carton, J.A., Chang, P., Doney, S.C., Hack, J.J., Henderson, T.B., Kiehl, J.T., Large, W.G., McKenna, D.S., Santer, B.D., and Smith, R.D. (2006) The Community Climate System Model Version 3 (CCSM3). Climate, 19(11):2122-2143.

CONAGUA – Comisión Nacional del Agua. (2004). "Registro Público de Derechos de Agua." México, D.F.

Coulibaly, P, and Burn, D.H. (2004). "Wavelet Analysis of Variability in annual Canadian flows". Water Resources Research, 40(W03105):1-14.

Chow, V., Maidment, D., and Mays, L. (1988). <u>Applied Hydrology</u>. McGraw-Hill, New

York.

Diaz-Nieto J, Wilby R.L. (2005). "A comparison of statistical downscaling and climate change factor methods: Impacts on low flows in the River Thames, United Kingdom". Climatic Change 69: 245–268.

Draper, S.E., Kundell, J.E. (2007). "Impact of climate change on transboundary water sharing". Journal of Water Resources Planning and Management. ASCE, 133(5), 405-415.

Elshamy, M.E., Wheater, H.S., Gedney, N., and Huntingford, C. (2006). "Evaluation of the rainfall component of a weather generator for climate impact studies", Journal of Hydrolply. 326 (2006), pp. 1–24.

Englehart, P.J; and Douglas, A.V. (2002). "On some characteristic variations in warm season precipitation over the central United States (1910-2000)". J. Geo. Research, 107(16), 4286, 10.1029/2001JD000972.

Flato, G.M. and Boer, G.J. (2001) Warming Asymmetry in Climate Change Simulations. Geophys. Res. Lett., 28:195-198.

Fleming, M., and Neary, V. (2004). "Continuous modeling study with the hydrologic modeling system. *J. Hydrol. Eng.* 9(3):175-183.

Fowler, H. J., Kilsby, C.G; and O'Connell, P.E. (2003). "Modeling the impacts of climatic change and variability on the reliability, resilience, and vulnerability of a water resource system". Water Resour. Res., 39(8), 1222, doi:10.1029/2002WR001778, 1-11.

Fowler, H.J., Blenkinsop, S., and Tebaldi, C. (2007). "Linking climate change modeling to impacts studies: recent advances in downscaling techniques for hydrological modeling". International Journal of Climatology. 27, 1547-1578.

Fowler H.J, Kilsby C.G., and Stunell J. (2007). "Modelling the impacts of projected future climate change on water resources in northwest England". Hydrology and Earth System Sciences 11(3): 1115-1126.

Fowler, H. J., and Kilsby, C.G. (2007). "Using regional climate model data to simulate historical and future river flows in northwest England". Climatic Change. 80:337–367 DOI 10.1007/s10584-006-9117-3.

Gao, Ch., Gemer, M., Zeng, X., Liu, B., Su, B., and Wen, Y. (2009). "Projected streamflow in the Huaihe River Basin (2010-2100) using artificial neural network". Stochastic Environmental Res Risk Assessment, DOI 10.1007/s00477-009-0355-6.

Gomez-Martinez, J., Mejia R., and A. Gutierrez. 2005. Study of Distributed Models for the Simulation of basin runoff: Application to the Rio Conchos basin, Tributary of Bravo River. Mexican Institute of Water Technology (IMTA). SEMARNAT-2002-C01-0569.A3. Final Report.

Gordon C., Cooper, C., Senior, C.A., Banks, H.T., Gregory, J.M., Johns, T.C., Mitchell, J.F.B., and Wood, R.A. (2000). The simulation of SST, sea ice extents and ocean heat transports in a version of the Hadley Centre coupled model without flux adjustments. Climate Dynamics 16:147-168

Griffis, V.W, and Stedinger, J.R. (2007). "Log-Pearson Type 3 distribution and its application in flood frequency analysis". Hydrologic Engineering, 12(5):482-491.

Hamlet, A.L., and Lettenmaier, D. (1999). "Effect of climate change on hydrology and water resources in the Columbia river basin". Journal of the American Water Resources Association. AWRA, Vol. 35(6), 1597-1623.

Hashimoto, T., Stedinger, J.R; and Loucks, D.P. (1982). "Reliability, resiliency, and vulnerability criteria for water resource system performance evaluation". Water Resour. Res., 18(1), 14 – 20, doi:10.1029/WR018i001p00014, 14-20.

Hay L.E., Wilby, R.L and Leavesly, H.H. (2000). "Comparison of delta change and downscaled GCM scenarios for three mountainous basins in the United States". Journal of the American Water Resources Association 36 (2), pp. 387–397.

Hay, L.E., and Clark, M.P. (2003). "Use of statistically and dynamically downscaled atmospheric model output for hydrologic simulations in three mountainous basins in the western United States". Journal of Hydrology 282 (2003) 56–75.

Hertig, E., and Jacobeit, J. (2007). "Assessments of Mediterranean precipitation changes for the 21st century using statistical downscaling techniques". International Journal of Climatology, DOI: 10:1002/joc.1597.

Helsel, D.R; and Hirsch, R.M. (2002). "Statistical methods in water resources". USGS Geological Survey. Book4, Hydrologic Analysis and Interpretation. Reston. 524 pp.

Ingol-Blanco, E. (2008). "Climate change impacts on the water resources: An overview of global Impacts and techniques to assess at local scale". Physical Climatology paper class, Literature Review, The University of Texas. at Austin.

Ingol-Blanco, E., and McKinney, D. (2009). "Hydrologic model for the Rio Conchos Basin: calibration and validation". Center for Research in Water Resources, The University of Texas at Austin, Online Report 08-09.

Ingol-Blanco, E., and D. C. McKinney. (2009). "Hydrologic Model of the Rio Conchos." EWRI World Environmental and Water Resources Conference, Kansas City, KS May 2009.

Ingol-Blanco, E., and D. C. McKinney. (2010). "Transboundary Climate Change Effects on the Hydrologic Regime in the Rio Conchos Basin", EWRI World Environmental and Water Resources Conference, Providence, RI, May 2010

Ingol-Blanco, E., and McKinney, D.C. (2010). "Development of a hydrological model for the Rio Conchos Basin". Paper submitted to the Hydrologic Engineering.

Ingol-Blanco, E., and McKinney, D.C. (2011). "Modeling Climate Change Impacts on Flow in the Rio Conchos Basin". Paper submitted to the J. Water Resour. Planning and Management.

Ingol-Blanco, E., and McKinney, D.C. (2011). "Analysis of Adaptation Scenarios for Climate Change Impacts in the Rio Conchos Basin". EWRI World Environmental and Water Resources Conference, Palm Spring, CA May 2011.

International Boundary Water Commission (IBWC, 2008). Rio Grande Historical Mean Daily Discharge Data. http://www.ibwc.state.gov/Water_Data/histflo1.htm

International Boundary and Waters Commission (IBWC). (1944). "Utilization of waters of the Colorado and Tijuana Rivers and of the Rio Grande." Treaty between the United States of America and Mexico. Washington, US.

IPCC. (2008). "Climate Change and Water".   Contribution to the Fourth Assessment Report of the Intergovernmental Panel on Climate Change. Bates, B.C., Kundzewicz, Z.W., Wu, S., and Palutikof, J.P. IPCC technical paper VI. http://www.ipcc.ch/ipccreports/tp-climate-change-water.htm

IPCC - Intergovernmental Panel on Climate Change. (2000). Emissions Scenarios. Nebojsa Nakicenovic and Rob Swart (Eds.). Cambridge University Press, Cambridge. pp 570

IPCC. (2001). Climate Change 2001. "The Scientific Basis". Contribution of Working Group I to the Third Assessment Report of the Intergovernmental Panel on Climate Change [Houghton, J.T.,Y. Ding, D.J. Griggs, M. Noguer, P.J. van der Linden, X. Dai, K. Maskell, and C.A. Johnson (eds.)]. Cambridge University Press, Cambridge, United Kingdom and New York, NY, US, 881pp.

IPCC. (2001). Climate Change 2001. "Impacts, adaption and vulnerability". Hydrology and water resources chapter. Contribution of working group II to the Third Assessment Report of the Intergovernmental Panel on Climate Change. Cambridge University Press, Cambridge, United Kingdom and New York, NY, US, 913 pp.

IPCC. (2007). Summary for Policymakers, Climate Change 2007. "Impacts, Adaptation and Vulnerability". Contribution of Working Group II to the Fourth Assessment Report of the Intergovernmental Panel on Climate Change, M.L. Parry, O.F. Canziani, J.P. Palutikof, P.J. van der Linden and C.E. Hanson, Eds., Cambridge University Press, Cambridge, UK, 7-22. http://www.ipcc.ch/pdf/assessment-report/ar4/wg2/ar4-wg2-spm.pdf

Jenkinson, A.F. (1955). "The frequency distribution of the annual maximum (or minimum) of meteorological elements". World Meteorological Office, London, 158-171.

Jimenez, G.G. (2002). "Agriculture use of water in the Rio Conchos basin". Texas Center for Policies Studies. Chihuahua, Mexico.

JISAO - Joint Institute for the Study of the Atmosphere and Ocean. (2010). PDO Index
Monthly Values. University of Washington. Seattle.
http://jisao.washington.edu/pdo/

Joyce, B., Vicuna, S., Dale, L., Purkey, D., and Yates, D. (2006). "Climate change
impacts on water for agriculture in California: A case study in the Sacrament
Valley". California Energy Commission and the California Environmental
Protection Agency.

Jungclaus, J.H., Botzet, M., Haak, H., Keenlyside, N., Luo, J-J, Latif, M., Marotzke, J.,
Mikolajewicz, U., and Roeckner, E. (2006). Ocean circulation and tropical
variability in the AOGCM ECHAM5/MPI-OM. J Climate 19:3952-3972

K-1 Model Developers. (2004). "K-1 coupled model (MIROC) description", K-1
Technical Report, 1. In: Hasumi H., Emori S. (eds). Center for Climate System
Research, University of Tokyo, Tokoyo. 34 pp

Kahya, E., and Kalayl, S. (2004). "Trend analysis of flow in Turkey". Journal of
Hydrology, 289:128-144.

Karl, T.M. (2002). "The U.S national climate change assessment: do the climate models
project a useful picture of regional climate?" National Data Center, NOAA.

Kang, B., and Ramirez, J.A. (2007). "Response of streamflow to weather variability
under climate change in the Colorado Rockies". Journal of Hydrologic
Engineering, ASCE, Vol. 12, No. 1, 63-72.

Kim, B.S., Hung Soo Kim., Byung Ha Seoh., and Nam Woon Kim. (2006). "Impact of
climate change on water resources in Yongdam Dam Basin, Korea". Journal of
Stochastic Environmental Research and Risk Assessment 21:355–373.

Kim, T.W. and J., Valdes. 2005. "Synthetic Generation of Hydrology Time Series Based
on Nonparmetric Random Generation". Journal of Hydrologic Engineering.
ASCE, 10(5), 395-404.

Kim, U., J. Jagath., J.J. Kaluarachchi., and V.U Smakhtin. (2008). "Climate Change
Impacts on the Hydrology and Water Resources of the Upper Blue Nile River
Basin, Ethiopia". Research Report 126 of the International Water Management
Institute and the Utah State University. 21 pp.

Kim, T.W., J. Valdés, and J. Aparicio. (2002). "Frequency and Spatial Characteristics of Droughts in the Rio Conchos basin, Mexico". Water International. International Water Resources Association. 27(3), 420-430.

Moriasi, D. N., Arnold, J.G; Van Liew, M.V; Bingner, R.L; Harmel, R.D; and Veith, T.L. (2007). "Model evaluation guidelines for systematic quantification of accuracy in watershed simulations. Trans. American Society of Agricultural and Biological Engineers 50(3): 885−900.

Legates, D.R., and McCabe, G.J. Jr. (1999). "Evaluating the use of goodness-of-fit measures in hydrologic and hydroclimatic model validation". Water Resources Res. 35(1):233-241.

Li, L., Hao, Z-C., Wang, J-H., Wang, Z-H., and Yu, Z-B. (2008). "Impact of future climate change on runoff in the head region of the Yellow river". Journal of Hydrologic Engineering, ASCE, Vol. 13, No.5, 347-354.

Lin, J.L., Mapes, B.E; Weickmann, K.M; Schubert, S.D; and Bacmeister, J.T. (2008). "North American Monsoon and convectively coupled equatorial waves simulated by IPCC AR4 coupled GCMs". American Meteorological Society, Vol. 21, No.5, 2919-2937.

Loucks, D.P. (1997). "Quantifying trends in system sustainability". J. of Hydrol. Sci; 42(4), 513-530.

Loukas, A., and Quick, M. (1996). "Effect of climate change on hydrology regime of two climatically different watersheds". Journal of Hydrologic Engineering, Vol. 1, No.2, ASCE, 77-87.

Luizzo, L., Noto, L.V., Vivoni, E.R., and La Loggia, G. (2010). "Basin-scale water resources assessment in Oklahoma under synthetic climate change scenarios using a fully distributed model". *J. Hydrol. Eng.* 15(2):107-122.

Martinez, J. and Zermeno, R.M and Lopez, A.G. (2005). "Estudio Para la Gestion Integrada del Agua en la Cuenca del Rio Bravo, Instituto Mexicano De Tecnologia Del Agua. Report No. 2002-C-01-0569-A3, (in Spanish).

Maurer, E.P. (2007). "Uncertainty in hydrologic impacts of climate change in the Sierra Nevada, California under two emissions scenarios". Climatic Change, 82, 10.1007/s10584-006-9180-9.

Maurer, E. P., Brekke, L., Pruitt, T., and Duffy, P. B. (2007). "Fine-resolution climate projections enhance regional climate change impact studies", Eos Trans. AGU, 88(47):504. <http://gdo-dcp.ucllnl.org/downscaled_cmip3_projections >

Maurer, E.P. and Duffy, P.B. (2005). "Uncertainty in Projections of Streamflow Changes due to Climate Change in California". Geophysical Research Letter. 32(3), L03704 doi:10.1029/2004GL021462.

Meselhe, E.A., Habib, E.H., Oche, O.C., and Gautam, S. (2009). "Sensitivity of conceptual and physically based hydrologic models to temporal and spatial rainfall sampling". *J. Hydrol. Eng*., 14(7):711-720.

Minville, M., Brisette, F., and Leconte, R. (2008). "Uncertainty of the impact of climate change on the hydrology of a Nordic watershed". Journal of Hydrology, 358, 70-83.

Munoz-Arriola, F; Avissar, R; Zhu, C; and Lettenmaier, D.P. (2009). "Sensitivity of the water resources of Rio Yaqui Basin, Mexico, to agriculture extensification under multiscale climate condictions". Journal Water Resources Research, 45, W00A20, 13 pp.

NARR - North American Regional Reanalysis. (2008). National Centers for Environmental Prediction (NCEP). National Oceanographic and Atmospheric Administration. Washington DC.
http://nomads.ncdc.noaa.gov/thredds/catalog/narr/catalog.html <accessed 13 November 2010>

NOAA - National Oceanographic and Atmospheric Administration. (2010). Monthly Bivariate ENSO Time Series (BEST) Index. Earth System Research Laboratory. Washington DC. http://www.esrl.noaa.gov/psd/data/ <accessed 13 November 2010>

Orive, A.A. (1945). "Informe técnico sobre el tratado internacional de aguas" Comisión Nacional de Irrigación. México D.F., Sep. 1945.

Patiño-Gomez, C; and McKinney, D.C. (2005). "GIS for Large-Scale Watershed Observational Data Model". Center for Research in Water Resources, Online Report 05-07, University of Texas at Austin, 283 pp. www.crwr.utexas.edu/reports/2005/rpt05-7.shtml

Payne, J., Wood, A.W., Hamlet, A.F., Palmer, R.N., and Lettenmaier, D.P. (2004). "Mitigating the effects of climate change on the water resources of the Columbia river basin". Climatic change 62: 233-256.

Phillips, N. (1956). "The general circulation of the atmosphere". Quarterly Journal of the Royal Meteorological Society, **82**, 123-164.

Pro Fauna. (2003). "Physical and hydrological condition indicators of the Rio Conchos, Chihuahua, Mexico". Pro Fauna A.C. Chihuahua, Mexico.

Randall, D.A., R.A. Wood, S. Bony, R. Colman, T. Fichefet, J. Fyfe, V. Kattsov, A. Pitman, J. Shukla, J. Srinivasan, R.J. Stouffer, A. Sumiand K.E. Taylor. (2007). "Climate Models and Their Evaluation". Climate Change 2007. The Physical Science Basis. Contribution of Working Group I to the Fourth Assessment Report of the Intergovernmental Panel on Climate Change. Cambridge University Press, Cambridge, United Kingdom and New York, NY, US.

Richardson, C.W. (1981). "Stochastic Simulation of Daily Precipitation, Temperature, and Solar Radiation". Water Resources Research, 17( 1):182-190**.**

Ruiz-Barradas, A., Nigam, S. (2006). "IPCC's twentieth-century climate simulations: varied representations of North American hydroclimate variability". American Meteorological Society, pages 4041-4058.

Sandoval-Solis, S., D. C. McKinney and R. L. Teasley (2008). Water Management Scenarios for the Rio Grande/Bravo Basin, Center for Research in Water Resources, Online Report 08-01, University of Texas at Austin. www.crwr.utexas.edu/reports/2006/rpt08-01.shtml

Sandoval-Solis, S., D. C. McKinney, and D. P. Loucks. (2011) Sustainability Index for Water Resources Planning and Management, J. Water Resour. Planning and Management, accepted, in press. Doi: 10.1061/(ASCE)WR.1943-5452.0000134.

Santa Clara University and Bureau of Reclamation. (2008). "Statistically Downscaled WCRP CMIP3 Climate Projections". http://gdo-dcp.ucllnl.org/downscaled_cmip3_projections/

Scurlock, J. M. O., Asner, G.P; and Gower, S.T. (2001). Global Leaf Area Index data from field measurements, 1932-2000". Dataset available on-line [http://www.daac.ornl.gov] from the Oak Ridge National Laboratory Distributed Active Archive Center, Oak Ridge, Tennessee, U.S.A.

Smagorinsky, J., Manabe, S. and Holloway, J.L. (1965). "Numerical results from a nine level general circulation model of the atmosphere". Monthly Weather Review, 93, 727-768.

Smagorinsky, J. (1963). "General circulation experiments with the primitive equations, the basic experiment". Monthly Weather Review, vol. 91, No. 3, Mar. 1963, pp. 99-164.

SEI - Stockholm Environment Institute. (2007). "Water Evaluation and Planning System, WEAP". Boston, US.

Sulis, M., Marrocu, M., and Paniconi, C. (2009). "Conjunctive use of a hydrological model and a multicriteria decision support system for a case study on the Caia catchment, Portugal". Journal of Hydrologic Engineering, ASCE, Vol. 14, No.2, 141-152.

Taylor, K.E; Stouffer, R.J; and Meehl, G.A. (2009). "A Summary of the CMIP5 Experiment Design". Program for Climate Model Diagnosis and Intercomparison (PCMDI), NOAA's Geophysical Fluid Dynamics Laboratory (GFDL), and National Center for Atmospheric Research (NCAR).

Torrence, C; and Compo, G.P. (1998). "A practical guide to wave analysis". Bull. Am. Meteorol. Soc 79:61-78.

Towler, E; Rajagopalan, B; Gilleland, E; Summers, S; Yates, D; and Katz, R.W. (2010). "Modeling hydrologic and water quality extreme in a changing climate: A statistical approach based on extreme value theory". Water Resources Research 46(W011504):1-11.

United Nations. World population prospects: the 2009 revision. Department of Economic and Social Affairs, Population Division, New York, NY. http://esa.un.org/unpd/wpp2008/index.htm

Vicuna, S., Maurer, E.P, Joyce, B., Dracup, J.A., and Purkey, D. (2007). "The sensitivity of California water resources to climate change scenarios". Journal of American Water Resources Association, Vol. 43, No. 2, 482-498.

Warren, W., and Parkinson, C. (2005). An Introduction to Three–Dimensional Climate Modeling. Second Edition, National Center for Atmospheric Research and NASA Goddard Space Flight Center. University Science Books, California. Herndon VA. 368 pp.

Wilby, R.L., and Wigley, T.M.L. (1997). "Downscaling General Circulation Model Ouput: Review of Methods and Limitations". Progress in Physical Geography 21, 4: 530-548.

Wilby, R.L., Charles, S.P., Zorita, E., Timbal, B., Whetton, P., Mearns, L.O. (2004). "Guidelines for use of climate scenarios developed from statistical downscaling methods", Supporting material of the Intergovernmental Panel on Climate Change (IPCC).
www.ipcc-data.org/guidelines/dgm_no2_v1_09_2004.pdf

Wilby, R.L., Hay, L.E., Gutowski, W.J., Arritt, E.S., Pan, Z., Leavesley, G.H., and Clark, M.P. (2000). "Hydrological responses to dynamically and statistically downscaled climate model output". Geophysical Research Letters, Vol. 21, No. 8, 1199-1202.

Wiley, M.W., and Palmer, R.N. (2008). "Estimating the impacts and uncertainty of climate change on a municipal water supply system". Journal of Water Resources Planning and Management, ASCE, Vol. 134, No.3, 239-246.

Wood, A.W., Leung, L. R., Sridhar, V., and Lettenmaier, D. P. (2004). "Hydrologic implications of dynamical and statistical approaches to downscaling climate model outputs". Climatic Change 62, 189–216.

Wood, A.W., Maurer, E.P., Kumar, A., and Lettenmaier, D. (2002). "Long-range experimental hydrologic forecasting for the eastern United States". Journal of Geophysical Research, Vol. 107, No. D20, ACL 6-15.

Xie, H., Wayland Eheart, J., and Hyunhee An. (2008). "Hydrologic and economic implications of climate change for typical river basins of the agricultural Midwestern United States". Journal of Water Resources Planning and Management, ASCE, Vol. 134, No.3, 205-213.

Xu, Chong-yu., Widen, E., Halldin, E. (2005). "Modeling hydrological consequences of climate change –progress and challenges". Advances in Atmospheric Sciences, Vol. 22, No. 6, 789-797

Yates, D., Purkey, D., Sieber, J., Hubber-Lee, A., Galbraith, H., West, J., Herrod-Julius, S., Young, Ch., Joyce, B., and Reyej, M. (2009). "Climate driven water resources model of the sacrament basin, California". *J. of Water Resources Planning and Management* 135(5):303-313.

Yates, Purkey, D., Sieber, J., and Hubber-Lee, A. (2005). "A demand, priority, and preference driven water planning model. Part 1: Model characteristics". Water International 30(4):487-500.

Yates, D., Purkey, D., Sieber, J., Huber-Lee, A., West, J, and Galbraith, H. (2006). "A physically-based, water resources planning model of the Sacrament Basin, California". ASCE, Journal of Water Resources Management.

Yates, D., and Strzepek, K.M. (1998). "Modeling the Nile basin under climate change". Journal of Hydrologic Engineering, ASCE, Vol. 3, No. 2, 98-108.

Zhu, T., Jenkins, M., and Lund, J. (2005). "Estimated Impacts of Climate Warming on California Water Availability Under Twelve Future Climate Scenarios". Journal of the American Water Resources Association. AWRA, 41(5), 1027-1038.

# Vita

Eusebio Ingol Blanco was born in a small town, Mocupe in Peru. He is the son of Mercedes Ingol Vigo and Natalia Blanco Guevara. He attended to Colegio San Francisco de Asis in Peru where he completed his school in 1986, with excellence award. After graduating valedictorian, Eusebio enrolled in the Agricultural Engineering department at the Universidad Nacional Pedro Ruiz Gallo in 1989. He received a bachelor degree in 1994, with graduated valedictorian, first class honor 1989-1994. In 1996, Eusebio graduated as Agricultural Engineer. He has worked in several water projects along to the coast and mountain in Peru. In 2000, Eusebio was awarded with a fellowship to study a master in hydrosciences in the Colegio de Postgraduados, Mexico from 2001-2002. He developed his maters thesis in hydraulic modeling of an irrigation channel using a 1-D hydrodynamic model. After completing his master degree in January 2003, he went back to Peru to work in projects of Water Resources Intendance. In 2005, he was awarded by the Ford Foundation with a fellowship for doctoral studies in the United States. Eusebio enrolled the Doctoral program in Environmental and Water Resources Engineering at the University of Texas at Austin in September 2006 and worked under the supervision of Dr. Daene McKinney. He is married to Juliana Leon, and they have two children: Nathaly and Gavin, and one little baby coming in October 2011. Eusebio is currently interested in faculty position in academia and international organizations for employment upon completion his Doctor of Philosophy degree in Civil Engineering in May 2011.

Permanent address:     3359 Lake Austin Blvd. Apt. B, Austin, TX 78703.
This dissertation was typed by the author.